

## Binocular, Accommodative and Oculomotor Alterations In Multiple Sclerosis: A Review

Amparo Gil-Casas, David P Piñero & Ainhoa Molina-Martin

To cite this article: Amparo Gil-Casas, David P Piñero & Ainhoa Molina-Martin (2020): Binocular, Accommodative and Oculomotor Alterations In Multiple Sclerosis: A Review, *Seminars in Ophthalmology*, DOI: [10.1080/08820538.2020.1744671](https://doi.org/10.1080/08820538.2020.1744671)

To link to this article: <https://doi.org/10.1080/08820538.2020.1744671>



Published online: 31 Mar 2020.



Submit your article to this journal [↗](#)



Article views: 12



View related articles [↗](#)



View Crossmark data [↗](#)



# Binocular, Accommodative and Oculomotor Alterations In Multiple Sclerosis: A Review

Amparo Gil-Casas<sup>1</sup>, David P Piñero<sup>2</sup>, and Ainhoa Molina-Martin<sup>2</sup>

<sup>1</sup>*Clínica Optométrica, Foundation Lluís Alcanyís, University of Valencia, Valencia, Spain and* <sup>2</sup>*Optics and Visual Perception Group (GOPV). Department of Optics, Pharmacology and Anatomy, University of Alicante, Alicante, Spain*

## ABSTRACT

Multiple sclerosis (MS) is an acquired demyelinating and inflammatory neurodegenerative disease affecting the central nervous system (CNS). Clinical and subclinical ocular disturbances occur in almost all patients with MS. The objective of this narrative review was to collect and summarize the available scientific information on oculomotor, accommodative and binocular alterations that have been reported in MS. A systematic search strategy with the following descriptors was carried out: multiple sclerosis, ocular motility disorders, internuclear ophthalmoplegia, nystagmus, vergences, fixation, pupil reflex, accommodation and stereopsis. According to the search, some oculomotor alterations were found to be commonly reported in MS, such as alterations in saccades and nystagmus. In contrast, accommodative, vergence and stereopsis alterations have not been comprehensively studied despite their relevance, with only minimal evidence showing a potential negative impact of the disease on these aspects. In conclusion, oculomotor impairment is a common component of disability in MS patients and should be considered when managing this type of patients. More research is still needed to know the real impact of this disease on binocular vision and accommodation.

**Keywords:** Accommodation, multiple sclerosis, saccades, stereopsis, vergence

## INTRODUCTION

Multiple sclerosis (MS) is an acquired demyelinating and inflammatory neurodegenerative disease affecting the central nervous system (CNS). It is characterized by relapses, followed by total or partial remissions.<sup>1</sup> It is most common at 25–35 years, although it can appear at any age. MS is the leading cause of non-traumatic disability in young adults<sup>2</sup>, with at least two times more women than men suffering this condition.<sup>3</sup>

Multiple clinical alterations can occur during MS, including visual dysfunctions that are among the most common. In the early stages of the disease<sup>4</sup>, signs and symptoms of visual disability can be present in one in three MS patients.<sup>5</sup> Specifically, oculomotor alterations can be present in up to 90–95% of cases in the course of MS, being more frequent in the progressive form.<sup>6</sup>

The objective of the present review was to conduct a narrative review of all oculomotor alterations that

have been reported to be present in MS, providing a synthesis of the available scientific information. Likewise, the scarce peer-reviewed literature available on binocular and accommodative alterations in MS was collected and summarized.

## SEARCH DESCRIPTION

A search strategy was performed using the scientific electronic database *Pubmed*. The bibliographic search was carried out using the Boolean operator AND in the following combinations of terms:

“multiple sclerosis” AND “ocular motility disorders”  
“multiple sclerosis” AND “internuclear ophthalmoplegia”  
“multiple sclerosis” AND nystagmus  
“multiple sclerosis” AND vergences  
“multiple sclerosis” AND fixation  
“multiple sclerosis” AND “pupil reflex”

Received 8 December 2019; accepted 14 March 2020; published online 30 March 2020.

Correspondence: David P Piñero, Optics and Visual Perception Group (GOPV). Department of Optics, Pharmacology and Anatomy. University of Alicante Spain. E-mail: [david.pinyero@ua.es](mailto:david.pinyero@ua.es)

“multiple sclerosis” AND accommodation  
 “multiple sclerosis” AND stereopsis

Inclusion criteria were articles published in Spanish, English or French showing results of clinical studies evaluating different oculomotor aspects of patients with multiple sclerosis. All types of articles were considered, including those describing case reports and series. No restrictions were considered in terms of the year of publication. Exclusion criteria were experimental studies with animals. According to this, a total of 147 references were revised in detail and their information included in the current narrative review (Figure 1). A total of 852 articles were identified in the search but excluded from the review according to the inclusion and exclusion criteria defined.

## OCULAR MOTILITY DISORDERS

Oculomotor alterations produced by MS are mainly caused by the presence of demyelination in different locations of the visual pathway. Depending on the

location, different mechanisms can be affected producing a wide range of alterations, including the medial longitudinal fasciculus, paramedian pontine reticular formation (PPRF), ocular motor cranial nerves CN III, IV, or VI, the medulla, the cerebellar peduncles, the posterior pontine tegmentum and the midbrain.<sup>7</sup>

The prevalence of oculomotor problems in MS is commonly underestimated, because these potential problems are not analyzed in detail in clinical practice if the patient does not report symptoms. Eye movement disorders are even more frequent in long-duration diseases<sup>8</sup> and therefore the evaluation of ocular motility is critical in patients with MS with and without symptoms. A great variety of alterations related to ocular motility in MS have been reported in the literature. A classification and description of these alterations are described in detail below.

### Saccades

Saccades are fast conjugated movements of the eyes between two targets. It can be executed voluntarily or

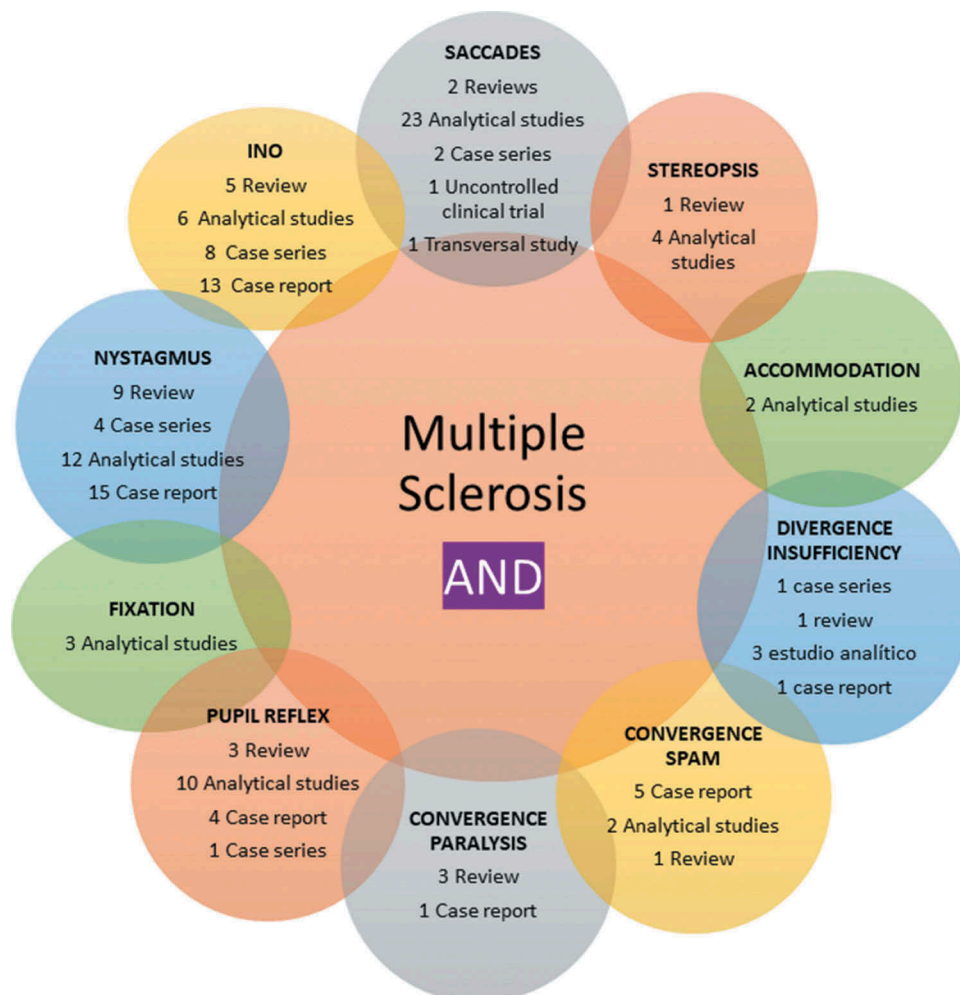


FIGURE 1. Summary of the articles considered for the current narrative review.

in response to visual stimuli. Depending on the direction of the movement, saccades can be directed to the new stimulus (pro-saccade) or move away from it (anti-saccades). The size of the saccadic pulse is controlled by the posterior fastigial nuclei and dorsal vermis in the cerebellum. Any damage in the fastigial nuclei causes hypermetric saccades (saccades that overshoot the target), and usually are binocular because axons cross to the contralateral nucleus. Lesion in dorsal vermis produces hypometric saccades (saccades that undershoot the target). Other impaired smooth pursuit can occur, such as saccadic intrusions and oscillations, and depending on the amplitude can be classified as square-wave jerks, macro square-wave jerks and macrosaccadic oscillations. When there is a pause between saccades back and forth, it has been postulated that the cause is a disruption of feedback between nuclei that control the saccades.<sup>2,9</sup>

Table 1 summarizes the saccadic alterations reported in MS patients in the studies revised. The most reported saccadic alterations in advanced MS and clinically isolated syndrome (CIS)<sup>10</sup> are saccadic dysmetria (41.7%) and impaired smooth pursuit (42.3%)<sup>11–13</sup>, which relates to prolonged saccadic latency, no matter if they have suffered or not optic neuritis (ON) or internuclear ophthalmoplegia (INO).<sup>14</sup> An increase in saccadic latency has been even found in children with MS.<sup>15</sup> Saccadic initiation time (SI time)<sup>16,17</sup> and average inter-saccadic intervals (ISI)<sup>18</sup> are also higher in patients with MS. Reduced saccade velocity is present in 44% of the cases with clinical MS and 18% of cases with the subclinical form.<sup>19</sup> Likewise, poor accuracy of saccades has been reported in MS, with a tendency to be hypometric.<sup>20</sup> Alterations of the vertical saccades (SVV) have also been found in 36% of MS patients<sup>13</sup>, combined with oblique saccades directed towards the side of the lesion.<sup>24</sup> The versional dysconjugacy index (VDI) has been proposed by several authors as a more appropriate measurement of the saccade limitation in MS rather than focusing only on the reduction of the saccade velocity.<sup>19,21,22</sup> VDI is a ratio between abducting to adducting eye movements for velocity, acceleration, latency and amplitude, allowing the elimination of the inter- and intraindividual variability. VDI has been found altered in patients with and without INO and NO.<sup>14</sup>

Saccades values are also used to characterize INOs, fixation and to quantify the effect of fatigue.<sup>25,26</sup> Fatigue increases saccade abnormalities, including large amplitude and latencies as well as larger decrease of saccadic peak velocity, which is the most characteristic sign of fatigue.<sup>27,28</sup> The saccades in the INO have been widely studied. Abduction saccadic velocities are normal while adduction saccades are slowed binocularly.<sup>22,29</sup> Obviously, fatigue also worsens the symptomatology and signs in INO.<sup>30</sup> Saccades alterations have been related to dynamic balance<sup>31</sup> and decrease in cognitive function, particularly working memory.<sup>32</sup>

These functions are valued by the anti-saccadic task that requires inhibiting an automatic saccade directed towards a visual stimulus that is presented and generating a saccade of similar amplitude in the opposite direction. Patients with MS make more errors in this test. Another test is memory-guided saccade that shows inaccurate responses in MS. Finally, saccades are measured to assess the effect of some pharmacological treatments, such as high-dose 6-methylprednisolone, which resulted in an improvement in latency.<sup>33</sup>

In all these studies, different methods have been used to measure the saccades. The most common are infrared oculography<sup>24,34</sup>, electro-oculographic technique,<sup>14,17,35</sup> infrared eye-tracker<sup>28</sup>, infrared reflection oculography<sup>19,34</sup> and the combination of infrared oculography and diffusion tensor imaging (DTI).<sup>36</sup> Other methods used analyze saccades but in relation to other cognitive abilities, such as the King-Devick test<sup>18</sup>, which is based on the speed of rapid number naming, and requires intact eye movements, particularly saccades. With this test, longer (worse) values have been found in MS patients. Another similar test is the Mobile Universal Lexicon Evaluation System (MULES)<sup>37</sup>, which is similar to the previous one, but images are named and time is measured. This evaluates the V4 area and the lower temporal projections needed for object recognition.

### Internuclear Ophthalmoplegia (INO)

Internuclear ophthalmoplegia (INO) is the slowing, limitation or incapacity of the adductor eye (inward) in horizontal gaze and the appearance of nystagmus in the abductor eye (outward)<sup>38</sup> (Figure 2). The adduction limitation is the same for pursuit and saccades, and saccadic latency is increased.<sup>23</sup> Convergence is preserved, which makes a differential diagnosis with paralysis of III cranial nerve. Patients do not necessarily manifest strabismus if fusional vergences are intact in primary gaze position. However, these patients may experience transient blur vision, oscillopsia, or diplopia for evoked nystagmus and transient tropia, while looking sideways.

INO is caused by damage to medial longitudinal fasciculus (MLF), which is the internuclear component that connects the oculomotor, trochlear, abducens, and vestibular nuclei, as well as the subnucleus of the medial rectus of the III cranial nerve. The lesion is on the same side of the eye showing the adduction weakness (Figure 3). MLF is also involved in the regulation of vertical eye movements, and therefore alterations such as skew deviation, ocular torsion, subjective visual vertical (SVV), decreased vertical smooth pursuit, or decreased vertical vestibulo-ocular reflex (VOR) gain can be present.<sup>39</sup> There are some hypotheses<sup>40</sup> about the origin of nystagmus in INO. First, these saccadic oscillations could be an

TABLE 1. Saccades studies.

Study (year)	N	Method	Type of MS	Measured Parameter	Conclusions
Lizak <i>et al.</i> <sup>10</sup>	20 CIS <sup>a</sup> 40 CDMS 20 H	EyeLink II dark pupil, video-oculography system	ND	- Latency of pursuit onset - Closed-loop pursuit gain - Summed saccade amplitudes during pursuit	CDMS patients had longer pursuit latency at all velocities. Closed-loop pursuit gain was significantly lower in CIS at all speeds. CDMS gain was lower at medium pursuit velocity. All patients increased summed saccade amplitudes at slow and medium pursuit speeds. Infrequent high-amplitude saccades at the fast speed.
Solingen <i>et al.</i> <sup>11</sup>	16 MS <sup>b</sup> 25 H	Electro-oculography	ND	- Saccade dysmetria - Delayed saccade reaction time - Slowing of adducting saccades - Impaired smooth pursuit - Examination of the eyes in primary position, horizontal and vertical conjugate gaze - Pursuit ocular movements - Horizontal and vertical saccades - Vertical VOR <sup>c</sup>	8 patients with MS present saccade dysmetria 5 patients with delayed saccade reaction time. 4 patients with bilateral saccade slowing. 1 patient with slowing of adducting saccades 3 patients with impaired smooth pursuit in both directions and 3 patients in one direction. 42.3% impaired smooth pursuit. 41.7% saccadic dysmetria. 14.7% unilateral internuclear ophthalmoplegia. 14.7% slowing of saccades 13.5% skew deviation. 13.5% gaze evoked nystagmus.
Servillo <i>et al.</i> <sup>12</sup>	163 MS	Bedside clinical examination	ND	- Eye convergence - Speed and accuracy of saccades - Vestibulo-ocular reflex - Subjective visual vertical (SVV)	16 patients with saccadic dysmetria in one plane and 14 in both 15 patients with smooth pursuit impaired 5 patients with VOR impaired 36% of patients with SVV abnormally large
Serra <i>et al.</i> <sup>13</sup>	50 MS	Bedside clinical examination	23 R-R <sup>d</sup> 8 P-P 12 S-P 7 P-R	- Latency - Accuracy - Peak velocity - Ratio of abduction and adduction peak velocities (VDI) - Latency saccadic and antisaccadic - Saccadic initiation time (SI time) - Saccadic initiation time (SI time) - Inter-saccadic intervals (ISI)	An increase in latency was the most frequent No asynchrony between abducting eye and adducting eye in MS patients without clinical INO 56% presented slowing of saccades VDI was significantly increased in the groups of MS patients without clinical INO. (VDI>1) Saccadic and antisaccadic latency was longer SI was longer in MS patients SI time was longer in RRMS Inter-saccadic intervals (ISI) were longer associated with prolonged K-D times
Ventre <i>et al.</i> <sup>14</sup>	32 MS (23 MS; 9 MSINO <sup>e</sup> ) 20 H	Electro-oculography	ND	- Latency saccadic and antisaccadic - Saccadic initiation time (SI time) - Inter-saccadic intervals (ISI)	Saccadic and antisaccadic latency was longer SI was longer in MS patients SI time was longer in RRMS Inter-saccadic intervals (ISI) were longer associated with prolonged K-D times
Yousef <i>et al.</i> <sup>15</sup>	15 MS 6 H 44 MS	Eye Brain tracker T2 Eye-tracker	ND R-R	Accuracy Peak velocity Latency and Accuracy in Predictable and unpredictable saccades	1/3 cases presented saccadic abnormalities, reduced velocity and hyper-and hypometria Unpredictable saccades, latencies prolonged and less accurate Predictable saccades were hypometric and normal latency
Nygaard <i>et al.</i> <sup>16</sup>	44 MS	Eye-tracker	R-R	Accuracy Peak velocity Latency and Accuracy in Predictable and unpredictable saccades	1/3 cases presented saccadic abnormalities, reduced velocity and hyper-and hypometria Unpredictable saccades, latencies prolonged and less accurate Predictable saccades were hypometric and normal latency
Mastaglia <i>et al.</i> <sup>17</sup>	108 MS	Electro-oculograms	R-R	Accuracy Peak velocity Latency and Accuracy in Predictable and unpredictable saccades	1/3 cases presented saccadic abnormalities, reduced velocity and hyper-and hypometria Unpredictable saccades, latencies prolonged and less accurate Predictable saccades were hypometric and normal latency
Hainline <i>et al.</i> <sup>18</sup>	25 MS	K-D <sup>f</sup> test Infrared video-oculography (Eyelink 1000+)	ND	Accuracy Peak velocity Latency and Accuracy in Predictable and unpredictable saccades	1/3 cases presented saccadic abnormalities, reduced velocity and hyper-and hypometria Unpredictable saccades, latencies prolonged and less accurate Predictable saccades were hypometric and normal latency
Meinenberg <i>et al.</i> <sup>19</sup>	79 MS	Infrared reflection oculography	ND	Accuracy Peak velocity Latency and Accuracy in Predictable and unpredictable saccades	1/3 cases presented saccadic abnormalities, reduced velocity and hyper-and hypometria Unpredictable saccades, latencies prolonged and less accurate Predictable saccades were hypometric and normal latency
Fielding <i>et al.</i> (2009) <sup>20</sup>	25 MS 25 H	IRIS infrared eye-tracker	22 R-R 3 S-P	Accuracy Peak velocity Latency and Accuracy in Predictable and unpredictable saccades	1/3 cases presented saccadic abnormalities, reduced velocity and hyper-and hypometria Unpredictable saccades, latencies prolonged and less accurate Predictable saccades were hypometric and normal latency

Flipse <i>et al.</i> <sup>21</sup>	26 MS 10 H	A scleral induction-coil magnetic system	ND	Peak velocities	Ratios between abducting eye/adducting eye showed significant differences while values of peak velocities and peak accelerations overlapped with the normal distribution
Jozefowicz-		Korczynsk <i>et al.</i> <sup>22</sup>	60 MSINO 50 H	Bedside ocularmotor examination and electrooculographic	ND
VDI for saccades velocity	32% with eye movements disorders Saccades velocity lower subclinical INO signs in 20%				
Reulen <i>et al.</i> <sup>23</sup>	84 MS	Electrodes on both canthi of both eyes. method developed by University of Amsterdam	ND	- Saccadic latency - Saccadic velocity - Accuracy of saccadic	80% with abnormal prolongation of saccadic latency. Significant correlation between prolonged saccadic latency and smooth pursuit deficit 19% with velocity disorders. 76% with abnormal pursuit eye movements

<sup>a</sup>CIS: clinically isolated syndrome; CDMS: clinically definite MS; H healthy.

<sup>a</sup>CIS: clinically isolated syndrome; CDMS: clinically definite MS; H healthy.

<sup>b</sup>MS: multiple sclerosis.

<sup>b</sup>MS: multiple sclerosis.

<sup>c</sup>VOR: Vestibulo-ocular reflex.

<sup>c</sup>VOR: Vestibulo-ocular reflex.

<sup>d</sup>R-R: relapsing-remitting; P-P: primary progressive- S-P: secondary progressive; P-R: progressive relapsing.

<sup>d</sup>R-R: relapsing-remitting; P-P: primary progressive- S-P: secondary progressive; P-R: progressive relapsing.

<sup>e</sup>MSINO: multiple sclerosis with internuclear ophthalmoplegia.

<sup>e</sup>MSINO: multiple sclerosis with internuclear ophthalmoplegia.

<sup>f</sup>K-D: King-Devick test.

<sup>f</sup>K-D: King-Devick test.



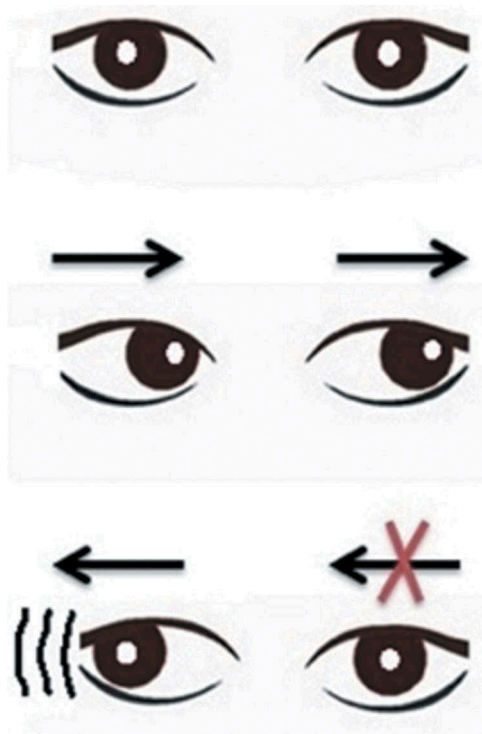


FIGURE 2. Ocular movements in internuclear ophthalmoplegia (INO) of the right medial longitudinal fasciculus (MLF). In the upper image: the primary gaze position is not affected. In the middle image, the left gaze is not altered. In the image below, in the right gaze, there is a paralysis or slowing down of the medial rectus of the right eye, as well as nystagmus in the left eye.

adaptive response rather than a true nystagmus (Hering's law). On the other hand, the structures responsible for the eccentric gaze are close to the MLF and might also be affected.

MS is the second cause of INO, with a prevalence of around 34%<sup>34,41–43</sup>, being preceded by vascular causes in a large portion of patients (36.9%).<sup>44</sup> The main findings in this dysfunction are present in the efferent visual system.<sup>45</sup> In children, INO is also present, with slightly more ophthalmological symptoms than adults.<sup>46</sup> Motor ocular findings may be the initial manifestations of MS and may predict additional demyelinating events.<sup>47,48</sup>

INO can be unilateral or bilateral. This last one is more frequent in MS<sup>40</sup>, with only 27% of the cases being unilateral.<sup>41</sup> Bilateral INOs have been reported in the literature as the first symptom of the disease and during the course of MS.<sup>49,50</sup> INO can be accompanied in some cases by complete bilateral horizontal gaze paralysis<sup>50,51</sup> or with right homonymous hemianopsia.<sup>52</sup> Bilateral INO is normally accompanied by vertical gaze deviation nystagmus.<sup>40</sup> INO can be also anterior or posterior, and the differential diagnosis depends on the integrity of convergence. If the lesion occurs at the level of the oculomotor nucleus, convergence is affected, whereas it is not

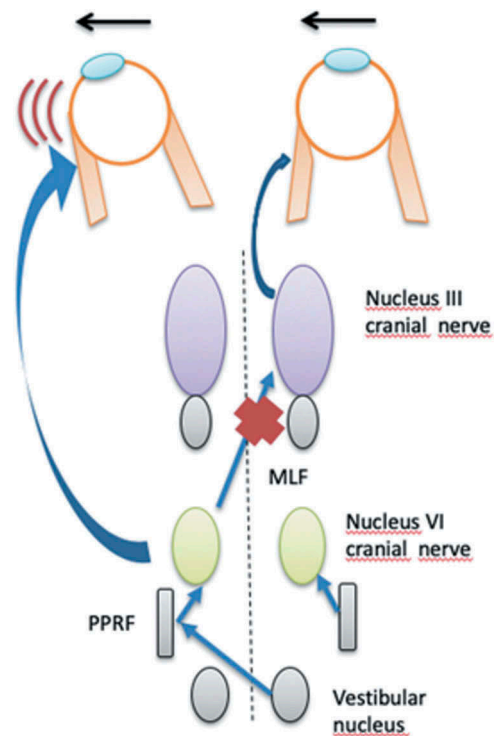


FIGURE 3. Internuclear ophthalmoplegia (INO): Paramedian pontine reticular formation (PPRF) projects a pulse of innervation to the VI nucleus. From here, through the cranial nerve VI (abducens nerve), the pulse of innervation is projected to the lateral rectus to generate an abduction of the left eye. Simultaneously, from the nucleus of the VI pair, the neurons come out to the nucleus of III cranial nerve (oculomotor) by medial longitudinal fasciculus (MLF) up to the right medial rectus. When the MLF is demyelinated, the size and timing of the pulse will be affected, altering the adduction of the medial rectus of the right eye.

affected in posterior INO because the MLF lesion is below the oculomotor nucleus.<sup>40</sup>

Another variant of INO is WEBINO (wall-eyed bilateral internuclear ophthalmoplegia), which is characterized by bilateral exotropia (wall-eyed) in primary position, bilateral INO, and affection of convergence.<sup>2</sup> Some rare cases of INO, such as INO of Lutz, also known as "INO of abduction", 'reverse INO' and 'pseudoabducens palsy', have been also reported in MS.<sup>53</sup> Different methods have been used to define and help in the diagnosis of INO, especially in early or subclinical cases.<sup>29</sup> The measurement of saccades, as mentioned above, is an important value in the diagnosis of INO.

INO can appear in combination with other alterations of the ocular movement, as one-and-a-half syndrome (OAHS) and its spectrum disorders. The one and a half syndrome is a horizontal movement disorder, which combines a paralysis of the ipsilateral-conjugated horizontal gaze (one) and INO (mean).<sup>54</sup> There is a sudden onset of double vision that gets worse when looking at one end. These patients cannot move their eyes to the opposite side. Vertical and

convergence movements are not affected. The one-and-a-half syndrome is caused by a lesion of unilateral tegmentum of pons, causing damage to the paramedian pontine reticular formation (PPRF), abducens nucleus and MLF ipsilateral. MS is the second most common cause of this syndrome after vascular disease.<sup>55,56</sup> It can occur as one of the first manifestations of the disease<sup>57</sup> or in the course of the disease.<sup>58</sup>

Twenty cases of OAHS in MS have been reported in the literature.<sup>44,57-61</sup> The range of age of presentation of clinical cases is 20 to 78 years. It is not specified in all cases whether the syndrome was the first symptom or it appeared during the course of the disease.

There are syndromes closely related to the OAHS called one-and-a-half spectrum syndromes, but only two of them have been reported in the literature associated to MS: eight-and-a-half syndrome and one-and-one syndrome. The eight-and-a-half syndrome was first named in 1998 by Eggenberger.<sup>62</sup> It is a combination of OAHS with ipsilateral seventh (facial) nerve palsy ( $7 + 1\frac{1}{2} = 8\frac{1}{2}$ ). It presents with one-sided facial paralysis and an OAHS on the same side. The demyelinating lesion occurs in the dorsal pontine tegmentum of the caudal pons involving the PPRF (or Abducens Nucleus) and the MLF, as well as the nucleus and fasciculus of the facial nerve. Few cases of eight-and-a-half syndrome have been reported in the literature: three cases<sup>63-65</sup> in adulthood and one in pediatric<sup>66</sup> age related to MS. In all cases, this syndrome was the first symptom of the disease.

The "one-and-one" syndrome term has been adopted by analogy with the "one-and-a-half" syndrome, leading to complete horizontal gaze paralysis. A case report of 24-year-old woman was published in 2010<sup>67</sup>, reporting as first symptom the diplopia. Abduction and adduction saccades were impossible, whereas vertical eye saccades and convergence were normal. The Marcus Gunn sign was observed, whereas nystagmus or other signs of brainstem dysfunction were not detected.

## Nystagmus

Nystagmus is a rhythmic oscillation of the eyes. The symptoms of acquired nystagmus include blurred vision due to the inability to fixate, vertigo and oscillopsia. The alteration of any of the following three mechanisms leads to nystagmus: (1) fixation: ability to detect the object and keep the visual axis on it; (2) the vestibulo-ocular reflex to compensate for head movements; (3) the gaze-holding system to hold the steady eccentric gaze. In MS, white matter usually affects the medial cerebellar, medullary posterior, central pontine and superior collicular regions, producing alterations in these mechanisms and therefore alterations of ocular movement and nystagmus.<sup>68,69</sup>

Each cycle of movement begins when the eye involuntarily moves away from the object (defoveating) and continues in motion to center the object in the fovea (foveating).<sup>70</sup> These movements may be slow or rapid. Normally, nystagmus is classified according to the rapid phase of the nystagmus. Nystagmus is one of the most frequent oculomotor alterations in MS, being permanent in 70% of cases.<sup>71</sup> However, in late-onset MS (after age 45), nystagmus is not as common as in the remaining cases.<sup>72</sup>

The first cause of acquired pendular nystagmus is MS.<sup>73,74</sup> Indeed, it has been one of the most studied nystagmus types by previous authors. The majority of patients with MS develops nystagmus later in a progressive phase of the disease.<sup>75</sup> The amplitude, asymmetry, irregularity and mean peak velocity of nystagmus in MS are lower than in oculopalatal tremor, but the frequency is higher in MS.<sup>76</sup> This type of nystagmus can also be associated with dissociated movements.<sup>77</sup>

Nystagmus may be due to visual deprivation due to optic neuritis<sup>75</sup> as the oscillations have been shown to be usually larger in the eye with more severe visual impairment. Another theory is that the oscillations are due to the instability of the neural integrator<sup>73,78</sup>, because in patients with MS demyelinating plaques are in the region of the paramedian tracts, which is an important area associated with feedback circuits of eye velocity signals.<sup>79,80</sup> In a clinical case, a vertical pendular nystagmus was reported in MS, with simultaneous involvement of optic nerve and asymmetric brain stem lesions.<sup>81</sup> Concerning the optokinetic nystagmus (OKN), it is one of the most common (around 60% of patients)<sup>82</sup> and disabling nystagmus in MS.<sup>83</sup>

Evoked nystagmus has been shown to be present in 45% of patients with MS.<sup>84</sup> This type of nystagmus may appear in conjunction with paralysis of the face, imbalance<sup>85</sup> and pupillary light-near dissociation.<sup>86</sup> Likewise, MS is the second cause of horizontal gaze-evoked nystagmus (hGEN) behind neuromyelitis optica spectrum disorder (NMOSD).<sup>87</sup> It is present in between 10-15% of patients with MS.<sup>12</sup> Another common type of nystagmus in MS is the acquired convergence-evoked nystagmus (CEN) (40% of patients), which is more frequent in its vertical mode (82%).<sup>88</sup> This type of nystagmus can occur as a first symptom<sup>89</sup> or in a relapse.<sup>90</sup> In this type of nystagmus, lesions occur in cortical eye fields and their descending connections.<sup>91</sup>

Upbeat nystagmus is not very common in MS, with only 5% of patients showing it.<sup>92</sup> It is related to damage of the vestibular-reflective ocular pathway and lesions in the medial longitudinal fasciculus (MLF) and ventral tegmental tract. Three clinical cases have been reported in combination with damage in the trigeminal nerve.<sup>93</sup> Another atypical case of upbeat nystagmus with a linear slow phase waveform has been reported, in which the velocity of nystagmus was intensified in downward gaze and



decreased during upward gaze. Lesions were located in the paramedian dorsal area of the caudal medulla, encompassing the most caudal part of the perihypoglossal nuclei.<sup>94,95</sup> Although downbeat nystagmus is related to neurological disorders, they are not as common in MS. Indeed, four cases have only been reported.<sup>96–98</sup> They are usually associated with lesions of the vestibulocerebellum and underlying medulla.

Central positional nystagmus is very rare in MS (1%), not being the primary cause.<sup>99,100</sup> However, it can be the first symptom of MS<sup>101</sup> because this type of nystagmus is a sign of pathology localized in the area of the vestibular nuclei. Only two cases of see-saw nystagmus (SSN) have been reported<sup>102,103</sup> even though MS is the second cause of SSN.<sup>104</sup> This nystagmus presents oscillopsia in two phases. In the first phase, three elevations are present, with intorsion of one eye and synchronous depression and extorsion of the other eye. In the second phase, the movements are the opposite.

A case of rotary nystagmus has also been reported, in which the visual axis of the eye involuntarily moves in the horizontal and vertical planes, describing a closed-loop trajectory.<sup>105</sup> Torsional nystagmus has only been reported in one case report in which a left dorsolateral medullary MS plaque was detected with MRI.<sup>106</sup> Finally, periodic alternating nystagmus (PAN) has been described in a clinical case<sup>107</sup>, in which multiple areas of demyelination scattered along the floor of the IV ventricle were present, involving portions of all vestibular nuclei. It is clinically presented with nystagmus in primary gaze position for 2 min, stopping then and starting beating in the opposite direction afterwards.<sup>104</sup>

## Fixation

Only two studies have been reported in the literature on fixation and MS. The first of them assessed fixation with scanning laser ophthalmoscope (SLO)-based eye-tracking during OCT scanning of retinal layer thickness.<sup>108</sup> Sixteen patients with MS were studied and concluded that MS patients have twofold of fixation instability. Likewise, there was no relationship between fixation instability and low-contrast letter acuity, and weakly with ganglion cell layer (GCL), suggesting that fixation instability may be due to demyelination or neurodegeneration affecting efferent pathways. These results were consistent with those obtained in another study<sup>25</sup>, which also did not find a relation between fixation instability in terms of frequency and amplitude with optic neuritis. These authors used infrared oculography in 213 patients to observe square-wave jerks, being larger in 25% of MS patients, but not in frequency.

Larger fixational eye movements around visual targets with intention tremor are present in patients with MS compared to controls.<sup>109</sup> The unsteady gaze

fixation on visual targets is proportional to the magnitude of the preceding saccades, influencing the severity of intention tremor during eye-hand coordinated visuomotor tasks.

## Pupil Reflex

The regulation of the pupil is controlled by the CGL of the retina through its projections to the olivary pretectal nucleus (OPN) and to the suprachiasmatic nucleus (SCN) in the middle brain. The rods mediate mainly the transient pupil contraction, whereas melanopsin retinal ganglion cells (mRGCs) contribute to the steady-state pupil constriction.

The reduction of the pupil sustained response to blue light has been associated with a decrease in thinner ganglion cell layer (GCL) and inner plexiform layer (IPL). This is also related to the abnormal rhythm of melatonin in MS patients, which is more remarked in patients with episodes of NO.<sup>110</sup> The pupil cycle time (PCT) is also reduced in 83% of patients with MS<sup>111</sup>, and even more in those combined with episodes of NO.<sup>112</sup> Pupil response deficits remain with standard visual field perimetry and chromatic thresholds isolating the use of color signals.<sup>113</sup>

The amplitude of pupillary response and maximum speed measured with multifocal objective pupillometry (mfPOP) are reduced in patients with MS with or without NO associated.<sup>114</sup> Another alteration in MS was a reduction of latency with a large pupil, and an increase of latency with a small pupil.<sup>115</sup> In some cases, this can be the first symptom of MS<sup>116</sup> as well as corectopia.<sup>117</sup>

A study assessed the dilating and contraction reaction of the pupil in patients with MS. It found that a lot of reaction to dilation was present, but with little reaction to constriction and greater recovery of pupil diameter after observing the light stimulus. The affection is nonspecific<sup>118</sup>, but when studied together with accommodation (parasympathetic system), no alteration was present in the pupillary reaction.<sup>119</sup> As the pupillary function is mediated by the autonomous system, it is related to the cognitive function. A study revealed that MS patients with low cognitive scores had lower pupil response measured with eye-tracker.<sup>120</sup>

Relative afferent pupillary defects are present in 18% of cases of MS. A relative afferent pupillary defect was found in 6% of patients with no history of optic neuritis and no optic atrophy.<sup>121</sup> Pupillary alterations such as Marcus Gunn have been reported in four clinical cases<sup>122,123</sup>, including a 15-month-old infant.<sup>124</sup> Others such as Argyll Robertson pupil have also been reported combined with lesions in the area of the nucleus of Edinger–Westphal.<sup>125</sup> Nine cases of III cranial nerve dysfunction in multiple sclerosis (MS) have been reported.<sup>126,127</sup>

## BINOCULAR VISION AND ACCOMMODATION

Vergences are coordinated movements of the eyes to maintain bifoveal fixation by excitation and inhibition of the lateral and medial rectus muscles. The impulses pass from lateral rectus subnucleus motor neurons to medial by means of the oculomotor internuclear complex and additional regions related to vergence areas 19 and 22 of the occipital lobes and the pontine tegmentum.<sup>40</sup> Degenerative conditions can cause vergence impairment<sup>128</sup>, producing symptomatology, such as diplopia, asthenopia and reduced depth perception. Some vergence disorders have been reported in the literature associated with MS.

### Convergence Paralysis

A pure study of convergence has not been done. In the peer-reviewed literature, the convergence paralysis or its deficit is associated with INO, as it affects the demyelination of MLF, and in consequence abductors or convergence pathways can also be damaged.<sup>129</sup> Only one case report in MS with dorsal midbrain syndrome has been published, showing pupillary light-near dissociation, upward gaze paresis, convergence-retraction nystagmus and skew deviation.<sup>86</sup>

### Convergence Spasm

Spasm of the near reflex is characterized by excessive convergence, accommodation and miosis that are often associated with psychogenic disorders, although it may be secondary to several organic conditions.<sup>130</sup> The spasm of the near point is considered as a paroxysmal symptom. In other words, it is a brief symptom that appears suddenly, being repeated multiple times a day during a variable period (days or weeks) and finally disappearing.

In 1975, a paroxysmal attack with double vision presentation in MS was described for the first time.<sup>131</sup> Although this anomaly was first mentioned in 1884<sup>132</sup>, it was not studied in depth due to the rarity of its clinical entity. Currently, the cases reported in the literature are not abundant. Indeed, the percentage of MS patients with paroxysmal symptoms ranges from 9% to 17%.<sup>131</sup> Paroxysmal symptoms have been described in the early stages of MS in patients who do not have a neurological disability or only a minor disability<sup>131</sup>, although they have also been described in advanced stages of the disease. It is suggested that these attacks occur by ephaptic activation, i.e. when axonal propagation in the plaques is abnormal, with the transmission of nerve impulses taking place through the membrane by synapses.<sup>133</sup>

Magnetic resonance studies have revealed the association of convergence spasm in MS with lesions of the brainstem in the region of the longitudinal cord.<sup>134,135</sup> In other cases, demyelinating plates have been found in the corpus callosum, white pericallosal matter and protons in the brainstem.<sup>136,137</sup>

### Divergence Insufficiency (ID)

ID is a rare-acquired disorder of binocular vision that has been associated with neurological disorders, such as ischemic brainstem disorder, brain stem malformation, tumors, CNS infections, demyelinating disorders, head trauma and intracranial hypertension.<sup>138</sup> ID in MS is very rare, also called divergence paralysis. The clinical features of ID are low magnitude esotropia at distance vision, but orthophoria or mild esophoria is usually present at near. In lateral gaze, the deviation is concomitant. Divergence fusion is reduced, but abduction is complete and saccadic velocities are normal in abduction.<sup>139</sup>

The cause of this condition is not clearly localized.<sup>140</sup> Many different regions (diffuse or focal) have been described for the lesions leading to ID. Although some authors support the hypothesis of the existence of a divergence control centre, diffuse and distributed lesions would not support such existence, with the possibility of multiple neural or diffusely distributed structures governing divergence.<sup>140</sup> Currently, the etiology of ID is undefined, being continuously in controversy.<sup>141</sup> It should be considered that divergence is an active process, not passive, associated with the relaxation of the middle rectus muscles.<sup>142</sup>

ID may be an initial symptom of a probable demyelinating disease in young and previously healthy subjects. Patients with ID should undergo a complete neurological evaluation, including neurological images<sup>143</sup> to rule out neurological alterations. Only one case of ID in MS has been reported<sup>143</sup>, showing a 38-year-old woman with an episode of diplopia at distance (esotropia) and orthophoria at near. Neurological evaluation was normal, but multiple demyelinating lesions were observed on MRI.

### Accommodative Disorders

Currently, little has been studied about accommodative alterations in MS. In fact, only two studies have studied accommodation in patients with MS. The first study<sup>119</sup> was carried out in 1992 that analyzed the accommodative range using a Badal optical system and the reaction time, pressing a button when they perceived the blur. The sample consisted of nine patients (7 women and 2 men) aged between 23 and 34 years, with no significant differences in accommodation range or tonus position. The only finding that differed between controls and

patients with MS was the reaction time that was slowest to detect optotypes at far and near distance.

The second study on accommodation<sup>144</sup> showed 25 MS subjects with alterations in the visual-evoked potentials (PEV), other 25 without alteration in the PEV and 25 controls. The study showed that patients with altered VEP and reduction in the retinal nerve fiber layer (RNFL) had a lower amplitude of accommodation measured with the negative lens method compared to controls. Considering that different methods used for measuring accommodation were used in both studies, no precise comparisons can be performed, being necessary more studies to assess the accommodation in patients with MS.

### Stereopsis

Deficits in stereoscopic vision may be due to alterations in the ocular movements, but also to the demyelization progress during the disease.<sup>145, 146</sup> Three studies have been made on MS and stereopsis. In the first study<sup>147</sup>, stereopsis was measured with the Randot Stereoacuity Test (RST) and these values were positively related with evoked potentials (PEV). In this study, 73.9% of the subjects showed a significant decrease in stereoacuity, even when their VA was 20/20. The second study<sup>148</sup> obtained similar conclusions with a sample of 27 patients with VA 20/20 and no history of NO, but the rate of stereoscopic anomalies was 22.2%, independently of the disease duration. The third study led to the same conclusion, with a decrease in stereoacuity in patients with MS, with or without AV involvement.<sup>149</sup>

### CONCLUSIONS

A great variety of oculomotor alterations are present in MS, either during the course of the disease or as a first sign. Oculomotor impairment is not severe in most of the cases, but chronic oculomotor alterations may be present at all stages of the disease, with the potential of affecting binocularity. In any case, a complete ophthalmological and optometric evaluation of the visual system is essential to assess the oculomotor impairment caused by MS.

### DECLARATION OF INTEREST

The authors have no proprietary or commercial interest in the medical devices that are involved in this manuscript.

### FUNDING

The author David P Piñero has been also supported by the Ministry of Economy, Industry

and Competitiveness of Spain within the program Ramón y Cajal, [RYC-2016-20471].

### REFERENCES

1. Lublin FD, Reingold SC, Cohen JA, et al. Defining the clinical course of multiple sclerosis: the 2013 revisions. *Neurology*. 2014;83:278–286.
2. Serra A, Chisari CG, Matta M. Eye movement abnormalities in multiple sclerosis: pathogenesis, modeling, and treatment. *Front Neurol*. 2018;9:31.
3. Pozzilli C, Tomassini V, Marinelli F, et al. “Gender gap” in multiple sclerosis: magnetic resonance imaging evidence. *Eur J Neurol*. 2003;10:95–97.
4. Graves J, Balcer LJ. Eye disorders in patients with multiple sclerosis: natural history and management. *Clin Ophthalmol*. 2010;4:1409–1422.
5. Jasse L, Vukusic S, Durand-Dubief F, et al. Persistent visual impairment in multiple sclerosis: prevalence, mechanisms and resulting disability. *Mult Scler J*. 2013;19:1818–1826
6. Frohman EM, Frohman TC, Zee DS, et al. The neuro-ophthalmology of multiple sclerosis. *Lancet Neurol*. 2005;4:111–121.
7. Rufa A, Cerase A, De Santi L, et al. Impairment of vertical saccades from an acute pontine lesion in multiple sclerosis. *J Neuroophthalmol*. 2008;28:305–307.
8. Alpini D, Milanese C, Berardi C. Value of otoneurological tests in the staging of multiple sclerosis. *Ital J Neurol Sci*. 1987;Suppl 6:103–108.
9. Prasad S, Galetta SL. Eye movement abnormalities in multiple sclerosis. *Neurol Clin*. 2010;28:641–655.
10. Lizak N, Clough M, Millist L, et al. Impairment of smooth pursuit as a marker of early multiple sclerosis. *Front Neurol*. 2016;7:206.
11. Solingen LD, Baloh RW, Myers L, et al. Subclinical eye movement disorders in patients with multiple sclerosis. *Neurology*. 1977;27:614–619.
12. Servillo G, Renard D, Taieb G, et al. Bedside tested ocular motor disorders in multiple sclerosis patients. *Mult Scler Int*. 2014;2014:732329.
13. Serra A, Derwenskus J, Downey DL, et al. Role of eye movement examination and subjective visual vertical in clinical evaluation of multiple sclerosis. *J Neurol*. 2003;250:569–575.
14. Ventre J, Vighetto A, Bailly G, et al. Saccade metrics in multiple sclerosis: versional velocity disconjugacy as the best clue? *J Neurol Sci*. 1991;102:144–149.
15. Yousef A, Devereux M, Gourraud P-A, et al. Subclinical saccadic eye movement dysfunction in pediatric multiple sclerosis. *J Child Neurol*. 2019;34:38–43.
16. Nygaard GO, de Rodez Benavent SA, Harbo HF, et al. Eye and hand motor interactions with the symbol digit modalities test in early multiple sclerosis. *Mult Scler Relat Disord*. 2015;4:585–589.
17. Mastaglia FL, Black JL, Collins DWK. Quantitative studies of saccadic and pursuit eye movements in multiple sclerosis. *Brain*. 1979;102:817–834.
18. Hainline C, Rizzo JR, Hudson TE, et al. Capturing saccades in multiple sclerosis with a digitized test of rapid number naming. *J Neurol*. 2017;264:989–998.
19. Meienberg O, Muri R, Rabineau PA. Clinical and Oculographic Examinations of Saccadic Eye Movements in the Diagnosis of Multiple Sclerosis. *Arch Neurol*. 1986;43:438–443.
20. Fielding J, Kilpatrick T, Millist L, et al. Control of visually guided saccades in multiple sclerosis: disruption to

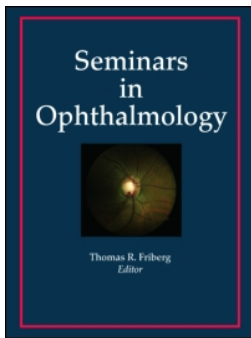


- higher-order processes. *Neuropsychologia*. 2009;47:1647–1653.
21. Flipse J, Straathof CS, Van der Steen J, et al. Binocular saccadic eye movements in multiple sclerosis. *J Neurol Sci*. 1997;148:53–65.
  22. Jozefowicz-Korczynska M, Łukomski M, Pajor A. Identification of internuclear ophthalmoplegia signs in multiple sclerosis patients. *J Neurol*. 2008;255:1006–1011.
  23. Reulen JP, Sanders EA, Hogenhuis LA. Eye movement disorders in multiple sclerosis and optic neuritis. *Brain*. 1983;106:121–140.
  24. Frohman EM, Frohman TC, Fleckenstein J, et al. Ocular contrapulsion in multiple sclerosis: clinical features and pathophysiological mechanisms. *J Neurol Neurosurg Psychiatry*. 2001;70:688–692.
  25. Nij Bijvank JA, Petzold A, Coric D, et al. Quantification of visual fixation in multiple sclerosis. *Invest Ophthalmol Vis Sci*. 2019;60:1372–1383
  26. Santinelli FB, Barbieri FA, Pinheiro CF, et al. Postural control complexity and fatigue in minimally affected individuals with multiple sclerosis. *J Mot Behav*. 2019;51:551–560.
  27. Finke C, Pech LM, Sömmer C, et al. Dynamics of saccade parameters in multiple sclerosis patients with fatigue. *J Neurol*. 2012;259:2656–2663.
  28. Ferreira M, Pereira PA, Parreira M, et al. Using endogenous saccades to characterize fatigue in multiple sclerosis. *Mult Scler Relat Disord*. 2017;14:16–22.
  29. Metz HS. Saccadic velocity measurements in internuclear ophthalmoplegia. *Am J Ophthalmol*. 1976;81:296–299.
  30. Matta M, Leigh RJ, Pugliatti M, et al. Using fast eye movements to study fatigue in multiple sclerosis. *Neurology*. 2009;73:798–804.
  31. Garg H, Dibble LE, Schubert MC, et al. Gaze stability, dynamic balance and participation deficits in people with multiple sclerosis at fall-risk. *Anat Rec*. 2018;301:1852–1860.
  32. Fielding J, Kilpatrick T, Millist L, et al. Multiple sclerosis: cognition and saccadic eye movements. *J Neurol Sci*. 2009;277:32–36.
  33. Versino M, Bergamaschi R, Callieco R, et al. Eye movement quantitative evaluation before and after high-dose 6-methylprednisolone in multiple sclerosis. *Acta Neurol Scand*. 2009;89:105–110.
  34. Müri RM, Meienberg O. The clinical spectrum of internuclear ophthalmoplegia in multiple sclerosis. *Arch Neurol*. 1985;42:851–855.
  35. Alpini D, Caputo D, Hahan A, et al. Grading brainstem involvement in multiple sclerosis - by means of electro-oculography. *J Neurovirol*. 2000;6(Suppl 2):S156–9.
  36. Fox RJ, McColl RW, Lee JC, et al. A preliminary validation study of diffusion tensor imaging as a measure of functional brain injury. *Arch Neurol*. 2008;65:1179–1184.
  37. Seay M, Akhand O, Galetta MS, et al. Mobile Universal Lexicon Evaluation System (MULES) in MS: evaluation of a new visual test of rapid picture naming. *J Neurol Sci*. 2018;394:1–5.
  38. Subei AM, Eggenberger E. Efferent manifestations of multiple sclerosis. *Curr Opin Ophthalmol*. 2012;23:506–509.
  39. Zwergal A, Cnyrim C, Arbusow V, et al. Unilateral INO is associated with ocular tilt reaction in pontomesencephalic lesions: INO plus. *Neurology*. 2008;71:590–593.
  40. Karatas M. Internuclear and supranuclear disorders of eye movements: clinical features and causes. *Eur J Neurol*. 2009;16:1265–1277.
  41. Nij Bijvank JA, van Rijn LJ, Balk LJ, et al. Diagnosing and quantifying a common deficit in multiple sclerosis: internuclear ophthalmoplegia. *Neurology*. 2019;92:e2299–e2308.
  42. Keane JR. Internuclear Ophthalmoplegia: unusual causes in 114 of 410 patients. *Arch Neurol*. 2005;62:714.
  43. Tilikete C, Jasse L, Vukusic S, et al. Persistent ocular motor manifestations and related visual consequences in multiple sclerosis. *Ann N Y Acad Sci*. 2011;1233:327–334.
  44. Bolanos I, Lozano D, Cantu C. Internuclear ophthalmoplegia: causes and long-term follow-up in 65 patients. *Acta Neurol Scand*. 2004;110:161–165.
  45. Maxner CE. Neuro-ophthalmology and multiple sclerosis. *Am Orthopt J*. 2006;56:72–85.
  46. Steinlin MI, Blaser SI, MacGregor DL, et al. Eye problems in children with multiple sclerosis. *Pediatr Neurol*. 1995;12:207–212.
  47. Chen L, Gordon LK. Ocular manifestations of multiple sclerosis. *Curr Opin Ophthalmol*. 2005;16:315–320.
  48. Brown P. A new clinical technique for demonstrating changes in eye acceleration during horizontal saccades in patients with partial internuclear ophthalmoplegias. *J Neuroophthalmol*. 1998;18:36–39.
  49. Hassen GW, Bhardwaj N. Bilateral internuclear ophthalmoplegia in multiple sclerosis. *N Engl J Med*. 2013;368:e3.
  50. Vidal de Francisco D, Argente Alcaraz J, Espinosa Rosso R. Complete bilateral horizontal internuclear ophthalmoplegia as a sign of multiple sclerosis relapse. *Neurologia*. 2014;29:252–253.
  51. Milea D, Napolitano M, Dechy H, et al. Complete bilateral horizontal gaze paralysis disclosing multiple sclerosis. *J Neurol Neurosurg Psychiatry*. 2001;70:252–255.
  52. Gündüz K, Cansu K, Bulduklar S, et al. Homonymous hemianopsia as the initial manifestation of multiple sclerosis. *Ophthalmologica*. 1998;212:215–220.
  53. Nij Bijvank JA, Balk LJ, Tan HS, et al. A rare cause for visual symptoms in multiple sclerosis: posterior internuclear ophthalmoplegia of Lutz, a historical misnomer. *J Neurol*. 2017;264:600–602.
  54. Fisher CM. Some neuro-ophthalmological observations. *J Neurol Neurosurg Psychiatry*. 1967;30:383–392.
  55. Xue F, Zhang L, Zhang L, et al. One-and-a-half syndrome with its spectrum disorders. *Quant Imaging Med Surg*. 2017;7:691–697.
  56. Martyn CN, Kean D. The one-and-a-half syndrome. clinical correlation with a pontine lesion demonstrated by nuclear magnetic resonance imaging in a case of multiple sclerosis. *Br J Ophthalmol*. 1988;72:515–517.
  57. Espinosa PS. Teaching NeuroImage: one-and-a-half syndrome. *Neurology*. 2008;70:e20.
  58. de Seze J, Vukusic S, Viallet-Marcel M, et al. Unusual ocular motor findings in multiple sclerosis. *J Neurol Sci*. 2006;243:91–95.
  59. Ilnczyk S, Kamondi A, Várallyay G, et al. One-and-a-half syndrome—two cases. *Ideggyogy Sz*. 2007;60:489–493.
  60. Wall M, Wray SH. The one-and-a-half syndrome—a unilateral disorder of the pontine tegmentum: a study of 20 cases and review of the literature. *Neurology*. 1983;33:971–980.
  61. Westerink M, van Woerkom TCAM, Tavy DLJ. Transcranial magnetic stimulation in peripheral facial nerve palsy of central origin. *Clin Neurol Neurosurg*. 1991;93:45–49.
  62. Eggenberger E. Eight-and-a-half syndrome: one-and-a-half syndrome plus cranial nerve VII palsy. *J Neuroophthalmol*. 1998;18:114–116.
  63. Jacob S, Murray A. Rare occurrence of eight-and-a-half syndrome as a clinically isolated syndrome. *BMJ Case Rep*. 2018;2018:bcr-2017-222057.
  64. Keskin Guler S, Güneş N, Gokce Cokal B, et al. As the first sign of multiple sclerosis, eight-and-a-half syndrome. *Neurol Sci*. 2018;39:945–947.
  65. Wanono R, Daelman L, Maarouf A, et al. Eight and a half plus syndrome as a first presentation of multiple sclerosis. *Rev Neurol (Paris)*. 2014;170:553–554.

66. Mortzos P, Nordling MM, Sørensen TL. Eight-and-a-half syndrome as presenting sign of childhood multiple sclerosis. *J Aapos*. 2014;18:490–492.
67. Bourre B, Collongues N, Bouyon M, et al. Un cas d'ophtalmoplégie horizontale bilatérale: le syndrome 1 +1. *Rev Neurol (Paris)*. 2010;166:1028–1031.
68. Warner J, Lessell S. Neuro-ophthalmology of multiple sclerosis. *Clin Neurosci*. 1994;2:180–188.
69. Bede P, Finegan E, Chipika RH, et al. Oculomotor neural integrator dysfunction in multiple sclerosis: insights from neuroimaging. *Front Neurol*. 2018;9:691.
70. Stahl JS, Averbuch-Heller L, Leigh RJ. Acquired Nystagmus. *Arch Ophthalmol*. 2000;118:544.
71. Duquette J. *Multiple Sclerosis, Vision Problems and Visual Impairment Interventions*. Institut Nazareth & Louis Braille; 2011. [www.inlb.qc.ca/wp-content/uploads/2015/01/Multiple-sclerosis-and-vision-impairment.pdf](http://www.inlb.qc.ca/wp-content/uploads/2015/01/Multiple-sclerosis-and-vision-impairment.pdf). accessed December 2nd 2019.
72. Lyon-Caen O, Izquierdo G, Marteau R, Lhermitte F, Castaigne P, Hauw JJ. Late onset multiple sclerosis. A clinical study of 16 pathologically proven cases. *Acta Neurol Scand*. 2009;72:56–60.
73. Kang S, Shaikh AG. Acquired pendular nystagmus. *J Neurol Sci*. 2017;375:8–17.
74. Choudhuri I, Sarvananthan N, Gottlob I. Survey of management of acquired nystagmus in the United Kingdom. *Eye*. 2007;21:1194–1197.
75. Barton JJ, Cox TA. Acquired pendular nystagmus in multiple sclerosis: clinical observations and the role of optic neuropathy. *J Neurol Neurosurg Psychiatry*. 1993;56:262–267.
76. Tilikete C, Jasse L, Pelisson D, et al. Acquired pendular nystagmus in multiple sclerosis and oculopalatal tremor. *Neurology*. 2011;76:1650–1657.
77. Barton JJ. Is acquired pendular nystagmus always phase locked? *J Neurol Neurosurg Psychiatry*. 1994;57:1263–1264.
78. Das VE, Oruganti P, Kramer PD, et al. Experimental tests of a neural-network model for ocular oscillations caused by disease of central myelin. *Exp Brain Res*. 2000;133:189–197.
79. Stahl JS, Leigh RJ. Nystagmus. *Curr Neurol Neurosci Rep*. 2001;1:471–477.
80. Averbuch-Heller L, Zivotofsky AZ, Das VE, et al. Investigations of the pathogenesis of acquired pendular nystagmus. *Brain*. 1995;118:369–378.
81. Singhvi JP, Singh AS. Unilateral vertical pendular nystagmus in multiple sclerosis: a distinctive neuro-ophthalmological sign. *Ann Indian Acad Neurol*. 2019;22:116–117.
82. Grénman R. Involvement of the audiovestibular system in multiple sclerosis. An otoneurologic and audiologic study. *Acta Otolaryngol Suppl*. 1985;420:1–95.
83. Todd L, King J, Darlington CL, et al. Optokinetic reflex dysfunction in multiple sclerosis. *Neuroreport*. 2001;12:1399–1402.
84. Cipparrone L, Fratiglioni L, Siracusa G, et al. Electronystagmography in the diagnosis of multiple sclerosis. *Acta Neurol Scand*. 1989;80:193–200.
85. Luis-Rosell E, Ramírez-Rivera J. Multiple sclerosis originating in childhood associated with seizures and hallucinations. *Bol Asoc Med P R*. 2006;98:203–205.
86. Slyman JF, Kline LB. Dorsal midbrain syndrome in multiple sclerosis. *Neurology*. 1981;31:196–198.
87. Lee SU, Kim HJ, Choi JH, et al. Comparison of ocular motor findings between neuromyelitis optica spectrum disorder and multiple sclerosis involving the brainstem and cerebellum. *Cerebellum*. 2019;18:511–518.
88. Oliva A, Rosenberg ML. Convergence-evoked nystagmus. *Neurology*. 1990;40:161–162.
89. Gstoettner W, Swoboda H, Müller C, et al. Preclinical detection of initial vestibulocochlear abnormalities in a patient with multiple sclerosis. *Eur Arch Otorhinolaryngol*. 1993;250:40–43.
90. Ikeda KM, Lee DH, Fraser JA, et al. Plasma exchange in a patient with tumefactive, corticosteroid-resistant multiple sclerosis. *Int J MS Care*. 2015;17:231–235.
91. Iyer PM, Fagan AJ, Meaney JF, et al. Horizontal nystagmus and multiple sclerosis using 3-Tesla magnetic resonance imaging. *Irish J Med Sci*. 2016;185:881–886.
92. Kim JA, Jeong IH, Lim YM, et al. Primary position upbeat nystagmus during an acute attack of multiple sclerosis. *J Clin Neurol*. 2014;10:37.
93. Nakamagoe K, Tozaka N, Nohara S, et al. Upbeat nystagmus is a useful sign in the regional diagnosis of trigeminal nerve disorder with multiple sclerosis. *Mult Scler Relat Disord*. 2018;19:59–61.
94. Kim HA, Yi HA, Lee H. Can upbeat nystagmus increase in downward, but not upward, gaze? *J Clin Neurosci*. 2012;19:600–601.
95. Adamec I, Gabelić T, Krbot M, et al. Primary position upbeat nystagmus. *J Clin Neurosci*. 2012;19:161–162.
96. Masucci EF, Kurtzke JF. Downbeat nystagmus secondary to multiple sclerosis. *Ann Ophthalmol*. 1988;20:347–348.
97. Lemos J, Pereira D, Amorim M, et al. Downbeat nystagmus elicited by eyelid closure. *J Neuroophthalmol*. 2014;34:350–353.
98. Baloh RW, Spooner JW. Downbeat nystagmus: A type of central vestibular nystagmus. *Neurology*. 1981;31:304.
99. Rosenhall U. Positional nystagmus. *Acta Otolaryngol Suppl*. 1988;455:17–20.
100. Thomsen J, Zilstorff K, Johnsen NJ. Positional Nystagmus of the Persistent Type. *ORL*. 1978;40:86–91.
101. Katsarkas A. Positional nystagmus of the “central type” as an early sign of multiple sclerosis. *J Otolaryngol*. 1982;11:91–93.
102. Samkoff LM, Smith CR. See-saw nystagmus in a patient with clinically definite MS. *Eur Neurol*. 1994;34:228–229.
103. Sandramouli S, Benamer HT, Mantle M, et al. See-saw nystagmus as the presenting sign in multiple sclerosis. *J Neuroophthalmol*. 2005;25:56–57.
104. Lee AG, Brazis PW. Localizing forms of nystagmus: symptoms, diagnosis, and treatment. *Curr Neurol Neurosci Rep*. 2006;6:414–420.
105. Gresty MA, Findley LJ, Wade P. Mechanism of rotatory eye movements in opsoclonus. *Br J Ophthalmol*. 1980;64:923–925.
106. Conger D, Beh SC. Seeing function in structure: “incidental” eye findings on OCT in a patient with multiple sclerosis. *Mult Scler Relat Disord*. 2019;31:72–73.
107. Keane JR. Periodic alternating nystagmus with downward beating nystagmus. *Arch Neurol*. 1974;30:399.
108. Mallery RM, Poolman P, Thurtell MJ, et al. Visual fixation instability in multiple sclerosis measured using SLO-OCT. *Invest Ophthalmol Vis Sci*. 2018;59:196–201.
109. Feys P, Helsen W, Nuttin B, et al. Unsteady gaze fixation enhances the severity of MS intention tremor. *Neurology*. 2008;70:106–113.
110. La Morgia C, Carelli V, Carbonelli M. Melanopsin retinal ganglion cells and pupil: clinical implications for neuro-ophthalmology. *Front Neurol*. 2018;9:1047.
111. Hamilton W, Drewry RD. Edge-light pupil cycle time and optic nerve disease. *Ann Ophthalmol*. 1983;15:714–721.
112. Karahan E, Karti O, Koskderelioglu A, et al. Pupil cycle time: as indicator of visual pathway dysfunction in multiple sclerosis. *Acta Neurol Belg*. 2017;117:75–81.
113. Moro SI, Rodriguez-Carmona ML, Frost EC, et al. Recovery of vision and pupil responses in optic neuritis



- and multiple sclerosis. *Ophthalmic Physiol Opt.* 2007;27:451–460.
114. Ali E, Maddess T, James A, et al. Pupillary response to sparse multifocal stimuli in multiple sclerosis patients. *Mult Scler J.* 2014;20:854–861
  115. Hawkes CH, Stow B. Pupil size and the pattern evoked visual response. *J Neurol Neurosurg Psychiatry.* 1981;44:90–91.
  116. Manor RS, Yassur Y, Ben-Sira I. Pupil cycle time in non-compressive optic neuropathy. *Ann Ophthalmol.* 1982;14:546–550.
  117. Braverman RS, Enzenauer RW. Incidental detection of bilateral corectopia by photo screening leads to the diagnosis of multiple sclerosis. A case report. *Binocul Vis Strabismus Q.* 2010;25:37–39.
  118. Pozzessere G, Rossi P, Valle E, et al. Autonomic involvement in multiple sclerosis: a pupillometric study. *Clin Auton Res.* 1997;7:315–319.
  119. Ogden NA, Raymond JE, Seland TP. Visual accommodation and sustained visual resolution in multiple sclerosis. *Invest Ophthalmol Vis Sci.* 1992;33:2744–2753.
  120. de Rodez Benavent SA, Nygaard GO, Harbo HF, et al. Fatigue and cognition: pupillary responses to problem-solving in early multiple sclerosis patients. *Brain Behav.* 2017;7:e00717.
  121. Cox TA. Relative afferent pupillary defects in multiple sclerosis. *Can J Ophthalmol.* 1989;24:207–210.
  122. DeRosa L. Two cases of the diagnosis of optic neuritis leading to the diagnosis of multiple sclerosis. *J Am Optom Assoc.* 1985;56:120–122.
  123. Fischer LG. The ocular manifestations of multiple sclerosis. *J Am Optom Assoc.* 1977;48:1511–1515.
  124. Giroud M, Semama D, Pradeaux L, et al. Hemiballismus revealing multiple sclerosis in an infant. *Childs Nerv Syst.* 1990;6:236–238.
  125. Dacso CC, Bortz DL. Significance of the Argyll Robertson pupil in clinical medicine. *Am J Med.* 1989;86:199–202.
  126. Bhatti MT, Schmalfuss IM, Williams LS, et al. Peripheral third cranial nerve enhancement in multiple sclerosis. *AJNR Am J Neuroradiol.* 2003;24:1390–1395.
  127. Newman NJ, Lessell S. Isolated pupil-sparing third-nerve palsy as the presenting sign of multiple sclerosis. *Arch Neurol.* 1990;47:817–818.
  128. Searle A, Rowe FJ. Vergence neural pathways: a systematic narrative literature review. *Neuro-ophthalmology.* 2016;40:209–218.
  129. Bronstein AM, Rudge P, Gresty MA, et al. Abnormalities of horizontal gaze. Clinical, oculographic and magnetic resonance imaging findings. II. Gaze palsy and internuclear ophthalmoplegia. *J Neurol Neurosurg Psychiatry.* 1990;53:200–207.
  130. Shabbir S, O Gl T, Robbins M. Convergence spasm in Wernicke's encephalopathy. *Neurohospitalist.* 2018;8:NP1–NP2.
  131. Tüzün E, Akman-Demir G, Eraksoy M. Paroxysmal attacks in multiple sclerosis. *Brain.* 1975;98:189–202.
  132. Goldstein JH, Schneekloth BB. Spasm of the near reflex: a spectrum of anomalies. *Surv Ophthalmol.* 1996;40:269–278.
  133. Matthews WB. Paroxysmal symptoms in multiple sclerosis. *Neurosurg Psychiatry.* 1975;38:617–623.
  134. Anlıaçık S, Uca AU, Kozak HH, et al. A very rare paroxysmal symptom in multiple sclerosis: convergence spasm. *Am J Emerg Med.* 2016;34:117.e5–117.e6.
  135. Postert T, McMonagle U, Büttner T, et al. Paroxysmal convergence spasm in multiple sclerosis. *Acta Neurol Scand.* 1996;94:35–37.
  136. Ghosh A, Padhy SK, Gupta G, et al. Functional convergence spasm. *Indian J Psychol Med.* 2014;36:332–334.
  137. Sitole S, Jay WM. Spasm of the near reflex in a patient with multiple sclerosis. *Semin Ophthalmol.* 2007;22:29–31.
  138. Kirkham TH, Bird AC, Sanders MD. Divergence paralysis with raised intracranial pressure. An electro-oculographic study. *Br J Ophthalmol.* 1972;56:776–782.
  139. Li YP, Zhang W. Advances in research of divergence insufficiency. *Zhonghua Yan Ke Za Zhi.* 2017;53:552–556.
  140. Lepore FE. Divergence paresis: a nonlocalizing cause of diplopia. *J Neuroophthalmol.* 1999;19:242–245.
  141. Jacobson DM. Divergence insufficiency revisited: natural history of idiopathic cases and neurologic associations. *Arch Ophthalmol.* 2000;118:1237–1241.
  142. Tamler E, Jampolsky A. Is divergence active? An electromyographic study. *Am J Ophthalmol.* 1967;63:452–459.
  143. Reche Sainz JA, Espinet Badia R, Puig Ganau T. Divergence insufficiency and demyelinating disorder. *Eur J Ophthalmol.* 2002;12:238–240.
  144. Küçük B, Hamamcı M, Aslan Bayhan S, Ali Bayhan H, Ertuğrul İnan L. Amplitude of accommodation in patients with multiple sclerosis. *Curr Eye Res.* 2019;44:1271–1277.
  145. Cumming BG, Deangelis GC. The physiology of stereopsis. *Annu Rev Neurosci.* 2001;24:203–238.
  146. Reis A, Mateus C, Macário MC, et al. Independent patterns of damage to retinocortical pathways in multiple sclerosis without a previous episode of optic neuritis. *J Neurol.* 2011;258:1695–1704.
  147. Sobaci G, Demirkaya S, Gundogan FC, Mutlu FM. Stereoacuity testing discloses abnormalities in multiple sclerosis without optic neuritis. *J Neuroophthalmol.* 2009;29:197–202.
  148. Heravian J, Moghaddam AAS, Najjaran M, et al. Visual evoked potentials, short wave-length automated perimetry, standard automated perimetry, contrast sensitivity and stereoacuity testing in visually asymptomatic eyes of patients with multiple sclerosis. *Iran J Ophthalmol.* 2013;25:45–52.
  149. Saxena R, Bandyopadhyay G, Singh D, et al. Evaluation of changes in retinal nerve fiber layer thickness and visual functions in cases of optic neuritis and multiple sclerosis. *Indian J Ophthalmol.* 2013;61:562–566.



# Clinical Accuracy of an Advanced Corneal Topographer with Tear-Film Analysis in Functional and Structural Evaluation of Dry Eye Disease

Jihei Sara Lee, Ikhyun Jun, Eung Kweon Kim, Kyoung Yul Seo & Tae-Im Kim

To cite this article: Jihei Sara Lee, Ikhyun Jun, Eung Kweon Kim, Kyoung Yul Seo & Tae-Im Kim (2020): Clinical Accuracy of an Advanced Corneal Topographer with Tear-Film Analysis in Functional and Structural Evaluation of Dry Eye Disease, *Seminars in Ophthalmology*, DOI: [10.1080/08820538.2020.1755321](https://doi.org/10.1080/08820538.2020.1755321)

To link to this article: <https://doi.org/10.1080/08820538.2020.1755321>



Published online: 18 Apr 2020.



Submit your article to this journal [↗](#)



View related articles [↗](#)



View Crossmark data [↗](#)



# Clinical Accuracy of an Advanced Corneal Topographer with Tear-Film Analysis in Functional and Structural Evaluation of Dry Eye Disease

Jihei Sara Lee<sup>1</sup>, Ikhyun Jun<sup>1,2</sup>, Eung Kweon Kim<sup>1,2</sup>, Kyoung Yul Seo<sup>1</sup>, and Tae-Im Kim<sup>1,2</sup>

<sup>1</sup>The Institute of Vision Research, Department of Ophthalmology, Yonsei University College of Medicine, Seoul, South Korea and <sup>2</sup>Corneal Dystrophy Research Institute, Department of Ophthalmology, Yonsei University College of Medicine, Seoul, South Korea

## ABSTRACT

**Purpose:** Dry eye disease (DED) is a common condition that significantly lowers the quality of life. As the disease grows more prevalent, multiple commercial instruments have been developed to measure the ocular surface of dry eyes, but no single device has yet been successful in comprehensive measurements. The current study aimed to investigate the clinical accuracy and utility of the Antares topographer in the diagnosis of DED.

**Methods:** Thirty-three consecutive patients underwent analyses of their non-invasive first tear-film break-up time (NIF-BUT), tear meniscus height (TMH) and meibography with the Antares topographer. The meibography with the LipiView scan was conducted. Slit-lamp examinations were done for assessments of meibomian glands (MG) and fluorescein tear-film break-up time (FBUT). Schirmer 1 test was done. The Ocular Surface Disease Index (OSDI) scores were graded.

**Results:** Thirty-three eyes of 33 patients (mean age  $61.5 \pm 10.6$  years, range 37.5–76.4 years, 27.3% males) completed the study. According to the Antares measurements, the NIF-BUT of the patient population was  $5.0 \pm 3.4$  seconds on average (1.1–15.0 seconds), and the TMH was  $0.2 \pm 0.1$  mm at center (0.1–0.5 mm). The average OSDI score was  $22.4 \pm 16.6$  points (0.0–79.5 points). When correlations were calculated, significant correlations were found between the NIF-BUT from the Antares topographer and FBUT ( $r = 0.538$ ,  $P = .001$ ), and between MG dropout from the Antares topographer and that from the LipiView interferometer ( $r = 0.446$ ,  $P = .009$ ). Antares NIF BUT and FBUT were in agreement with one another (95% limits of agreement (LOA)  $-5.04 \pm 6.37$ ,  $P = .198$ ) as were the infrared images from the Antares topographer and those from the LipiView interferometer (95% LOA  $-0.25 \pm 0.35$ ,  $P = .073$ ).

**Conclusion:** The Antares topographer is useful in the diagnosis of DED. Among its outputs, the NIF-BUT and MG dropout most closely correlated with currently accepted modes of diagnosis. However, concurrent clinical examinations are recommended for clinical follow-up.

**Keywords:** Antares topographer, dry eye, meibomian gland dysfunction, tear break-up time

## INTRODUCTION

In 2017, the Tear Film and Ocular Surface Dry Eye Workshop has defined the dry eye disease (DED) as “a multifactorial disease of the ocular surface characterized by a loss of homeostasis of the tear film, and accompanied by ocular symptoms.”<sup>1</sup> As evident in the convoluted definition, the disease is complex and remains incompletely understood. So far, an increase

in tear osmolarity and subsequent instability in the tear film have been touted as the key concept in the pathogenesis.<sup>2</sup> The meibomian gland dysfunction has also gained significant attention as a major cause of tear deficiency and evaporative dry eyes.<sup>2–4</sup> Until now, slit-lamp examinations as well as clinical tests like Schirmer tests were employed, and they have somewhat allowed the evaluation of the disease in various aspects. The imaging of meibomian glands

Received 6 February 2020; accepted 9 April 2020; published online 16 April 2020.

Correspondence: Tae-im Kim, Department of Ophthalmology, Yonsei University College of Medicine, 50-1 Yonsei-ro, Seodaemun-gu, Seoul 03722. Email: [taeimkim@gmail.com](mailto:taeimkim@gmail.com)

has evolved from the transillumination on an everted eyelid by Tapie in 1977 to infrared photography and enabled easy visualization.<sup>5</sup> However, demands for devices that combine multiple modalities to parallel expanding knowledge about the disease remain high. Numerous analytical tools for DED have emerged in response; yet no single diagnostic device has assumed the role of gold standard mode of diagnosis.

The Antares topographer (Lumenis, Australia), the topic of our present study, is one of the latest efforts to qualify as well quantify the ocular surface of DED. It is a part of a growing list of DED diagnostic apparatuses that include Keratograph 5 M and LipiView interferometer. Like many of its predecessors, it generates outputs on tear meniscus height (TMH), tear-film break-up time (BUT) and infrared images of the meibomian glands (MG). Before its clinical applications, however, vigorous testing of its accuracy is in order. Therefore, in this study, we examined the clinical accuracy of the outputs provided by the Antares topographer and identified whether the results have correlations with currently accepted modes of diagnosis in the DED.

## MATERIALS AND METHODS

### Subjects

The study protocol was approved by the Institutional Review Board of Yonsei University College of Medicine (1-2019-0072). The procedures followed the tenets of the Declaration of Helsinki, and all patients provided written informed consent. A total of 33 consecutive patients who visited our clinic in December 2018 were prospectively recruited for enrollment in the study. Patients were recruited regardless of the diagnosis of dry eye disease or their symptoms. Patients over the age of 20 were considered eligible for inclusion. Those meeting any of the following criteria were excluded: (1) presence of any severe ocular surface disease and/or corneal epithelial pathology, (2) previous ocular trauma or surgery other than uncomplicated cataract extraction, (3) ocular comorbidities such as glaucoma and uveitis, (4) disease of the eyelid that led to unacceptable discomfort during eyelid eversion, and (5) any ocular surgery within 1 year of study. All subjects underwent examinations in the order of invasiveness to minimize the effect of the previous test on the next: first the Antares topographer, then the LipiView interferometer, followed by slit-lamp examinations and finally OSDI questionnaires.

### Antares Corneal Topographer

The Antares topographer (Lumenis, Australia) is a non-contact Placido ring-based corneal topographer. It is also equipped with an infrared (IR) illumination

system for imaging of meibomian glands. The device has also incorporated fluoroscopy to measure non-invasive first BUT (NIF BUT). It provides TMH along the lower lid margin at three different locations. A patient was seated in front of the device and asked to focus on the central target while information on TMH and NIF BUT was obtained. In order to visualize the lower palpebral conjunctiva, the lower lid was everted and held in place by a cotton-tip applicator by an investigator, and IR option was chosen for meibography. While exams with the Antares topographer were conducted for both eyes for each individual, the eye to be included in the analysis was chosen at random.

### Infrared Meibography

Meibography was performed with the LipiView II Ocular Surface Interferometer (Tear-Science, Morrisville, NY, USA) following the standard operating procedure for the device. The Lid Everter was positioned on the lower eyelid, and the palpebral conjunctiva was exposed by everting the lower lid and holding in place with a cotton-tip applicator as much as possible. The best Dynamic Illumination photograph for each eye was chosen for analysis.

### Clinical Parameters

All subjects underwent slit-lamp biomicroscopy examinations as well as clinical tests that included fluorescein tear break-up time (FBUT) and Schirmer 1 test. The subjects were instructed to not use any eyedrops for 2 hours before examinations. For FBUT measurement, a single fluorescein strip (Haag-Streit, Koeniz, Switzerland) was applied over the inferior meniscus. In order to control for possible variations in fluorescein volume and concentration, the average value of 3 repeated tests was taken as the final measurement. The Schirmer test was conducted using a standard paper strip (Eagle Vision, Memphis, TN, USA). The strips were placed without topical anesthesia and left for 5 minutes before the final reading. Lid margin abnormalities were assessed with slit-lamp biomicroscopy. The following four factors were used to grade abnormalities: vascular engorgement, plugged meibomian gland orifice, displacement of the mucocutaneous junction and irregularity of the lid margin.<sup>6-8</sup> Based on the presence of any of the four factors, abnormalities were graded from 0 to 4. The meibum quality was assessed based on the secretion from the eight glands in the center of the lower lid and graded out of 24 points.<sup>6,7</sup> The expressibility of meibum was graded semi-quantitatively also by assessing the secretion after applying firm digital pressure onto the five lower lid glands.<sup>6,9</sup> The protocol is defined in detail elsewhere.<sup>10</sup>

The slit-lamp examinations were conducted by a single clinician (I.J) for consistency. During the same visit, the subjects were asked to fill out the Ocular Surface Disease Index (OSDI) questionnaire. The questions were taken from the set developed by the Outcomes Research Group at Allergan (Irvine, CA, USA).

## Image Analysis

A single-masked observer analyzed the infrared images of the MG from the Antares topographer and the LipiView interferometer in a darkened room using ImageJ (<http://imagej.nih.gov/ij/>, National Institutes of Health, Bethesda, MD, USA). Using a technique initially described by Pult et al.,<sup>11</sup> the free-hand tool was used to trace the non-glandular areas. The non-glandular area was divided by the total exposed area of the lower palpebral conjunctiva to obtain the percentage of MG dropout.

## Statistical Analyses

All continuous data are expressed as mean  $\pm$  standard deviation while categorical data were presented as the number and percentage of the total population. The degree of correlations was calculated with Pearson's correlation coefficients as appropriate, and scatterplot graphs were drawn. Statistical analyses were performed using SPSS statistics software (version 23; IBM Corporation, Armonk, NY). In order to confirm interchangeability between Antares and other diagnostic tests, Bland-Altman plots were produced with MedCalc (version 19.1.6; MedCalc Software Ltd, Ostend, Belgium). A  $p$ -value  $<0.05$  was considered statistically significant.

## RESULTS

### Patient Population

A total of 33 patients were included in the study. Table 1 illustrates the baseline characteristics of the patient population. They were  $61.5 \pm 10.6$  years old on average, ranging from 37.5 to 76.4 years old. Nine of the patients (27.3%) were males. Seventeen left eyes and 16 right eyes were included in the study.

### Use of the Antares Topographer in Diagnosis

The Antares topographer was utilized to evaluate the tear film in multiple aspects. The results are illustrated in detail in Table 2. The NIF BUT was evaluated by detecting changes in the edges of mires illuminated onto the

TABLE 1. Summary of clinical findings.

Parameters	Median	Mean $\pm$ SD (Range)
Age (years)	63.3	61.5 $\pm$ 10.6 (37.5–76.4)
Sex		
Male		9 (27.3%)
Female		24 (72.7%)
Eyes		
Right		16 (48.5%)
Left		17 (51.5%)
Schirmer 1 test (mm)	10.0	13.5 $\pm$ 9.7 (2.0–35.0)
Fluorescein break-up time (sec)	4.0	4.3 $\pm$ 2.1 (0.0–13.0)
Lid margin abnormality	2.0	2.2 $\pm$ 1.1 (0.0–4.0)
Meiboscore		
Quality	12.0	12.5 $\pm$ 4.4 (6.0–24.0)
Expressibility	2.0	2.0 $\pm$ 0.9 (1.0–3.0)
Digital pressure	2.0	1.9 $\pm$ 1.0 (0.0–3.0)
OSDI score	20.5	22.4 $\pm$ 16.6 (0.0–79.5)
Meibomian gland dropout (%)	13.0	16.1 $\pm$ 11.8 (2.5–59.2)

SD, standard deviation; OSDI, ocular surface disease index.

TABLE 2. Summary of Antares topographer measurements.

Parameters	Median	Mean $\pm$ SD (Range)
<b>NIF BUT (sec)</b>	4.2	5.0 $\pm$ 3.4 (1.1–15.0)
<b>Tear meniscus height (mm)</b>		
Center	0.2	0.2 $\pm$ 0.1 (0.1–0.5)
Nasal	0.2	0.3 $\pm$ 0.1 (0.1–0.5)
Temporal	0.2	0.2 $\pm$ 0.1 (0.1–0.5)
Average	0.2	0.2 $\pm$ 0.1 (0.1–0.5)
SD	0.0	0.0 $\pm$ 0.0 (0.0–0.1)
<b>Meibomian gland dropout (%)</b>	16.0	21.4 $\pm$ 16.3 (1.5–69.1)

SD, standard deviation; NIF BUT, non-invasive first break-up time.

corneal surface. The break-up time was  $5.0 \pm 3.4$  seconds (1.1–15.0 seconds). There were generally no noticeable differences in the heights of tear lake at different locations. Except for the nasal part of the eyes, where the height was slightly higher at  $0.3 \pm 0.1$  mm (0.1–0.5 mm), the TMH at center and temporal parts of the eyes were  $0.2 \pm 0.1$  mm (0.1–0.5 mm for both center and temporal parts). The meibomian glands were visualized again with the topographer using an infrared system. The dropout was  $21.4 \pm 16.3\%$ ; the dropout calculated from the Antares images ranged from 1.5% to 69.1%.

### Clinical Evaluation of Dry Eyes

The structural as well as functional aspects of the DED were evaluated (Table 1). When meibomian glands were visualized with a non-contact infrared meibography, LipiView interferometer, the MG dropout for the patient population was on average  $16.1 \pm 11.8\%$ . The dropout measured with LipiView interferometer was as low as 2.5% and as high as 59.2% in our study population. The mean FBUT was



4.3 ± 2.1 seconds (0.0–13.0 seconds). Schirmer 1 test showed 13.5 ± 9.7 mm on average. The results ranged from 2.0 mm to 35.0 mm. When lid margin abnormality was examined and graded, the average score was 2.2 ± 1.1 points for the patient population (0.0–4.0 points). The meibomian gland function was evaluated through meibum quality, expressibility and digital pressure. The quality was 12.5 ± 4.4 points (6.0–24.0 points); the expressibility was 2.0 ± 0.9 points (1.0–3.0 points); and the digital pressure was 1.9 ± 1.0 points (0.0–3.0 points). The OSDI score was 22.4 ± 16.6 points. The score ranged from 0 to 79.5.

### Correlations between Parameters

The correlations between clinical measurements and outputs of the Antares topographer were analyzed (Table 3). The correlation between FBUT and NIF BUT from the Antares topographer reached a statistical significance (Pearson  $r = 0.538$ ,  $P = .001$ ; Figure 1a). The MG dropout calculated from the infrared images provided by the Antares topographer also significantly correlated

with that from the LipiView interferometer (Pearson  $r = 0.446$ ,  $P = .009$ ; Figure 1b). When the differences of the two techniques were plotted against the averages (Figure 2), the Antares NIF BUT and FBUT were in agreement with one another (95% limits of agreement (LOA)  $-5.04 \pm 6.37$ ,  $P = .198$ ; Figure 2a). The Bland-Altman plot also indicated that the infrared images from the Antares topographer may be used interchangeably with those from the LipiView interferometer for the approximation of gland dropout (95% LOA  $-0.25 \pm 0.35$ ,  $P = .073$ ; Figure 2b). No significant correlations were found for Antares NIF BUT, TMH, MG dropout against clinical measurements such as Schirmer test score, lid margin abnormality, meibum quality and OSDI score.

### DISCUSSION

The current study investigated the clinical accuracy and utility of the Antares topographer in quantification and diagnosis of the DED. The results of our analyses showed that the Antares topographer gave

TABLE 3. Correlations of Antares parameters to clinical measurements.

Antares measurements	Meibomian gland							
	TBUT	Schirmer	Lid margin abnormality	Quality	Expressibility	Digital pressure	OSDI	LipiView MG dropout
NIF BUT	$r = 0.538$ $p = .001$	$r = 0.204$ $p = .254$	$r = -0.050$ $p = .781$	$r = 0.108$ $p = .548$	$r = 0.159$ $p = .385$	$r = -0.068$ $p = .711$	$r = -0.305$ $p = .085$	$r = 0.020$ $p = .912$
Tear meniscus height	$r = -0.219$ $p = .207$	$r = -0.145$ $p = .406$	$r = 0.143$ $p = .412$	$r = 0.298$ $p = .082$	$r = 0.052$ $p = .772$	$r = 0.113$ $p = .523$	$r = 0.050$ $p = .776$	$r = -0.040$ $p = .821$
MG dropout	$r = 0.084$ $p = .637$	$r = 0.110$ $p = .536$	$r = 0.220$ $p = .211$	$r = 0.208$ $p = .237$	$r = 0.043$ $p = .813$	$r = 0.077$ $p = .670$	$r = 0.101$ $p = .569$	$r = 0.446$ $p = .009$

TBUT, tear break-up time; OSDI, ocular surface disease index; MG, meibomian gland; NIF BUT, non-invasive first break-up time.  $r$  = Pearson's correlation coefficient

A  $p$ -value <0.05 was considered statistically significant.

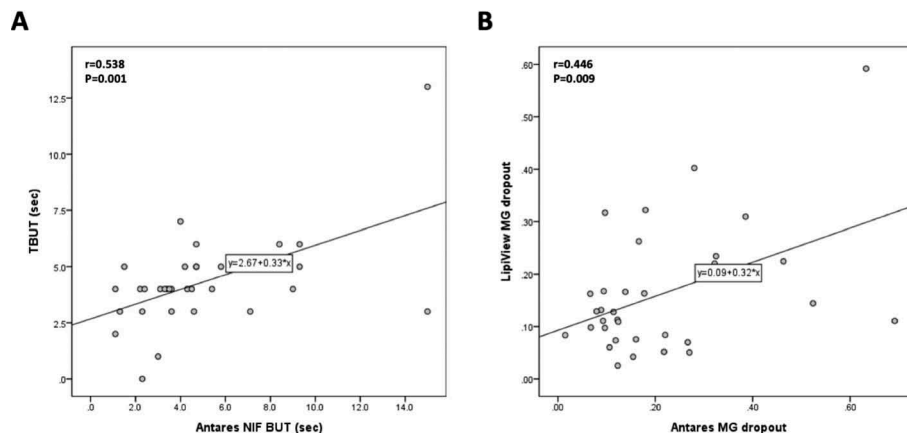


FIGURE 1. Scatterplots of BUT and MG dropout. A scatterplot between the NIF BUT obtained with the Antares topographer and FBUT (a). A scatterplot of the percentage dropout detected with Image J from infrared images of the Antares topographer and LipiView interferometer (b). Solid black lines indicate the regression. A  $p$ -value <0.05 was considered statistically significant.

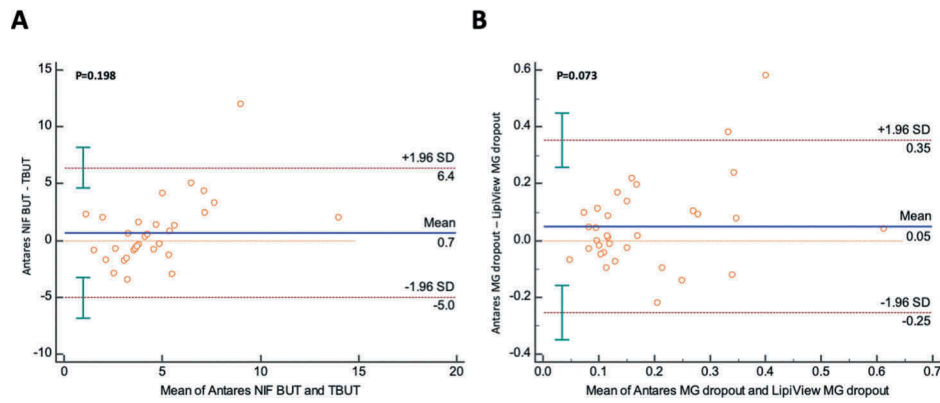


FIGURE 2. Bland-Altman plots of BUT and MG dropout. The Bland-Altman plots calculated interchangeability between the NIF BUT from the Antares topographer and clinically acquired FBUT (a), and between the percentage area of dropout from the infrared images of the Antares topographer and LipiView interferometer (b).

a consistent output of NIF BUT, TMH and meibomian gland imaging. Based on the correlation analyses, we found that the NIF BUT and percentage area of gland dropout obtained by the Antares topographer also had statistically significant correlations with FBUT and dropout calculated from the images of the LipiView interferometer, respectively.

The results of our current study demonstrated that the NIF BUT obtained with the new corneal topographer was positively correlated with BUT obtained with fluorescein, where the correlation coefficient was 0.538 ( $P = .001$ ). The results of the Bland-Altman plot also confirmed the clinical applicability of NIF BUT of the Antares topographer in place of the FBUT. While the NIF BUT did show correlations with FBUT in our study, the correlation between NIF BUT and OSDI scores did not reach a statistical significance. Studies on the association between BUT and dry eye symptoms have put forth different results. Similar to our own, some studies have also shed light on the lack of association between BUT and dry eye symptoms. Abdelfattah et al. have previously demonstrated that NIF BUT obtained with Oculus Keratograph 5 M did not differ significantly between the ocular surface disease group and the control.<sup>12</sup> Other studies on similar commercial devices, however, have found correlations between the NIF BUT with dry eye symptoms.<sup>13</sup> For instance, Fuller et al. have demonstrated that the NIF-BUT values obtained with Keratograph 4 were negatively correlated with the OSDI scores.<sup>14</sup> Although its role in predicting dry eye symptoms requires further studies, the detection of BUT by non-invasive means such as the Antares topographer nonetheless offers several advantages over BUT measured with fluorescein. Not only does it circumvent invasive clinical tests, the assessment of the corneal surface by illuminating mires allows the assessment of the entire cornea.<sup>15,16</sup> The lack of variability in the concentration and amount of the dye installed in the fornix improves the accuracy and

repeatability of the result.<sup>17</sup> The measurement by non-invasive means also provides results unaffected by reflex tearing. Based on our study, the Antares topographer can be used for reliable measurements of tear-film break-up time in a clinical setting.

In the present study, the infrared images from the Antares topographer were compared against the LipiView scans, and the dropout of MG, defined as the ratio of the gland loss area to the total palpebral conjunctival area, was found to be significantly correlated ( $r = 0.446$ ,  $P = .009$ ) with one another. In contrast to previous reports that showed correlations with the symptom scores and meibum quality,<sup>11,18</sup> however, the dropout calculated from images of the Antares topographer did not present any correlations with clinical parameters in our study. The insignificant results from correlation analyses may be explained partly by poorly standardized clinical techniques in assessing the gland function. For example, the force with which digital pressure should be applied and subjective assessment of secreted meibum may not have been consistent.<sup>18,19</sup> Many investigators also have argued for modification of the definition of the dropout itself, such as counting the number of partial glands or limiting the scope to the central lid, in order to account for some of the conjunctival areas that may have never had any glands at all.<sup>5,20,21</sup> In addition, the differences in the quality of the obtained images may have affected dropout calculations. The poorer contrast, lighter background and greater reflections of the Antares images did make evaluations more difficult. In fact, starker contrasts and clearer distinction of gland margins of the LipiView scans have been pointed out by other studies in the past.<sup>5</sup> Despite the superiority of LipiView in image quality, however, this study, too, was unsuccessful in establishing correlations between the percentage dropout and clinical signs such as erythema and meibum secretion. The repeated failure of correlations by multiple studies, including our own, suggests that ocular surface

factors other than impaired gland function exist in generating symptoms of DED. As the assessment of the glands has so far been limited to two-dimensional imaging, modalities that better reflect their function and explain symptoms need to be developed in the future for a comprehensive assessment of MG in the DED.

The Antares topographer was able to measure the TMH at three different locations along the lower lid margin. Increasingly, the measurements of tear meniscus are gaining attention in the study of DED. This is because studies over the years have shown that the TMH reflects the severity of DED.<sup>22–24</sup> In addition, the TMH is thought to reflect real-time changes of the ocular surface in response to different artificial tear drops.<sup>25</sup> Studies, especially those that assessed tear meniscus with optical coherence tomography, have shown that statistically significant correlations exist between tear meniscus height, volume and area with TBUT and Schirmer test.<sup>22,26</sup> In our study, we have attempted to find whether TMH obtained with the Antares topographer had any meaningful correlations with other clinical parameters, but with no success. There may be several possible explanations for the unforeseen results. First, the measurements of heights by taking images like the Antares topographer are affected by the time points at which images are taken in relation to blinking.<sup>27</sup> The relevant literature states that the height increases by approximately 10% immediately after blinking.<sup>28</sup> Second, the lid morphology such as the palpebral aperture, lid length and lid-parallel conjunctival folds (LIPCOF) may have affected tear distribution.<sup>29,30</sup> Third, Schirmer test has low reproducibility in part due to the invasive nature of the study that induces reflex tear secretion.<sup>31,32</sup> More importantly, the topographer must be applied to a greater number of patients to confirm the applicability of TMH measurements in DED diagnosis.

There are several limitations that should be considered in interpreting the results of our study. First, the relatively small number of patients included in the study may have affected the results. However, a retrospective calculation of the post-hoc power based on the assumption of a type I error equal to 0.05 revealed that the main outcome of the study – BUT and MGD – had sufficient powers. The required sample sizes for reliable outcomes were 22 and 34, respectively. Nonetheless, the results should be confirmed with a larger number of patients. The study subjects were also homogenous, consisting only of the Korean population. Second, the population was not classified according to the severity of dry eye disease and clinical parameters were not compared among different severity groups. Third, no other non-invasive BUT measurements were performed other than Antares topographer. Despite the limitations, we believe that our results

showed a clear correlation between clinical parameters of dry eyes and the outputs of the Antares topographer to validate its use in a clinical setting. In conclusion, the Antares topographer provided a reliable and comprehensive review of ocular parameters, including NIF BUT, TMH and infrared images of the meibomian glands. The NIF BUT and MG dropout showed significant correlations with FBUT and images of the LipiView interferometer. However, concurrent clinical examinations are recommended for thorough clinical assessments of dry eye disease.

## ACKNOWLEDGMENTS

We thank Lumenis (Australia) for providing the Antares corneal topographer.

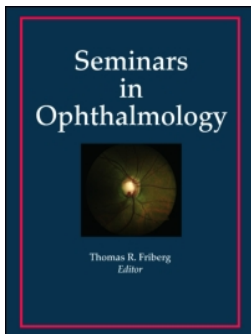
## FUNDING

The study was supported by the Basic Science Research Program through the National Research Foundation of Korea (NRF) funded by the Ministry of Education, Science and Technology [NRF-2019R1F1A1062468].

## REFERENCES

1. Craig JP, Nichols KK, Akpek EK, et al. TFOS DEWS II definition and classification report. *Ocul Surf.* 2017;15:276–283. doi:10.1016/j.jtos.2017.05.008.
2. Heidari M, Noorizadeh F, Wu K, Inomata T, Mashaghi A. Dry eye disease: emerging approaches to disease analysis and therapy. *J Clin Med.* 2019;8(9):1439. doi:10.3390/jcm8091439.
3. Craig JP, Tomlinson A. Importance of the lipid layer in human tear film stability and evaporation. *Optom Vis Sci.* 1997;74:8–13. doi:10.1097/00006324-199701000-00014.
4. Nelson JD, Shimazaki J, Benitez-del-Castillo JM, et al. The international workshop on meibomian gland dysfunction: report of the definition and classification subcommittee. *Invest Ophthalmol Vis Sci.* 2011;52:1930–1937. doi:10.1167/iovs.10-6997b.
5. Wong S, Srinivasan S, Murphy PJ, Jones L. Comparison of meibomian gland dropout using two infrared imaging devices. *Cont Lens Anterior Eye.* 2019;42:311–317. doi:10.1016/j.clae.2018.10.014.
6. Choi YJ, Park SY, Jun I, et al. Perioperative ocular parameters associated with persistent dry eye symptoms after cataract surgery. *Cornea.* 2018;37:734–739. doi:10.1097/ICO.0000000000001572.
7. Tomlinson A, Bron AJ, Korb DR, et al. The international workshop on meibomian gland dysfunction: report of the diagnosis subcommittee. *Invest Ophthalmol Vis Sci.* 2011;52:2006–2049. doi:10.1167/iovs.10-6997f.
8. Arita R, Itoh K, Inoue K, Kuchiba A, Yamaguchi T, Amano S. Contact lens wear is associated with decrease of meibomian glands. *Ophthalmology.* 2009;116:379–384. doi:10.1016/j.ophtha.2008.10.012.

9. Pflugfelder SC, Tseng SC, Sanabria O, et al. Evaluation of subjective assessments and objective diagnostic tests for diagnosing tear-film disorders known to cause ocular irritation. *Cornea*. 1998;17:38–56. doi:10.1097/00003226-199801000-00007.
10. Nichols KK, Foulks GN, Bron AJ, et al. The international workshop on meibomian gland dysfunction: executive summary. *Invest Ophthalmol Vis Sci*. 2011;52:1922–1929. doi:10.1167/iovs.10-6997a.
11. Pult H, Riede-Pult BH. Non-contact meibography: keep it simple but effective. *Cont Lens Anterior Eye*. 2012;35:77–80. doi:10.1016/j.clae.2011.08.003.
12. Abdelfattah NS, Dastiridou A, Satta SR, Lee OL. Noninvasive imaging of tear film dynamics in eyes with ocular surface disease. *Cornea*. 2015;34(Suppl 10):S48–52. doi:10.1097/ICO.0000000000000570.
13. Pult H, Purslow C, Murphy PJ. The relationship between clinical signs and dry eye symptoms. *Eye (Lond)*. 2011;25:502–510. doi:10.1038/eye.2010.228.
14. Fuller DG, Potts K, Kim J. Noninvasive tear breakup times and ocular surface disease. *Optom Vis Sci*. 2013;90:1086–1091. doi:10.1097/OPX.0000000000000023.
15. Goto T, Zheng X, Okamoto S, Ohashi Y. Tear film stability analysis system: introducing a new application for videokeratography. *Cornea*. 2004;23:S65–70. doi:10.1097/01.icc.0000136685.88489.70.
16. Hong J, Sun X, Wei A, et al. Assessment of tear film stability in dry eye with a newly developed keratograph. *Cornea*. 2013;32:716–721. doi:10.1097/ICO.0b013e3182714425.
17. Johnson ME, Murphy PJ. The effect of instilled fluorescein solution volume on the values and repeatability of TBUT measurements. *Cornea*. 2005;24:811–817. doi:10.1097/01.icc.0000154378.67495.40.
18. Srinivasan S, Menzies K, Sorbara L, Jones L. Infrared imaging of meibomian gland structure using a novel keratograph. *Optom Vis Sci*. 2012;89:788–794. doi:10.1097/OPX.0b013e318253de93.
19. Korb DR, Blackie CA. Meibomian gland diagnostic expressibility: correlation with dry eye symptoms and gland location. *Cornea*. 2008;27:1142–1147. doi:10.1097/ICO.0b013e3181814c4f.
20. Arita R, Minoura I, Morishige N, et al. Development of definitive and reliable grading scales for meibomian gland dysfunction. *Am J Ophthalmol*. 2016;169:125–137. doi:10.1016/j.ajo.2016.06.025.
21. Nichols JJ, Berntsen DA, Mitchell GL, Nichols KK. An assessment of grading scales for meibography images. *Cornea*. 2005;24(4):382–388. doi:10.1097/01.icc.0000148291.38076.59.
22. Cox SM, Nichols KK, Nichols JJ. Agreement between automated and traditional measures of tear film breakup. *Optom Vis Sci*. 2015;92:e257–263. doi:10.1097/OPX.0000000000000648.
23. Qiu X, Gong L, Lu Y, Jin H, Robitaille M. The diagnostic significance of Fourier-domain optical coherence tomography in Sjogren syndrome, aqueous tear deficiency and lipid tear deficiency patients. *Acta Ophthalmol*. 2012;90:e359–366. doi:10.1111/j.1755-3768.2012.02413.x.
24. Tung CI, Perin AF, Gumus K, Pflugfelder SC. Tear meniscus dimensions in tear dysfunction and their correlation with clinical parameters. *Am J Ophthalmol*. 2014;157:301–310 e301. doi:10.1016/j.ajo.2013.09.024.
25. Napoli PE, Satta GM, Coronella F, Fossarello M. Spectral-domain optical coherence tomography study on dynamic changes of human tears after instillation of artificial tears. *Invest Ophthalmol Vis Sci*. 2014;55:4533–4540. doi:10.1167/iovs.14-14666.
26. Akiyama R, Usui T, Yamagami S. Diagnosis of dry eye by tear meniscus measurements using anterior segment swept source optical coherence tomography. *Cornea*. 2015;34(Suppl 11):S115–120. doi:10.1097/ICO.0000000000000583.
27. Palakuru JR, Wang J, Aquavella JV. Effect of blinking on tear dynamics. *Invest Ophthalmol Vis Sci*. 2007;48:3032–3037. doi:10.1167/iovs.06-1507.
28. Savini G, Goto E, Carbonelli M, Barboni P, Huang D. Agreement between stratus and visante optical coherence tomography systems in tear meniscus measurements. *Cornea*. 2009;28:148–151. doi:10.1097/ICO.0b013e31818526d0.
29. Chan TC, Ye C, Ng PK, Li EY, Yuen HK, Jhanji V. Change in tear film lipid layer thickness, corneal thickness, volume and topography after superficial cauterization for conjunctivochalasis. *Sci Rep*. 2015;5:12239. doi:10.1038/srep12239.
30. Pult H, Riede-Pult BH. Impact of conjunctival folds on central tear meniscus height. *Invest Ophthalmol Vis Sci*. 2015;56:1459–1466. doi:10.1167/iovs.14-15908.
31. Chan TCY, Wan KH, Shih KC, Jhanji V. Advances in dry eye imaging: the present and beyond. *Br J Ophthalmol*. 2018;102:295–301. doi:10.1136/bjophthalmol-2017-310759.
32. Nichols KK, Mitchell GL, Zadnik K. The repeatability of clinical measurements of dry eye. *Cornea*. 2004;23:272–285. doi:10.1097/00003226-200404000-00010.



## Concentrations of Selected Cytokines and Vascular Endothelial Growth Factor in Aqueous Humor and Serum of Diabetic Patients

Katarina Cvitkovic, Antonio Sesar, Irena Sesar, Anita Pusic-Sesar, Renato Pejic, Tomislav Kelava, Alan Sucur & Ivan Cavar

To cite this article: Katarina Cvitkovic, Antonio Sesar, Irena Sesar, Anita Pusic-Sesar, Renato Pejic, Tomislav Kelava, Alan Sucur & Ivan Cavar (2020): Concentrations of Selected Cytokines and Vascular Endothelial Growth Factor in Aqueous Humor and Serum of Diabetic Patients, *Seminars in Ophthalmology*, DOI: [10.1080/08820538.2020.1755320](https://doi.org/10.1080/08820538.2020.1755320)

To link to this article: <https://doi.org/10.1080/08820538.2020.1755320>



Published online: 20 Apr 2020.



Submit your article to this journal [↗](#)



Article views: 4



View related articles [↗](#)



View Crossmark data [↗](#)





# Concentrations of Selected Cytokines and Vascular Endothelial Growth Factor in Aqueous Humor and Serum of Diabetic Patients

Katarina Cvitkovic<sup>1,2</sup>, Antonio Sesar<sup>2</sup>, Irena Sesar<sup>2</sup>, Anita Pusic-Sesar<sup>2</sup>, Renato Pejic<sup>2</sup>, Tomislav Kelava<sup>3</sup>, Alan Sucur<sup>3</sup>, and Ivan Cavar<sup>1,2</sup>

<sup>1</sup>Department of Immunology, School of Medicine, University of Mostar, Mostar, Bosnia and Herzegovina,

<sup>2</sup>Department of Ophthalmology, University Hospital Center, Mostar, Bosnia and Herzegovina, and

<sup>3</sup>Department of Physiology and Immunology, School of Medicine, University of Zagreb, Zagreb, Croatia

## ABSTRACT

**Purpose:** To investigate the aqueous humor and serum levels of selected cytokines and vascular endothelial growth factor (VEGF) in diabetic patients, implicating their role in the pathogenesis of diabetic eye complications.

**Materials and methods:** A total of 65 patients (27 males and 38 females) who underwent cataract surgery were recruited into the study. The study group consisted of 30 cataract patients with type 2 diabetes mellitus, and this group was divided into two subgroups: 14 patients with diabetic retinopathy (DR group) and 16 patients without DR (NDR group). The control group consisted of 35 non-diabetic cataract subjects.

**Results:** Patients in the DR group had significantly higher aqueous humor concentrations of interleukin (IL)-1 $\beta$ , IL-6, IL-8, IL-10, monocyte chemoattractant protein (MCP-1) and VEGF. Likewise, serum concentrations of IL-1 $\beta$ , IL-6, IL-8, IL-12, TNF- $\alpha$  and IFN- $\gamma$  were significantly higher in the DR group as compared to the controls. Aqueous humor concentrations of IL-1 $\beta$ , IL-8, MCP-1 and VEGF were significantly higher in the DR group as compared with the NDR group.

**Conclusion:** Our findings support the hypothesis that chronic inflammation and a disturbance of the immune system play important roles in the pathogenesis of diabetic cataract and DR.

**Keywords:** cataract, diabetic retinopathy, cytokines, aqueous humor, serum

## INTRODUCTION

The prevalence of diabetes mellitus (DM) and its associated complications is increasing and has an alarming rate in both developed and developing countries. Cataract, diabetic retinopathy (DR) and diabetic macular edema (DME) are the most frequent diabetes-related eye complications and major causes of visual impairment.<sup>1</sup> According to recent reports, chronic inflammation is an important pathogenetic mechanism that contributes to the development and progression of DR.<sup>2</sup> Previous studies have shown that increased concentrations of inflammatory cytokines in diabetic eyes may lead to microvascular occlusion and breakdown of the blood-retinal barrier, followed by

vascular leakage, capillary nonperfusion and neovascularization.<sup>3,4</sup> Because of this, most published studies on cytokine profiles in the serum, aqueous humor (AH) and vitreous were performed in diabetic patients who had DR and DME.<sup>5–9</sup>

Cataract is among the earliest complications, and it occurs 2–5 times more frequently in patients with DM.<sup>10</sup> The pathogenesis of diabetic cataracts is still not fully understood. Several different pathogenetic mechanisms have been proposed, including increased osmotic stress caused by activation of the polyol pathway, non-enzymatic glycation of lens proteins and increased oxidative stress.<sup>11</sup> Higher concentrations of inflammatory cytokines, such as interleukin (IL)-1, IL-6, IL-8, IL-12, vascular endothelial growth factor (VEGF) and

monocyte chemotactic protein-1 (MCP-1) have been found in aqueous humor samples of patients with diabetic cataract.<sup>1,5–8</sup> In addition, higher concentrations of MCP-1, VEGF, IL-8 and tumor necrosis factor- $\alpha$  (TNF- $\alpha$ ) were detected in serum samples of cataract diabetic patients.<sup>1,12,13</sup> However, it is not fully elucidated whether high concentrations of inflammatory cytokines in diabetic eyes are the result of intraocular inflammation or infiltration through the disrupted blood-eye barrier. Despite these findings, there is a relatively small number of studies in which aqueous and serum levels of cytokines were measured in diabetic cataract patients with and without DR.

So, the aim of our study was to determine the concentrations of selected cytokines, such as IL-1 $\beta$ , IL-6, IL-8, IL-10, IL-12, MCP-1, TNF- $\alpha$  and interferon-gamma (IFN- $\gamma$ ), and VEGF in aqueous humor and serum of type 2 DM (T2DM) patients who underwent cataract surgery, implicating their role in the pathogenesis of diabetic eye complications.

## MATERIALS AND METHODS

### Subjects

A total of 65 cataract patients (27 males and 38 females) who underwent cataract surgery (phacoemulsification) from March 2018 to March 2019 at the Eye Clinic of the University Hospital Center Mostar were recruited into the study. The study group consisted of 30 cataract patients with T2DM, and this group was divided into two subgroups: 14 patients with DR (DR group) and 16 patients without DR (NDR group). The control group consisted of 35 non-diabetic cataract subjects who were matched with diabetic patients according to sex and age ( $\pm 2$  years). Participants with glaucoma, history of ocular inflammation or ocular surgery, and any other retinal or optic nerve pathology other than DR and systemic inflammatory diseases were excluded from the study. Other ocular exclusion criteria for diabetic patients were previous steroid or anti-VEGF injections and argon laser photocoagulation in the last 6 months. The study was approved by the Ethics Committee of University Hospital Center Mostar and was performed in accordance with the Declaration of Helsinki. Written informed consent was obtained from all patients prior to their participation in the study.

### Procedures

Before cataract surgery, all participants underwent complete ophthalmological examination, including assessment of best-corrected visual acuity using a logarithm of the mild angle of resolution (LogMAR) charts, measuring of intraocular pressure (IOP) using

a Goldmann applanation tonometer, slit-lamp biomicroscopic examination of the anterior eye segment, fundus examination in mydriasis and central foveal thickness (CFT) and total macular volume (TMV) measurements using spectral-domain, high-definition optical coherence tomography (SD-OCT; Copernicus, Reichert Inc., USA). The presence of DR was diagnosed according to the results of indirect ophthalmoscopy and fundus camera (Carl Zeiss Mediatec, Jena, Germany). Hypertension was defined as a systolic blood pressure  $> 140$  mmHg and/or diastolic blood pressure  $> 90$  mmHg. Preoperative systemic examination, blood pressure measurement and routine blood analysis, including glycated hemoglobin (HbA1c), fasting blood glucose and C-reactive protein (CRP), were performed for all participants before cataract surgery.

### Sample Collection

Aqueous humor samples were collected at the beginning of cataract surgery through anterior chamber paracentesis with the 26 G needle of a tuberculin injector. After collection of 0.1–0.15 ml of aqueous humor, samples were immediately transported in a sterile plastic tube and frozen at  $-80^{\circ}\text{C}$  until final analysis. In the morning, before cataract surgery, peripheral blood samples were drawn from each participant by cubital venipuncture and sent to the laboratory for analysis. After separation, serum samples were stored at  $-80^{\circ}\text{C}$  until final analysis. The aqueous humor and serum concentrations of IL-1 $\beta$ , IL-6, IL-8, IL-10, IL-12, MCP-1, IFN- $\gamma$  and TNF- $\alpha$  were measured by performing cytometric bead array technique with the Human Inflammation Multiplex Immunoassay Core Kit (No ab213391, Abcam, Cambridge, UK) according to the manufacturer's instructions (Life Technologies, Carlsbad, CA, USA). The concentration of VEGF in the aqueous humor was determined with a commercially available enzyme-linked immunosorbent assay (ELISA) kit (Human VEGF ELISA Kit, No ab100663, Abcam, Cambridge, UK). The sensitivities and dynamic ranges for investigated cytokines are as follows: 1.2 pg/ml (4,57–10,000 pg/ml) for IL-1 $\beta$ , 8.86 pg/ml (4,57–10,000 pg/ml) for IL-6, 0.31 pg/ml (1.52–3,333 pg/ml) for IL-8, 2.58 pg/ml (4.57–10,000 pg/ml) for IL-10, 2.43 pg/ml (1.52–10,000 pg/ml) for IL-12, 1.0 pg/ml (1.52–3,333 pg/ml) for MCP-1, 1.73 pg/ml (4.57–10,000 pg/ml) for TNF- $\alpha$ , 3.6 pg/ml (4.57–10,000 pg/ml) for IFN- $\gamma$  and 10 pg/ml (8.23–6000 pg/ml) for VEGF.

### Statistical Analysis

Data were analyzed using the Statistical Package for the Social Sciences for Windows (SPSS version 20.0, IBM Corp., Armonk, N.Y., USA). The Chi square test

was used to test the significance of differences between categorical variables. The Shapiro-Wilk test was used to check the normality of non-categorical variables. The mean, standard deviation, t-test for independent samples and ANOVA test were used for normally distributed variables, while the median, interquartile range, Mann-Whitney U test and Kruskal-Wallis H test were used for variables that were not normally distributed. The correlations between study parameters were analyzed by Spearman's correlation coefficient. The level of statistical significance was set at  $p < .05$ .

## RESULTS

Demographic, clinical and biochemical characteristics of subjects in the DR, NDR and control groups are shown in Table 1. There were no significant differences between the three groups of patients with respect to age ( $p = .082$ ), sex ( $p = .567$ ), systolic ( $p = .956$ ) and diastolic blood pressures ( $p = .958$ ).

There were no significant differences between the NDR and DR groups considering the duration of DM ( $p = .355$ ), HbA1c ( $p = .377$ ) and fasting blood glucose level ( $p = .371$ ). Diabetic cataract patients, both in the NDR and DR groups, had a significantly higher CFT value in comparison to the control group ( $p < .001$ ), while the subjects in the DR group had a significantly higher TMV value as compared to those in the control group ( $p < .001$ ).

Figure 1 shows that concentrations of IL-6 were significantly higher in the aqueous humor ( $p = .037$ ) and serum ( $p = .027$ ) of patients with DR in comparison to that of the control group. Concentrations of IL-6 in the aqueous humor and serum of DR patients were higher in comparison to the NDR group, but without statistical significance ( $p = .355$  for both comparisons). Furthermore, the aqueous humor level of VEGF was significantly higher in the DR group in comparison to the NDR and control groups ( $p = .012$ , Figure 2).

The levels of IL-1 $\beta$ , IL-8, IL-10, IL-12, MCP-1, TNF- $\alpha$  and IFN- $\gamma$  in the aqueous humor and serum are

TABLE 1. Demographic, clinical and biochemical characteristics of patients.

Variable	Control group (n = 35)	NDR group (n = 16)	DR group (n = 14)	p	Significant difference between groups
Age (years)	69,9 (4,7)	71,9 (6,7)	73,2 (5,1)	0.082 <sup>A</sup>	
Female/Male	20/15	11/5	7/7	0.567 <sup>B</sup>	
SBP>130 mmHg	21/35	10/16	8/14	0.956 <sup>B</sup>	
DBP >80 mmHg	14/35	6/16	5/14	0.958 <sup>B</sup>	
Duration of diabetes (years)		8.5 [9.0]	10.0 [9.0]	0.355 <sup>D</sup>	
Fasting blood glucose level (mmol/L)	5.7 [1.1]	8.3 [3.0]	10.2 [4.6]	0.371 <sup>C</sup>	
HbA1c (%)		6.9 [1.5]	7.2 [1.3]	0.377 <sup>D</sup>	
CRP (mg/L)	1.2 [1.6]	1.1 [1.8]	2.6 [2.8]	0.216 <sup>C</sup>	
CFT ( $\mu$ m)	213.0 [44.0]	262.5 [64.0]	271.0 [130.0]	<0.001 <sup>C</sup>	NDR-Control <sup>D</sup> DR-Control <sup>D</sup>
TMV (mm <sup>3</sup> )	6.8 (0.7)	7.1 (0.5)	8.2 (1.7)	<0.001 <sup>A</sup>	DR-Control <sup>D</sup>

The results are expressed as m/n, M (SD) or C [IQR]

<sup>A</sup>ANOVA; <sup>B</sup>Chi-square test; <sup>C</sup>Kruskal-Wallis H Test; <sup>D</sup>Mann-Whitney U test

NDR group = type 2 diabetic subjects without diabetic retinopathy; DR group = type 2 diabetic subjects with diabetic retinopathy; SBP = systolic blood pressure; DBP = diastolic blood pressure; HbA1c = glycated hemoglobin; CRP = C-reactive protein, CFT = central foveal thickness; TMV = total macular volume

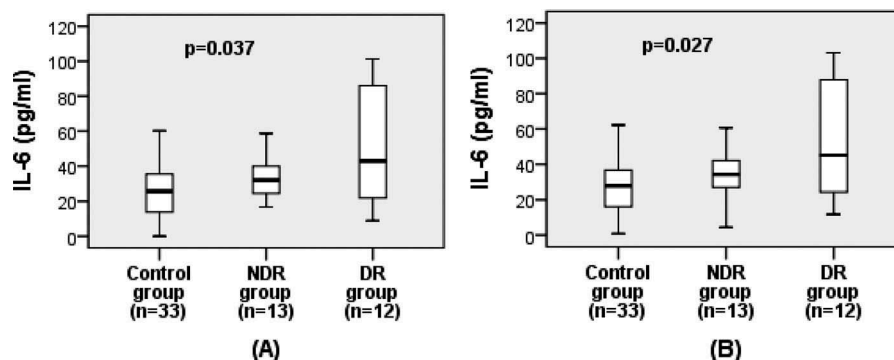


FIGURE 1. Aqueous humor (A) and serum (B) concentrations of interleukin (IL)-6. NDR group = type 2 diabetic subjects without diabetic retinopathy; DR group = type 2 diabetic subjects with diabetic retinopathy.

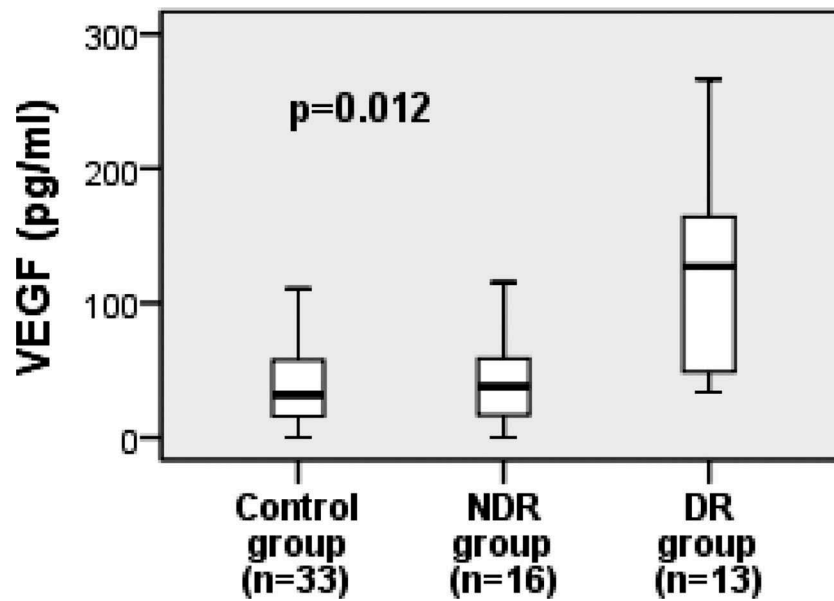


FIGURE 2. Aqueous humor concentration of vascular endothelial growth factor (VEGF).NDR group = type 2 diabetic subjects without diabetic retinopathy; DR group = type 2 diabetic subjects with diabetic retinopathy.

summarized in Table 2. The DR patients had significantly higher concentrations of IL-1 $\beta$  ( $p < .001$ ), IL-8 ( $p < .001$ ), IL-10 ( $p = .001$ ), MCP-1 ( $p = .005$ ) and VEGF

( $p = .003$ ) in their aqueous humor in comparison to the NDR and control groups. In parallel, serum concentrations of IFN- $\gamma$  ( $p = .001$ ), IL-1 $\beta$  ( $p = .009$ ), IL-6

TABLE 2. Aqueous humor and serum levels of the assayed cytokines.

	Control Group (n = 33)	NDR Group (n = 15)	DR Group (n = 13)	p <sup>A</sup>	Significant difference between groups <sup>B</sup>
<b>Aqueous humor concentrations</b>					
IL-1 $\beta$	4.2 [1.2]	4.6 [2.0]	6.9 [4.5]	<0.001	NDR-Control DR-Control
IL-8	69.2 [69.6]	69.3 [91.4]	263.7 [232.0]	<0.001	NDR-DR DR-Control
IL-10	0.6 [2.6]	2.8 [5.4]	4.4 [4.6]	0.001	NDR-DR DR-Control
IL-12	39.4 [66.5]	27.8 [90.9]	52.1 [81.7]	0.946	-
MCP-1	1404.7 [294.1]	1393.5 [300.7]	2250.0 [2232.0]	0.005	DR-Control NDR-DR
<b>Serum concentrations</b>					
TNF- $\alpha$	50.7 [12.5]	54.3 [11.2]	57.7[21.8]	0.011	NDR-Control DR-Control
IL-1 $\beta$	16.4 [1.5]	17.0 [3.7]	18.6 [3.6]	0.009	DR-Control
IL-8	27.7 [16.0]	30.6 [24.3]	39.8 [14.5]	0.046	DR-Control
IL-10	0 [1.1]	3.5 [4.8]	4.8 [7.8]	<0.001	NDR-Control DR-Control
IL-12	2.8 [9.0]	6.2 [10.8]	14.4 [7.7]	0.005	DR-Control NDR-DR
MCP-1	265.5 [129.8]	336.4 [103.1]	338.8 [281.3]	0.169	-
IFN- $\gamma$	2.9 [14.7]	27.8 [45.9]	56.8 [41.9]	0.001	NDR-Control DR-Control

The results are expressed as C[IQR]

<sup>A</sup>Kruskal-Wallis H Test; <sup>B</sup>Mann-Whitney U test

NDR group = type 2 diabetic subjects without diabetic retinopathy; DR group = type 2 diabetic subjects with diabetic retinopathy; IL = interleukin; MCP-1 = monocyte chemoattractant protein-1; VEGF = vascular endothelial growth factor; IFN- $\gamma$  = interferon gamma; TNF- $\alpha$  = tumor necrosis factor alpha



TABLE 3. Correlation between the aqueous humor levels of cytokines and CFT.

		CFT		
		Control group	NDR group	DR group
IL-1 $\beta$	Spearman's rho	-0.035	-0.009	0.302
	Sig. (2-tailed)	0.848	0.974	0.316
	N	33	16	13
IL-6	Spearman's rho	-0.148	-0.339	0.791**
	Sig. (2-tailed)	0.428	0.257	0.004
	N	31	13	11
IL-8	Spearman's rho	0.321	-0.455	0.242
	Sig. (2-tailed)	0.064	0.077	0.426
	N	34	16	13
IL-10	Spearman's rho	-0.318	-0.326	0.236
	Sig. (2-tailed)	0.067	0.217	0.437
	N	34	16	13
IL-12	Spearman's rho	-0.321	-0.158	-0.046
	Sig. (2-tailed)	0.068	0.574	0.881
	N	33	15	13
MCP-1	Spearman's rho	0.157	-0.401	0.253
	Sig. (2-tailed)	0.384	0.139	0.405
	N	33	15	13
VEGF	Spearman's rho	-0.120	-0.052	0.018
	Sig. (2-tailed)	0.513	0.854	0.958
	N	32	15	11

\* Correlation is significant at the 0.05 level (2-tailed).

\*\* Correlation is significant at the 0.01 level (2-tailed).

CFT = central foveal thickness; NDR group = type 2 diabetic subjects without diabetic retinopathy; DR group = type 2 diabetic subjects with diabetic retinopathy; IL = interleukin; MCP-1 = monocyte chemoattractant protein; VEGF = vascular endothelial growth factor.

( $p = .027$ ), IL-8 ( $p = .046$ ), IL-10 ( $p < .001$ ), IL-12 ( $p < .005$ ) and TNF- $\alpha$  ( $p = .011$ ) in the DR patients were significantly higher than that of those in the control group. Levels of TNF- $\alpha$  and IFN- $\gamma$  in the aqueous humor samples of all diabetic patients and controls were below the detection limit of the assay.

There was significant correlation between the aqueous humor concentration of IL-6 and CFT in the DR group (Table 3). There was also significant correlation between the aqueous humor concentration of IL-1 $\beta$  and HbA1c in the NDR group (Table 4).

## DISCUSSION

The role of inflammatory mediators in the development and progression of most common diabetic eye complications, such as cataract, DR and DME, has been studied for a long time. Inflammatory cytokines have been investigated in the tears<sup>14</sup> aqueous humor<sup>1,5-8</sup> and vitreous of diabetic patients.<sup>15,16</sup> Their importance in the pathogenesis of different stages of DR has been suggested by many authors. Furthermore, chronic hyperglycaemia-induced inflammation can be a critical contributing factor in the pathogenesis of DR.<sup>17</sup> The production of inflammatory cytokines in aqueous humor of patients with diabetic cataract and DR may

be induced locally by inflammatory cells, such as resident macrophages, fibroblasts and infiltrating leukocytes.<sup>18</sup> However, elevated levels of the same mediators have also been found in the serum, supporting the possibility that inflammatory cytokines are not produced only locally in diabetic patients. According to some research, the breakdown of the blood-retinal barrier in DR facilitates the leakage of serum proteins and other molecules and their passage from the bloodstream to the intraocular fluid.<sup>13</sup> Therefore, we measured the concentrations of selected cytokines and VEGF in aqueous humor and serum of diabetic cataract patients.

VEGF is an important mediator of microvascular complications of T2DM that causes angiogenesis and increased vascular permeability. Several clinical studies have shown a strong correlation between increased levels of VEGF and development of DR<sup>7,19</sup> and DME.<sup>9,12,20,21</sup> According to Mitrovic et al<sup>1</sup> and Cheung et al<sup>7</sup>, the aqueous humor level of VEGF was higher in diabetic cataract patients with or without DR as compared to the senile cataract group. In our study, the VEGF concentration in aqueous humor was significantly higher in the DR group as compared to the NDR and control groups, implicating its role in the progression of DR.

IL-6 is an inflammatory cytokine that is up-regulated early in inflammation<sup>22</sup>, and a previous study showed that IL-6 is involved in the breakdown of the blood-

TABLE 4. Correlation between the aqueous humor/serum levels of cytokines and HbA1 c.

	HbA1 c	Aqueous humor		Serum	
		NDR group	DR group	NDR group	DR group
TNF- $\alpha$	Spearman's rho			0.254	0.050
	Sig. (2-tailed)			0.343	0.871
	N			16	13
IL-1 $\beta$	Spearman's rho	0.630**	0.091	-0.052	-0.391
	Sig. (2-tailed)	0.009	0.757	0.847	0.167
	N	16	14	16	14
IL-6	Spearman's rho	-0.331	-0.224	-0.331	-0.224
	Sig. (2-tailed)	0.269	0.484	0.269	0.484
	N	13	12	13	12
IL-8	Spearman's rho	-0.073	0.042	0.313	-0.209
	Sig. (2-tailed)	0.789	0.886	0.238	0.474
	N	16	14	16	14
IL-10	Spearman's rho	0.070	0.084	-0.123	-0.281
	Sig. (2-tailed)	0.798	0.774	0.649	0.352
	N	16	14	16	13
IL-12	Spearman's rho	0.157	-0.221	0.031	-0.033
	Sig. (2-tailed)	0.576	0.448	0.909	0.914
	N	15	14	16	13
MCP-1	Spearman's rho	-0.129	-0.138	-0.105	-0.053
	Sig. (2-tailed)	0.647	0.639	0.699	0.864
	N	15	14	16	13
VEGF	Spearman's rho	-0.025	0.107		
	Sig. (2-tailed)	0.929	0.742		
	N	15	12		
IFN- $\gamma$	Spearman's rho			-0.013	0.302
	Sig. (2-tailed)			0.961	0.294
	N			16	14

\* Correlation is significant at the 0.05 level (2-tailed).

\*\* Correlation is significant at the 0.01 level (2-tailed).

HbA1 c = glycated hemoglobin; NDR group = type 2 diabetic subjects without diabetic retinopathy; DR group = type 2 diabetic subjects with diabetic retinopathy; IL = interleukin; MCP-1 = monocyte chemotactic protein; VEGF = vascular endothelial growth factor; IFN- $\gamma$  = interferon gamma; TNF- $\alpha$  = tumor necrosis factor alpha

retinal barrier in patients with DR.<sup>23</sup> In our study, concentrations of IL-6 in the aqueous humor and serum of diabetic cataract patients with DR were significantly higher than those in the control group, suggesting that inflammation has an important role in the pathogenesis of DR and cataracts.<sup>24,25</sup> Furthermore, our results showed significant correlation between the aqueous humor concentration of IL-6 and CFT in the DR group. This finding suggests that IL-6 contributes to the occurrence and progression of DME, which is in accordance with the study of Oh et al.<sup>26</sup> Besides, we also found up-regulation of the IL-1 $\beta$  in the aqueous humor and serum samples of patients with DR. IL-1 $\beta$  is known to induce vascular dysfunction and cell death with consequent increased endothelial permeability, which occurs during the progression of DR.<sup>27</sup> Other authors found that elevated serum<sup>28</sup> and aqueous humor<sup>8</sup> levels of IL-1 $\beta$  correlated with the presence and severity of DR. In our study, there was a significant correlation between the aqueous humor concentration of IL-1 $\beta$  and serum concentration of HbA1c in the NDR group. Another study showed significant correlation between IL-10 or MCP-1 and HbA1c in patients with DR.<sup>12</sup> TNF- $\alpha$  is an inflammatory cytokine

produced by monocytes, macrophages and activated endothelial cells. In the present study, we observed higher serum TNF- $\alpha$  concentrations in patients with DR as compared to controls, which is in accordance with the results of previous studies.<sup>29-31</sup> Our results also revealed that the both CFT and TMV values were significantly higher in cataract patients with DR as compared to controls. Previous studies reported that elevated levels of IL-1 $\beta$ , IL-6 and TNF- $\alpha$  correlated with the severity of DR and the presence of DME.<sup>8</sup>

Another cytokine investigated in our study was an IL-12, which has been hypothesized to have a role in inhibition of retinal neovascularization.<sup>31</sup> It has been found that the concentration of IL-12 in the aqueous humor was significantly higher in patients with proliferative DR.<sup>6</sup> Our study did not show significant differences between the groups considering the aqueous humor concentration of IL-12, while the serum level of IL-12 was significantly higher in the DR group as compared to the other two groups. IL-10 as an anti-inflammatory and anti-angiogenic mediator is produced by monocytes and macrophages. Our results showed that the aqueous humor and serum concentrations of IL-10 were

significantly increased in the NDR and DR groups as compared to controls, supporting the results of some previous research.<sup>12,20,32</sup> Nevertheless, Dong et al<sup>20</sup> found that the aqueous humor levels of IL-10 decreased with increasing severity of DR. Lee et al<sup>33</sup> reported that higher serum levels of IL-10 were related to a lower risk for DR in T2DM patients. MCP-1 has been shown to be a significant component of the retinal inflammation induced by diabetes, and its production is increased in patients with hyperglycemia.<sup>34</sup> According to Yoshimura et al<sup>35</sup> elevation of the aqueous humor levels of IL-8 and MCP-1 in eyes with less severe stages of DR suggests that inflammatory changes precede the development of neovascularization in DR. In our study, the aqueous humor concentrations of IL-8 and MCP-1 were significantly increased in the DR group as compared to the control group, which is consistent with previous reports.<sup>7,20,22,36,37</sup> On the other hand, systemic concentrations of these cytokines were not significantly different among the study groups, suggesting local production of MCP-1.

In conclusion, our study showed increased aqueous humor concentrations of IL-1 $\beta$ , IL-6, IL-8, MCP-1 and VEGF and serum concentrations of IL-1 $\beta$ , IL-6, IL-8, IL-12, TNF- $\alpha$  and IFN- $\gamma$  in diabetic cataract subjects. These findings support the hypothesis that chronic inflammation and a disturbance of the immune system play important roles in the pathogenesis of diabetic cataract and DR. According to the results of our and other research, it is necessary to carry out further studies to better understand the relationship between systemic and local inflammatory mediators in the development of diabetic eye complications.

## DECLARATION OF INTEREST

The authors report no conflict of interest. The authors are alone responsible for the writing and content of the paper. The funding organization had no role in the design or conduct of this study.

## ORCID

Katarina Cvitkovic  <http://orcid.org/0000-0001-7668-825X>

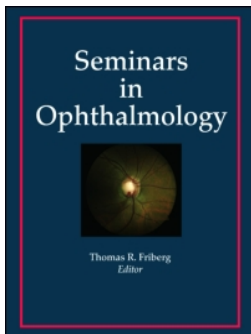
Ivan Cavar  <http://orcid.org/0000-0002-0685-3982>

## REFERENCES

- Mitrovic S, Kelava T, Sucur A, Grcevic D. Levels of selected aqueous humor mediators (IL-10, IL-17, CCL-2, VEGF, FasL) in diabetic cataract. *Ocul Immunol Inflamm.* 2016;24(2):159–166. doi:10.3109/09273948.2014.949779.
- Xu H, Chen M. Diabetic retinopathy and dysregulated innate immunity. *Vision Res.* 2017;139:39–46. doi:10.1016/j.visres.2017.04.013.
- Stitt AW, Curtis TM, Chen M. et al. The progress in understanding and treatment of diabetic retinopathy. *Prog Retin Eye Res.* 2016;51:156–186. doi:10.1016/j.preteyeres.2015.08.001.
- Simo R, Hernandez C. Novel approaches for treating diabetic retinopathy based on recent pathogenic evidence. *Prog Retin Eye Res.* 2015;48:160–180. doi:10.1016/j.preteyeres.2015.04.003.
- Funatsu H, Yamashita H, Noma H, Mimura T, Yamashita T, Hori S. Increased levels of vascular endothelial growth factor and interleukin-6 in the aqueous humor of diabetics with macular edema. *Am J Ophthalmol.* 2002;133(1):70–77. doi:10.1016/s0002-9394(01)01269-7.
- Gverovic Antunica A, Karaman K, Znaor LJ, Sapunar A, Buskov V, Puzovic V. IL-12 concentrations in aqueous humor and serum of diabetic retinopathy patients. *Graefes Arch Clin Exp Ophthalmol.* 2012;250(6):815–821. doi:10.1007/s00417-011-1905-4.
- Cheung CMG, Vania M, Ang M, Chee S, Li J. Comparison of aqueous humor cytokine and chemokine levels in diabetic patients with and without retinopathy. *Mol Vis.* 2012;18:830–837.
- Dong N, Xu B, Chu L, Tang X. Study of 27 aqueous humor cytokines in type 2 diabetic patients with or without macular edema. *PlosONE.* 2015;10(4):e0125329. doi:10.1371/journal.pone.0125329.
- Funatsu H, Noma H, Mimura T, Eguchi S, Hori S. Association of vitreous inflammatory factors with diabetic macular edema. *Ophthalmology.* 2009;116(1):73–79. doi:10.1016/j.ophtha.2008.09.037.
- Klein BE, Klein R, Moss SE. Prevalence of cataracts in a population – based study of persons with diabetes mellitus. *Ophthalmology.* 1985;92:1191–1196. doi:10.1016/s0161-6420(85)33877-0.
- Pollreis A, Schmidt-Erfurth U. Diabetic cataract - pathogenesis, epidemiology and treatment. *J Ophthalmol.* 2010;2010:e608751. doi:10.1155/2010/608751.
- Ozturk BT, Bozkurt B, Kerimoglu H, Okka M, Kamis U, Gunduz K. Effect of serum cytokines and VEGF levels on diabetic retinopathy and macular thickness. *Mol Vis.* 2009;15:1906–1914.
- Doganay S, Evereklioglu C, Er H. et al. Comparison of serum NO, TNF- $\alpha$ , IL-1 $\beta$ , sIL-2R, IL-6 and IL-8 levels with grades of retinopathy in patients with diabetes mellitus. *Eye.* 2002;16:163–170. doi:10.1038/sj.eye.6700095.
- Liu J, Shi B, He S, Yao X, Willcox MDP, Zhao Z. Changes to tear cytokines of type 2 diabetic patients with or without retinopathy. *Mol Vis.* 2010;16:2931–2938.
- Boss JD, Singh PK, Pandya HK, et al. Assessment of neurotrophins and inflammatory mediators in vitreous of patients with diabetic retinopathy. *Invest Ophthalmol Vis Sci.* 2017;58(12):5594–5603. doi:10.1167/iovs.17-21973.
- Endo H, Naito T, Asahara T, Kajima M, Shiota H. Cytokines in the vitreous fluid of patients with proliferative diabetic retinopathy-vascular endothelial growth factor and platelet-derived growth factor are elevated in proliferative diabetic retinopathy. *Nippon Ganka Gakkai Zasshi.* 2000;104:711–716.
- Koleva-Georgieva DN, Sivkova ND, Terzieva D. Serum inflammatory cytokines IL-1 $\beta$ , IL-6, TNF- $\alpha$  and VEGF have influence on the development of diabetic retinopathy. *Folia Med (Plovdiv).* 2011;53(2):44–50. doi:10.2478/v10153-010-0036-8.
- Hui C, Xiongze Z, Nanying L, Feng W. Increased levels of IL-6, sIL-6R and sgp130 in the aqueous humor and serum of patients with diabetic retinopathy. *Mol Vis.* 2016;22:1005–1014.
- Kocabora MS, Durmaz S, Taskapili M, Cekic O, Ozsutcu M. Increased levels of vascular endothelial growth

- factor in the aqueous humor of patients with diabetic retinopathy. *Indian J Ophthalmol.* 2010;58(5):375–379. doi:10.4103/0301-4738.67042.
20. Dong N, Xu B, Chu L, Tang X. Study of 27 aqueous humor cytokines in patients with type 2 diabetes with or without retinopathy. *Mol Vis.* 2013;19:1734–1746.
  21. Nguyen QD, Tatlipinar S, Shah SM, et al. Vascular endothelial growth factor is crucial stimulus for diabetic macular edema. *Am J Ophthalmol.* 2006;142(6):961–969. doi:10.1016/j.ajo.2006.06.068.
  22. Jones SA. Directing transition from innate to acquired immunity; defining a role for IL-6. *J Immunol.* 2005;175:3463–3468. doi:10.4049/jimmunol.175.6.3463.
  23. Moriarty AP, Spalton DJ, Moriarty BJ, Shilling JS, Flytche TJ, Bulsara M. Studies of the blood - aqueous barrier in diabetes mellitus. *Am J Ophthalmol.* 1994;117(6):768–771. doi:10.1016/S0002-9394(14)70320-4.
  24. Hamid S, Gul A, Hamid Q. Relationship of cytokines and AGE products in diabetic and non - diabetic patients with cataract. *Int J Health Sci (Qassim).* 2016;10(4):507–515. doi:10.12816/0048891.
  25. Zhu HC, Tao Y, Li YM. Correlations of insulin resistance and HbA1c with cytokines IGF-1, bFGF and IL-6 in the aqueous humor of patients with diabetic cataract. *Eur Rev Med Pharmacol Sci.* 2019;23(1):16–22. doi:10.26355/eurrev\_201901\_16742.
  26. Oh IK, Seong WK, Oh J, Lee TS, Huh K. Inflammatory and angiogenic factors in the aqueous humor and the relationship to diabetic retinopathy. *Curr Eye Res.* 2010;35:1116–1127. doi:10.3109/02713683.2010.510257.
  27. Kowluru RA, Odehbach S. Role of the interleukin -1beta in the pathogenesis of diabetic retinopathy. *Br J Ophthalmol.* 2004;88(10):1343–1347. doi:10.1136/bjo.2003.038133.
  28. Kaul K, Hodgkinson a, Tarr JM, Kohner EM, Chibber R. Is inflammation a common retinal- renal-nerve pathogenetic link in diabetes? *Curr Diabetes Rev.* 2010;6:294–303. doi:10.2174/157339910793360851.
  29. Gustavsson C, Agardth CD, Agardth E. Profile of intraocular tumor necrosis factor -  $\alpha$  and interleukin -6 in diabetic subjects with different degrees of diabetic retinopathy. *Acta Ophthalmol.* 2013;91:445–452. doi:10.1111/j.1755-3768.2012.02430.x.
  30. Gustavsson A, Agardth E, Bengtsson B, Agardth CD. TNF - alpha is an independent serum marker for proliferative retinopathy in type 1 diabetic patients. *J Diabetes Complications.* 2008;22(5):309–316. doi:10.1016/j.jdiacomp.2007.03.001.
  31. Zhou Y, Yoshida S, Kubo Y. et al. Interleukin-12 inhibits pathological neovascularization in mouse model of oxygen-induced retinopathy. *Sci Rep.* 2016;6:e28140. doi:10.1038/srep28140.
  32. Hailiang W, De-Kuang H, Xudong S, Yong T. Association between aqueous cytokines and diabetic retinopathy stage. *J Ophthalmol.* 2017;2017:e9402198. doi:10.1155/2017/9402198.
  33. Lee JH, Lee W, Kwon OH, et al. Cytokine profile of peripheral blood in type 2 diabetes mellitus patients with diabetic retinopathy. *Ann Clin Lab Sci.* 2008;38:361–367.
  34. Zhang W, Liu H, Al-Shabrawey M, Caldwell RW, Caldwell RB. Inflammation and diabetic retinal microvascular complications. *J Cardiovasc Dis Res.* 2011;2:96–103. doi:10.4103/0975-3583.83035.
  35. Yoshimura T, Sonoda KH, Sugahara M, et al. Comprehensive analysis of inflammatory immune mediators in vitreoretinal diseases. *PLoS One.* 2009;4(12):e8158. doi:10.1371/journal.pone.0008158.
  36. Chen H, Zhang X, Liao N, Wen F. Assessment of biomarkers using multiplex assays in aqueous humor of patients with diabetic retinopathy. *BMC Ophthalmol.* 2017;17(1):176. doi:10.1186/s12886-017-0572-6.
  37. Songfu F, Honghua Y, Ying Y. et al. Levels of inflammatory cytokines IL-1 $\beta$ , IL-6, IL-8, IL-17A and TNF- $\alpha$  in aqueous humor of patients with diabetic retinopathy. *J Diabetes Res.* 2018;2018:8546423. doi:10.1155/2018/8546423.





## Detection of structural and electrical disturbances in macula and optic nerve in Alzheimer's patients and their correlation with disease severity

Sagnik Sen, Rohit Saxena, Deepti Vibha, Manjari Tripathi, Pradeep Sharma, Swati Phuljhele, Radhika Tandon & Pawan Kumar

To cite this article: Sagnik Sen, Rohit Saxena, Deepti Vibha, Manjari Tripathi, Pradeep Sharma, Swati Phuljhele, Radhika Tandon & Pawan Kumar (2020): Detection of structural and electrical disturbances in macula and optic nerve in Alzheimer's patients and their correlation with disease severity, *Seminars in Ophthalmology*, DOI: [10.1080/08820538.2020.1748203](https://doi.org/10.1080/08820538.2020.1748203)

To link to this article: <https://doi.org/10.1080/08820538.2020.1748203>



Published online: 18 Apr 2020.



Submit your article to this journal [↗](#)



Article views: 28



View related articles [↗](#)



View Crossmark data [↗](#)



ARTICLE

# Detection of structural and electrical disturbances in macula and optic nerve in Alzheimer's patients and their correlation with disease severity

Sagnik Sen<sup>1</sup>, Rohit Saxena<sup>1</sup>, Deepti Vibha<sup>2</sup>, Manjari Tripathi<sup>2</sup>, Pradeep Sharma<sup>1</sup>, Swati Phuljhele<sup>1</sup>, Radhika Tandon<sup>1</sup>, and Pawan Kumar<sup>1</sup>

<sup>1</sup>Department of Ophthalmology, AIIMS, New Delhi, India and <sup>2</sup>Department of Neurology, AIIMS, New Delhi, India

## ABSTRACT

**Aim:** To evaluate and compare structural and functional changes in macula and optic nerve in Alzheimer disease (AD) patients and healthy subjects.

**Methods:** Both eyes of 20 AD patients and 40 age-matched healthy controls were evaluated. All subjects were evaluated by cognitive testing and comprehensive ophthalmological examination, including visual acuity, visual fields, color vision, contrast sensitivity, anterior, and posterior segment examination, optical coherence tomography, multifocal electroretinography (mfERG), and pattern-reversal visual evoked potential (pVEP).

**Results:** AD patients showed significantly reduced contrast sensitivity, thinner nerve fiber layer, ganglion cell layer and macular volume. Multifocal ERG wave amplitudes were significantly reduced with delayed implicit times, which correlated significantly with the inner retinal layer thinning and poorer disease severity scores. The correlation with structural changes and disease severity was highest for pVEP, which showed significant derangement in AD patients.

**Conclusion:** Subclinical visual dysfunction may be present in AD patients, which may be detected as inner retinal thinning. A probable photoreceptor abnormality may also form a part of the AD disease process.

**Keywords:** Alzheimer's, RNFL, GCL, OCT, mfERG

## INTRODUCTION

Alzheimer's disease (AD) is the most common form of dementia in the world with an incidence of 15.54 per 100 person-years (95% CI: 14.6–16.5) in age more than 65 years.<sup>1</sup> The morbidity associated with AD is due to the loss of activities of daily living and a reduced life expectancy. At present, diagnosis of AD is restricted to clinical evaluation with history and neurological examination using cognitive screening and diagnostic tests like National Institute of Neurological and Communication Disorders and Stroke-Alzheimer's disease and Related Disorders association (NINCDS-ADRDA) criteria, Mini-mental state examination scoring (MMSE), Cognitive Dementia Rating (CDR) scale, etc., followed by structural and functional brain imaging.<sup>2</sup> Recent AD research has focused on the

detection of downstream neuronal injury that reflects complex patterns of tissue changes through imaging. A number of studies have evaluated spectral-domain optical coherence tomography (OCT) of retina and optic nerve and found characteristic changes in AD patients involving the degeneration of the retinal nerve fiber layer (RNFL) and the retinal ganglion cell layer (RGC).<sup>3–6</sup> Moreover, electrophysiological dysfunction in the retina has been observed in AD using pattern electroretinogram (pERG) and pattern visual evoked potential (pVEP). pVEP and pERG abnormalities may correspond to the affection of RGCs in the inner retinal layers. Another significant question in this regard arises whether the outer retina also gets affected in AD patients. We designed the study in order to evaluate the posterior segment of the eye including the macula and try and find

a correlation between the structural retinal disease process and the electrical changes in the macula.

## METHODS

### Study Groups

The study was conducted at a tertiary care center after obtaining approval from the Institutional Ethics Review Board. The study adhered to the tenets of the Declaration of Helsinki and informed consent was taken from all subjects. Each patient needed to have an informant or caregiver. Primary caregivers were considered as surrogate decision-makers and informed consent was obtained from them in case the patient was extremely incapacitated to give consent. A total of 60 subjects (20 AD patients, 40 healthy controls) were included after obtaining written informed consent, the inclusion criteria being age more than 40 years and visual acuity better than 6/9. Sample size was calculated to evaluate a change of 10  $\mu\text{m}$  change of retinal nerve fiber layer thickness from a previous paper evaluating OCT changes in AD.<sup>7</sup> AD patients were diagnosed using the National Institute of Neurological and Communicative Disorders and Stroke and Alzheimer's disease and Related Disorders Association (NINCDS-ADRDA) criteria after consultation with two experienced neurologists. The subjects having other known cerebral pathology, cardiovascular diseases, psychiatric abnormalities, glaucoma/ocular hypertension, macular degeneration, high refractive error of  $\pm 5\text{D}$  and media opacities were excluded. In addition, subjects with head or neck injuries unable to maintain retinal fixation on a specified target were excluded. Disease duration was recorded based on patient and informant's memory of onset of symptoms. Controls comprised of cognitively normal elderly subjects (screened via MMSE score in the Neurology department), age matched within  $\pm 2$  years of the AD cases, taken from the outpatient department, without any ophthalmic diseases, neurodegenerative diseases, or cardiovascular risk factors.

### Cognitive Scoring

Initial screening using the MMSE score was performed for all subjects (cases and controls) by two Neurologists. Detailed evaluation of cognition of the AD cases using Global Deterioration Scale and Washington University Clinical Dementia Rating (CDR) scale was performed by two neurologists.<sup>8,9</sup> The patients were rated in each domain according to their cognitive functionality and the final score was determined based on an algorithm of clinical scoring rules after incorporating information from

both the patient and the informant. The sum of boxes score of CDR (CDR-SOB) was also calculated for each patient.

### Ophthalmic Evaluation

All subjects underwent comprehensive ophthalmological evaluation for each eye separately including best-corrected visual acuity (BCVA) measured using ETDRS charts, colour vision using Ishihara pseudo-isochromatic test plates, contrast sensitivity using Pelli-Robson chart and anterior and posterior segment examination. The subjects were required to take adequate sleep the night before ocular investigations to ensure compliance. All subjects were evaluated using a spectral-domain optical coherence tomography (OCT) device (Cirrus HD-OCT Model 4000, Carl Zeiss Meditec Inc., Dublin, CA). Analyzed features included retinal nerve fiber layer (RNFL) thickness in the  $200 \times 200$  scan and ganglion cell layer (GCL) thickness and macular volume (MV) in the  $512 \times 128$  scan. All scans deemed suitable for gradation in the study had a signal strength of at least 5 and re-scanning was performed if any motion artefact was detected. MfERG was performed according to ISCEV standards using a 61-scaled hexagon display (Metrovision, Monpack, Pirencies, France) with a mean luminance of 100  $\text{cd}/\text{m}^2$  and a contrast of  $>90\%$ .<sup>10</sup> Disposable monopolar scleral lenses and skin electrodes were used for mfERG. The display monitor was placed at a distance of 30 cm before the patient and one eye was tested at a time. Stimulus frequency of the hexagon display was kept at 17 Hz. Video monitoring based on a near infra-red sensor which recorded image of the eye was used for ensuring and monitoring eye-fixation. Five thousand responses were recorded over a period of 5 min for each eye. First-order kernel mfERG responses were documented for further analysis. Pattern-reversal VEP was also performed according to ISCEV standards using a single recording channel with a midline occipital positive electrode.<sup>11</sup> This active skin electrode was placed at the Oz position, the highest point of the occiput, with reference and ground electrodes at Fz and Cz (vertex) points, respectively. Recording was performed using the Nicolet Ganzfeld 2015 visual stimulator and a monitor (Nicolet Biomedical, Madison, WI). A checkerboard pattern (reversal time of 500 ms) was used with a field size of  $>150$  and mean luminance of 50  $\text{cd}/\text{m}^2$ , kept at a distance of 100 cm from the subjects' eye. The monitor presented black and white checks, whose phases were reversed, i.e., black to white and white to black, at a fixed rate of two reversal per second. Each eye was tested separately. A sweep length of 250 ms was used which recorded

more than 100 responses, at an amplification range of 20000 to 100000. Electrode impedance was kept less than 5 K $\Omega$ . Visual fields were recorded using automated Visual Field Analyser 750i (Carl Zeiss Meditec, Dublin, CA) with 30–2 SITA Standard Strategy. Automated static field results were considered reliable if false-positive and false-negative responses were lower than 33% and fixation loss lesser than 20%. MfERG, pattern VEP and fields were tested with the patient wearing full refractive correction.

All investigations were done by one Neuro ophthalmology laboratory personnel. The patient's name and identification number only were revealed to the person and whether the subject was a part of any study or that he suffered from a particular disease condition was not revealed to him.

### Statistical Analysis

Data were analysed using IBM SPSS Statistics version 21.0 (Armonk, NY). Generalized estimating equations (GEE) adjusted for age and inter-eye correlation were used to compare variables between AD patients and controls. In the GEE model, age was taken as a between-subject effect and eye of the patient as a within-subject effect. Disease status (Alzheimer's or healthy control) was kept as a dependent variable. Binary logistic model was used for GEE. The robust estimator matrix was used with an independent working correlation matrix to adjust estimators by number of non-redundant parameters. Eye (right or left) was considered a factor and age a covariate in the analysis. Pearson's correlation coefficients were used to correlate variables and determine the strength of such correlations. Receiver operating characteristic (ROC) curves were obtained to describe the discrimination ability of parameters by the area under the curves (AUC). Data was considered statistically significant for a 2-tailed  $p$  value of 0.05. For multiple comparisons within a given domain, to compare several parameters, modified  $p$  values using Bonferroni correction were used.

## RESULTS

### Demographics

The study evaluated 120 eyes of 20 cases of clinically diagnosed AD patients and 40 cognitively healthy control subjects (Table 1). Table 1 displays the GEE parameter estimates ( $p$  values and 95% confidence intervals) and the AUC obtained by the ROC curves. The mean (SD) age of AD patients was 61.5 (7.45) years (range, 45–78 years), that of controls being 60.94 (7.6) years (range, 44–72 years) ( $p = .79$ ).

The median MMSE score was 17.5 (range, 10–23) in AD patients and 28 (range, 26–29) in controls (Table 2). The median severity of disease (CDR) was 1 (range, 0.5–2) and the median sum-of-boxes CDR score was 5.5, indicating a mild dementia. The median duration of disease was 2 years (range, 6 months–3.5 years). The mean (SD) BCVA was similar in the two groups ( $p = .19$ ). Mean contrast sensitivity was significantly reduced in the AD eyes ( $p < .05$ ) (Table 1). Static visual fields were found to be within normal limits in all patients. The anterior segment, intraocular pressure, fundus examination, and colour vision were within normal limits in all subjects.

### OCT Measurements

AD patients showed significant average RNFL thinning with individual significant thinning (Table 1) in superior and inferior quadrants of RNFL ( $p < .001$ ) with the largest AUCs being for superior (0.863; 95% CI: 0.791–0.937) and inferior (0.8; 95% CI: 0.718–0.888) quadrants. The ratio of nasal to temporal RNFL thickness was higher in AD eyes ( $p < .001$ ) indicating thinner papillomacular bundle. AD eyes showed significant average GCL thickness reduction compared to controls; individually in superior, superonasal, inferonasal, inferior, inferotemporal, and superotemporal sectors ( $p < .005$ ) (Table 1). The inferotemporal quadrant showed the largest AUC (0.887; 95% CI: 0.826–0.948), followed by the superior quadrant (0.883; 95% CI: 0.812–0.955). AUC of RGCL average (0.947; 95% CI: 0.909–0.985) was higher than that of RNFL average (0.892; 95% CI: 0.832–0.953). Also, macular volume thinning was observed in the AD patients ( $p < .001$ ).

### Electrophysiological Parameters

A generalized suppression of electrical activity was observed in mfERG (Table 1). The mfERG anatomical areas corresponded to the following: ring 1 to fovea, ring 2 to parafovea, ring 3 to perifovea, ring 4 to near periphery, and ring 5 to mid-periphery. Mean P1, N1, and N2 amplitudes were significantly reduced ( $p < .001$ ) in AD cases in rings 1–5, while mean P1 implicit times were significantly prolonged ( $p < .001$ ) in rings 1–5. N1 and N2 implicit times were longer in AD group than healthy controls, however, the difference was not found significant. Pattern –reversal VEP amplitude was significantly reduced with latency prolonged significantly in the AD patients ( $p < .05$ ). VEP latency was higher than 115 ms in 26/40 eyes (65%). Ten AD patients (50%) had bilateral prolongation (20 eyes) of VEP latency while the rest six patients showed this unilaterally. Analysis of AUC



TABLE 1. Comparative evaluation of Alzheimer's patients and healthy controls.

	Cases (N = 40)	Controls (N = 80)	Difference (95% CI) <sup>c</sup>	S.E.	p value <sup>a</sup>	Effect size <sup>d</sup>	AUC (95% CI) <sup>b</sup>
<b>Age</b>	61.5 ± 7.45 (N = 20)	60.94 ± 7.6 (N = 40)			0.79		
<b>BCVA (logMAR)</b>	0.17 ± 0.132 (N = 40)	0.14 ± 0.112 (N = 80)			0.19		
<b>Contrast sensitivity</b>	1.326 ± 0.205 (N = 40)	1.853 ± 0.05 (N = 80)	-0.53 (-0.58, -0.47)	0.02	<0.05	4.22	
<b>Retinal nerve fibre layer thickness (µm)</b>							
Superior quadrant	76.2 ± 28.56	112.34 ± 15.87	-33.8 (-47.9, -19.7)	7.21	<0.001	1.72	0.863 (0.791-0.937)
Nasal quadrant	62.83 ± 16.69	71.23 ± 10.19	-4.4 (-10.3, 1.5)	3.0	0.141	0.66	0.683 (0.566-0.8)
Inferior quadrant	77.08 ± 25.09	105.88 ± 23.29	-23.1 (-36.4, -9.7)	6.82	<0.001	1.21	0.803 (0.718-0.888)
Temporal	53.23 ± 19.09	60.5 ± 11.83	-7.6 (-15.3, -0.4)	3.89	0.049	0.497	0.653 (0.544-0.761)
Average	67.33 ± 13.14	87.49 ± 9.2	-17.2 (-24.0, -10.5)	3.45	<0.001	1.89	0.892(0.832-0.953)
<b>Retinal ganglion cell layer thickness (µm)</b>							
Superior sector	68.38 ± 19.59	90.41 ± 8.6	-21.8 (-28.3, -15.3)	3.32	<0.001	1.66	0.883 (0.812-0.955)
Supero-nasal sector	67.93 ± 17.83	85.95 ± 8.83	-18.6 (-24.1, -13.1)	2.79	<0.001	1.44	0.871 (0.805-0.936)
Infero-nasal sector	66.75 ± 17.17	85.24 ± 8.29	-15.9 (-21.8, -9.9)	3.02	<0.001	1.54	0.861 (0.796-0.927)
Inferior sector	58.78 ± 18.78	81.44 ± 13.79	-18.2 (-26.4, -10.1)	4.15	<0.001	1.78	0.859 (0.788-0.93)
Infero-temporal	61.93 ± 18.19	85.23 ± 7.72	-24.3 (-31.9, -16.7)	3.89	<0.001	1.9	0.887 (0.826-0.948)
Supero-temporal sector	65.2 ± 18.86	87.46 ± 9.64	-20.6 (-27.3, -13.9)	3.43	<0.001	1.66	0.883 (0.818-0.947)
Average	64.83 ± 13.74	85.95 ± 6.28	-19.9 (-24.8, -14.9)	2.51	<0.001	2.24	0.947 (0.909-0.985)
<b>Macular volume (mm<sup>3</sup>)</b>	8.92 ± 0.78	9.78 ± 0.64	-0.83 (-1.15, -0.52)	0.15	<0.001	1.25	0.872 (0.801-0.944)
<b>mfERG Amplitudes (nV)</b>							
<b>P1 wave</b>							
Ring 1	990.38 ± 406.34	1495.58 ± 378.56	-448.3 (-656.1, -240.5)	106.0	<0.001	1.3	0.859 (0.775-0.943)
Ring 2	720.38 ± 235.25	1116.3 ± 263.87	-320.3 (-439.3, -201.3)	60.71	<0.001	1.55	0.859 (0.789-0.93)
Ring 3	794.05 ± 296.4	1049.75 ± 223.87	-200.4 (-305.9, -94.8)	53.8	<0.001	1.02	0.816 (0.734-0.898)
Ring 4	804.6 ± 233.65	1080.78 ± 231.84	-226.3 (-341.08, -111.5)	58.57	<0.001	1.19	0.788 (0.698-0.878)
Ring 5	958.73 ± 296.4	1160.3 ± 255.39	-168.9 (-297.6, -40.2)	65.65	0.01	0.747	0.698 (0.594-0.801)
Average	853.62 ± 228.93	1180.54 ± 237.65	-272.8 (-390.1, -155.5)	59.84	<0.001	1.39	0.836 (0.757-0.915)
<b>N1 wave</b>							
Ring 1	497.85 ± 211.254	876.45 ± 187.94	-360.7 (-462.7, -258.7)	52.06	<0.001	1.93	0.921 (0.859-0.984)
Ring 2	445.73 ± 209.27	599.77 ± 162.49	-114.2 (-192.3, -36.1)	39.8	<0.001	0.859	0.769 (0.658-0.878)
Ring 3	421.13 ± 133.39	539.33 ± 126.93	-105.4 (-171.3, -39.6)	33.6	<0.001	0.91	0.775 (0.674-0.877)
Ring 4	403.08 ± 97.79	515.19 ± 105.55	-100.5 (-148.1, -52.8)	24.31	<0.001	1.09	0.799 (0.703-0.892)
Ring 5	488.13 ± 188.94	538.1 ± 118.63	-46.1 (-122.3, 30.1)	38.8	0.236	0.34	0.709 (0.601-0.817)
Average	451.18 ± 122.12	613.77 ± 104.32	-145.4 (-199.1, -91.6)	27.43	<0.001	1.47	0.843 (0.75-0.93)
<b>N2 wave</b>							
Ring 1	751.35 ± 314.75	1399.65 ± 435.44	-776.7 (-1015.8, -537.6)	122.0	<0.001	1.62	0.901 (0.835-0.966)
Ring 2	639.08 ± 213.71	927.99 ± 192.47	-300.8 (-406.7, -195.0)	53.9	<0.001	1.45	0.85 (0.768-0.932)
Ring 3	581.96 ± 215.11	864.17 ± 205.15	-311.8 (-422.1, -201.6)	56.23	<0.001	1.35	0.838 (0.755-0.92)
Ring 4	672.65 ± 181.28	807.62 ± 286.05	-125.6 (-239.8, -11.28)	58.27	0.031	0.53	0.723 (0.627-0.819)
Ring 5	789.33 ± 285.99	942.99 ± 258.93	-194.9 (-316.16, -73.8)	61.8	<0.001	0.57	0.638(0.528-0.749)
Average	686.87 ± 189.43	988.48 ± 199.42	-341.9 (-442.9, -240.9)	51.53	<0.001	1.54	0.849 (0.77-0.928)
<b>P100 wave</b>							
Amplitude (µV)	7.62 ± 2.97	11.04 ± 2.89	-3.3 (-4.7, -1.8)	0.75	<0.05	1.17	0.825 (0.742-0.908)
<b>mfERG Implicit times (ms)</b>							
<b>P1 wave</b>							
Ring 1	51.36 ± 3.73	47.13 ± 4.47	3.9 (2.1, 5.8)	0.93	<0.001	0.997	0.781 (0.699-0.864)
Ring 2	49.31 ± 4.8	45.13 ± 3.29	3.7 (2.2, 5.2)	0.75	<0.001	1.08	0.827 (0.746-0.909)

Ring 3	48.2 ± 5.35	44.03 ± 3.48	4.07 (2.4, 5.7)	0.84	<0.001	0.994	0.785 (0.694–0.876)
Ring 4	48.61 ± 5.44	43.72 ± 3.29	4.25 (2.6, 5.9)	0.84	<0.001	1.185	0.81 (0.73–0.889)
Ring 5	48.42 ± 5.36	43.26 ± 3.29	4.3 (2.7, 6.04)	0.85	<0.001	1.26	0.818 (0.736–0.9)
Average	49.18 ± 4.47	44.65 ± 3.3	4.07 (2.58, 5.57)	0.76	<0.001	1.21	0.837 (0.762–0.911)
<b>N1 wave</b>							
Ring 1	31.1 ± 6.46	26.27 ± 3.59	3.9 (1.7, 6.2)	1.1	<0.001	1.02	0.813 (0.73–0.894)
Ring 2	28.42 ± 5.55	26.62 ± 3.92	2.04 (–0.5, 4.1)	1.1	0.056	0.39	0.678 (0.566–0.792)
Ring 3	28.31 ± 4.84	26.23 ± 3.5	2.3 (0.58, 4.1)	0.9	0.009	0.52	0.74 (0.64–0.839)
Ring 4	28.6 ± 5.29	26.3 ± 3.4	2.2 (0.46, 4.0)	0.9	0.014	0.56	0.724 (0.629–0.82)
Ring 5	27.9 ± 6.67	25.9 ± 4.93	2.8 (–0.11, 5.7)	1.48	0.059	0.36	0.645 (0.536–0.753)
Average	28.87 ± 5.19	26.27 ± 3.4	2.67 (0.78, 4.6)	0.97	0.006	0.64	0.746 (0.65–0.843)
<b>N2 wave</b>							
Ring 1	71.03 ± 5.49	67.38 ± 6.9	3.9 (0.87, 7.1)	1.58	0.012	0.56	0.739 (0.646–0.831)
Ring 2	66.12 ± 4.67	64.18 ± 6.14	1.3 (–1.07, 3.7)	1.21	0.281	0.34	0.685 (0.587–0.784)
Ring 3	62.23 ± 9.69	62.42 ± 5.77	1.57 (–0.74, 3.9)	1.18	0.183	0.02	0.645 (0.543–0.747)
Ring 4	63.79 ± 4.69	61.9 ± 5.65	1.21 (–1.17, 3.6)	1.21	0.32	0.35	0.701 (0.605–0.97)
Ring 5	63.22 ± 4.07	61.58 ± 5.45	1.62 (–0.59, 3.8)	1.12	0.15	0.32	0.685 (0.585–0.784)
Average	65.28 ± 4.32	63.49 ± 5.65	1.93 (–0.37, 4.2)	1.18	0.1	0.34	0.725 (0.63–0.819)
<b>P1/N1</b>							
Ring 1	1.76 ± 0.5	2.11 ± 0.66	0.34 (0.03, 0.65)	0.16	0.029	0.57	0.318 (0.215–0.944)
Ring 2	1.85 ± 0.73	1.95 ± 0.61	–0.106 (–0.47, 0.26)	0.19	0.568	0.15	0.526 (0.411–0.642)
Ring 3	2.01 ± 0.64	2.03 ± 0.58	0.07 (–0.26, 0.39)	0.17	0.692	0.03	0.521 (0.411–0.632)
Ring 4	2.06 ± 0.59	2.16 ± 0.58	–0.06 (–0.35, 0.23)	0.15	0.673	0.17	0.525 (0.413–0.638)
Ring 5	2.09 ± 0.66	2.23 ± 0.61	–0.103 (–0.39, 0.19)	0.15	0.484	0.22	0.552 (0.437–0.668)
Average	2.03 ± 0.49	2.02 ± 0.47	0.027 (–0.24, 0.04)	0.13	0.838	0.02	0.489 (0.379–0.599)
<b>P100 wave</b>							
Latency (ms)	120.01 ± 6.99	108.36 ± 4.84	12.0 (8.8, 15.1)	1.61	<0.05	2.06	0.94 (0.897–0.982)

<sup>a</sup>Generalised estimating equations parameter estimates.

<sup>b</sup>Area under Receiver operator characteristic curve.

<sup>c</sup>Wald's 95% confidence intervals as determined in GEE model.

<sup>d</sup>Effect size calculated by Hedge's *g*.

S.E.: Standard error

BCVA: Best-corrected visual acuity.

logMAR: log of minimum angle of resolution.

mfERG: multifocal electroretinogram.

CI: Confidence interval.

Bold signifies significant *p* values after considering multiple comparisons (Bonferroni)

AUC: area under curve.

TABLE 2. Disease characteristics of AD cases (Median).

AD cases (N = 20)	
Disease duration (years)	2
Mini Mental State Examination score	17.5
Global Deterioration Scale score	4
Global Cognitive Dementia Rating score	1
Cognitive Dementia Rating Scale Sum-of-boxes score	5.5

of the ROC curves (Table 1) of mfERG and pattern VEP revealed largest AUC of P100 latency (AUC = 0.94; 95% CI: 0.897-0.982) followed by N1 ring 1 amplitude (AUC = 0.921; 95% CI: 0.859-0.984), N2 ring 1 amplitude (AUC = 0.901; 95% CI: 0.835-0.966) and P1 ring 1 amplitude (AUC = 0.859; 95% CI: 0.775-0.943).

### Correlation of Structural and Functional Parameters with Disease Characteristics

Disease duration significantly correlated with contrast sensitivity reduction ( $r = -0.34$ ,  $p = .042$ ) (Table 3). Contrast sensitivity reduction was positively correlated with P100 amplitude ( $r = 0.385$ ,  $p = .014$ ). No correlation was found among MMSE scores and OCT or electrophysiological parameters. However, disease severity denoted by CDR-SOB was found to have negative correlation with RNFL average thickness ( $r = -0.596$ ,  $p < .001$ ) and also independently with RNFL thickness superior quadrant ( $r = -0.476$ ,  $p = 0.002$ ) and inferior quadrant ( $r = -0.383$ ,  $p = .015$ ). CDR-SOB also correlated with P1 average amplitude ( $r = -0.41$ ,  $p = .009$ ) and P100 amplitude ( $r = -0.333$ ,  $p = .036$ ). RNFL average thickness had positive association with RNFL thickness in superior quadrant ( $r = 0.771$ ,  $p < .001$ ) and RGCL thickness in superior sector ( $r = 0.388$ ,  $p = .013$ ) and infero-nasal sector ( $r = 0.322$ ,  $p = .043$ ).

TABLE 3. Summary of correlation among disease duration, MMSE, and CDR scale with the structural and functional changes detected in eyes of AD cases (N = 40) (<sup>a</sup>Pearson's correlation coefficient).

		$r^a$	$P$ value
Duration	Contrast	-0.34	.042
	RGCL supero-nasal sector	-0.367	.028
	RGCL average	-0.34	.042
	P1 amplitude average	-0.447	.006
	P1/N1 average	-0.414	.012
MMSE	P1/N1 average	-0.572	<.001
CDR sum of boxes	RNFL superior quadrant	-0.476	.002
	RNFL inferior quadrant	-0.383	.015
	RNFL average	-0.596	<.001
	P1 amplitude average	-0.41	.009
	P100 amplitude	-0.333	.036

MfERG and pattern VEP amplitudes were positively correlated with RNFL average thickness and negatively correlated with P100 latency ( $r = -0.4$ ,  $p = .011$ ) (Table 4). GCL average thickness was correlated independently with GCL infero-nasal sector ( $r = 0.853$ ,  $p < .001$ ) followed by inferior sector thickness ( $r = 0.828$ ,  $p < .001$ ) and with P100 amplitude ( $r = 0.331$ ,  $p = .037$ ). Macular volume was positively correlated with GCL thickness in infero-temporal sector ( $r = 0.331$ ,  $p = .037$ ). P100 amplitude positively correlated with mfERG amplitudes.

### Agreement between Cognitive Scales Used (Table 5)

Subgroup analysis was done to compare the discriminant abilities of the two scoring systems used to categorize patients into different stages of AD. It was observed that six patients labelled as mild AD by CDR were staged as moderate AD by GDS. Only two eyes were staged as belonging to a severe AD case, hence they were not included for analysis. The

TABLE 4. Correlation between structural and functional changes detected in inner and outer layers of retina in AD eyes (N = 40) (<sup>a</sup>Pearson's correlation coefficient).

		$r^a$	$P$ value	
Contrast sensitivity	p100 amplitude	0.385	.014	
	RNFL average			
	RNFL superior quadrant	0.771	<.001	
	RNFL inferior	0.682	<.001	
	RNFL temporal	0.458	.003	
	RGCL superior sector	0.388	.013	
	RGCL infero-nasal	0.322	.043	
	P1 amplitude average	0.454	.003	
	N1 amplitude average	0.417	.007	
	N2 amplitude average	0.408	.009	
	P100 amplitude	0.698	<.001	
	P100 latency	-0.4	.011	
RGCL average	RGCL superior sector	0.779	<.001	
	RGCL supero-nasal	0.825	<.001	
	RGCL infero-nasal	0.853	<.001	
	RGCL inferior	0.828	<.001	
	RGCL infero-temporal	0.575	<.001	
	RGCL supero-temporal	0.621	<.001	
	P100 amplitude	0.331	.037	
	Macular volume	RGCL inferotemporal	0.331	.037
		P100 amplitude	RNFL average	0.698
RGCL average			0.331	.037
RMS average			0.505	.001
P1 amplitude average			0.463	.003
N1 amplitude average	0.495		.001	
	N2 amplitude average	0.365	.02	
	N2 time average	-0.577	<.001	
	P100 latency	-0.355	.025	
P100 latency	RNFL superior	-0.323	.042	
	RGCL supero-nasal	-0.314	.049	
	RNFL average	-0.4	.011	
	P1 amplitude	-0.349	.027	
	P100 amplitude	-0.355	.025	

TABLE 5. Comparison of AD cases scored according to the two scales used.

		CDR		Total
		Mild	Moderate	
GDS	Mild	13	0	13
	Moderate	3	3	6
	Total	26	3	19

two scoring systems were found to have a moderate agreement (Cohen's kappa = 0.5778, 95% CI: 0.18 - 0.975) with each other.

## DISCUSSION

AD patients in our study demonstrated normal visual acuity in the presence of significantly reduced contrast sensitivity. Our study patients were comparatively in the milder stages of dementia explaining differing results in comparison to other reports, which have reported reduced visual acuity.<sup>12</sup> The median scores of CDR and GDS scales both indicated the presence of mild dementia with moderate concordance between the two scales used. Although frank visual deficit may occur only in the advanced stages of the disease, almost 43% of early AD patients may have complex visual symptoms like defects in contrast sensitivity, right left distinction, visuomotor skill impairment, prosopagnosia, hallucinations, complex deficits in colour vision, Balint's syndrome, etc.<sup>13</sup> This visual dysfunction was earlier thought to be due to aberrations in the visual cortex and higher cortical areas; however, pre-cortical degeneration has also been suggested to be playing a role.<sup>2,3,6</sup>

Obtaining the ophthalmological tests was a quite challenging task for the laboratory personnel since AD patients were often uncooperative and needed to be in a lucid state to clearly understand and follow commands. Hence, the caregivers were asked to ensure that all subjects were well rested after a good night's sleep before performing the ophthalmological investigations. All subjects were initially made comfortable in the presence of the primary caregiver before performing the tests, and then only testing was started, with adequate importance given to the maintenance of fixation. The electrophysiology station had a fixation monitor on screen which was used to ascertain maintenance of fixation throughout the duration of the tests.

### Structural Changes

We found that RNFL and RGCL thickness were significantly reduced in all quadrants. A number of studies has shown RNFL thinning using both time-domain and spectral-domain OCT machines with similar

findings.<sup>2,3,13</sup> RNFL thinning has been hypothesized to be due to a degeneration of the GCL axons which may precede the cognitive impairment in AD.<sup>14,15</sup> Advanced OCT technology allowed us to analyze the GCL separately from RNFL and nullified the effect of variability of RNFL in healthy population, in contrast to previous literature where the two layers have been studied together. Till date, few studies have separately analyzed GCL on OCT and found significantly reduced overall GCL thickness in AD eyes.<sup>16,17</sup>

Interestingly, most studies have shown a significant reduction of RNFL thickness in all quadrants of retina, but more predominantly in the superior and inferior quadrants.<sup>18,19</sup> In our study, higher AUCs for RNFL thickness reduction were seen in the superior and inferior quadrants and AUC of GCL was maximum in the inferotemporal and superior sectors, thereby corresponding to the changes in RNFL. Our observations may have reflected the fact that maximum number of nerve fibers converge on the optic disc superiorly and inferiorly and hence, neurodegeneration affected them preferentially. These changes were further reflected in the significant loss of macular volume in the AD group. In addition, based on the AUC findings, we infer that GCL may be a better indicator of disease status than RNFL, which is similar to one previous OCT-based study.<sup>16</sup> GCL thinning may precede loss of neurons in hippocampus of human brain, similar to what has been seen in mouse models of AD.<sup>20</sup> However, all of our AD patients already demonstrated cortical atrophy when we evaluated them, probably because of which the global GCL thinning was noted.

### Functional Changes

In mfERG, we found significant reduction of P1, N1, and N2 amplitudes with a significantly higher P1 implicit time in the foveal (central 2°) and parafoveal (2–15°) regions. One study has reported similar results previously.<sup>21</sup> Detection of mfERG dysfunction in AD cases was peculiar, and although the exact cause cannot be pointed out, it may be due to an underlying outer retinal involvement, probably secondary to local amyloid deposition.<sup>22</sup> This needs to be investigated further with pattern ERG and targeted investigations for the detection of local amyloid in the retina and by correlating them with structural parameters.

We found a reduced amplitude and prolonged latency of pattern VEP in AD cases. AD patients have previously been reported to have an abnormal flash VEP with prolonged latency of the positive component.<sup>23</sup> But pattern VEP studies have been equivocal, with varying results.<sup>24,25</sup> This change in pattern VEP may be because of an underlying

macular dysfunction, as has been proposed previously.<sup>26</sup> pVEP measures the integrity of the entire visual pathway. Since all of our AD patients had presence of cortical atrophy, this may also be the reason for deranged VEPs. We found that AUC of P100 latency was highest among all the electrophysiological parameters indicating that pattern reversal VEP may be a better predictor of the electrical disturbance in AD. We did not detect any changes in the visual fields of the patients and the threshold readings were within normal limits.

### Correlation between Structural and Functional Changes

Significant correlation found between contrast sensitivity reduction and pattern VEP amplitude signifies the early subclinical electrical disturbance in the neural system in AD. Disease duration also correlated with severity of OCT and mfERG changes in AD patients with patients having longer duration having more severe affection of the macula. While trying to correlate the disease severity scores with the ophthalmological investigations, we could find no correlation of MMSE with the investigations. Disease severity measured as CDR-SOB correlated significantly with OCT and electrophysiological derangement, the strongest correlation being with average RNFL thickness. This again reemphasizes the role of OCT in identifying retinal thinning and indicating a simultaneous analogy to the severity of the AD disease process also, which is a novel finding of our study.

We found that structural alterations in inner retinal layers on OCT were correlated significantly with foveal electrical dysfunction detected by mfERG. This structural-functional correlation was manifested only as a subclinical contrast sensitivity impairment since the visual acuities were normal for all subjects. OCT changes also correlated with pattern VEP amplitude and average RNFL thickness. Previously, AD patients have been shown to have a significant correlation between the VEP latency and disease severity and VEP amplitude with disease duration.<sup>26</sup> Since we did not perform detailed cognitive and psychophysical status evaluation of patients, we were not able to establish the extent of neurological defects present in the patients, e.g., apraxia or aphasias affecting the ocular function.

### Concept of Retinal Amyloid

Our findings may shed some light on the involvement of retina in AD. Recently ocular AD has been described, which involves localized amyloid deposition in the retina. Previously, histological studies in retina

from AD patients have found a vacuolated and 'frothy' appearance of the cytoplasm of degenerated RGCs instead of characteristic neurofibrillary tangles which is rather unique to AD.<sup>27</sup> Koronyo-Hamaoui *et al.* first visualized curcumin bound fluorescent amyloid beta (A $\beta$ ) in the retinas of transgenic mice.<sup>28</sup> Such curcumin binding of A $\beta$  has also been demonstrated in the retina and brain of AD donors, although this was absent in healthy controls. Although, A $\beta$  accumulation in photoreceptor outer segments associated with electrophysiological abnormalities has been seen in few animal models, photoreceptor death has not been noted in the progressed stages in another mouse AD model.<sup>29,30</sup> Few studies have reported A $\beta$  plaques in the GCL with ganglion cell destruction along with electrophysiological dysfunction.<sup>31,32</sup> Recent mice studies also have shown an association between retinal A $\beta$  burden and inner retinal function.<sup>33,34</sup> It is of importance that the GCL cell body destruction has been seen to precede the loss of dendrites in hippocampal pyramidal neurons in Tg2576 mice with frank pathological changes of AD.<sup>20</sup> Non-invasive hyperspectral imaging technology of retina also suggests that early A $\beta$  deposition-related retinal dysfunction may begin during the asymptomatic stage of AD.<sup>35</sup> In contrast to these findings, absence of A $\beta$  deposits in retina of confirmed AD patients has also been reported.<sup>36</sup> Recently, demonstration of tau deposits in the retina of 301 S human tau mouse line using *in vivo* scanning laser ophthalmoscopy, and also in AD patient retina, has led authors to suggest that hyperphosphorylated tau proteins in retina may also be another marker for AD.<sup>37</sup> Neuroscientists are unclear as to whether A $\beta$  accumulation facilitates the pathogenicity of tau in the cortex or tau accumulation precedes diffuse cortical A $\beta$  deposition.<sup>36</sup> To what extent this amyloid is pathogenetic in the retina or whether it is just an age-related change is unknown. Moreover, whether ocular AD is a completely different disease process or a part of the same spectrum as AD is also not known for sure. However, our findings may indicate the possibility of a primary photoreceptor dysfunction in AD patients apart from the ganglion cell dysfunction. A pattern ERG-based evaluation may be more specific towards the same.

### Future Direction

The primary diagnosis of Alzheimer's disease is based on NINDS-ADRDA clinical criteria and on a battery of cognitive tests like the MMSE, CDR, etc., supplanted by imaging modalities like MRI and FDG-PET. Efforts have been on for the identification of biomarkers for preclinical diagnosis of Alzheimer's or screening of patients at risk of Alzheimer's before definite cerebral atrophy sets in. The next generation of imaging for AD



diagnosis is targeted towards detection of amyloid/tau in brain and retina before the onset of full-fledged dementia, based on the observation that retinal A $\beta$  deposits precede brain A $\beta$  deposition.<sup>38</sup> PET imaging targeted for tau or A $\beta$  deposition early in the disease, in the inferior temporal cortex has been considered an early AD biomarker; however, the invasiveness of this test is a drawback. In this regard, as a non-invasive rapid screening or diagnostic tool, ocular examination is believed to gain an important status in future. Ganglion cell layer, contrast sensitivity, and mfERG have the potential to become sensitive indicators in early disease stages, with a significant correlation with disease attributes. Reduction of total brain volume has been found to have a weak association with GCL thinning; however, reduction of grey matter volume in occipital and temporal lobes has been seen to be strongly associated with GCL thinning, independent of systemic vascular risk factors.

Although OCT can assess this small part of the CNS (viz. retinal layers) with high accuracy, as seen in our findings, however, it has to be determined if these patterns are exclusive to AD. Recently, deep-learning-based tools of artificial intelligence (AI) have been studied to understand the progression and referral patterns of retinal diseases using OCT.<sup>39</sup> Also, a recurrent neural network-based predictive model for AD progression has been developed using the GDS and CDR scales.<sup>40</sup> However, they have not included more accurate diagnostic testing for AD, e.g., AD biomarkers. In future, such AI models may be developed, incorporating OCT and electrophysiology data along with cognitive classification schemes to accurately predict the progression from cognitively normal to dementia stage.

The limitation of this study was that we did not evaluate mild cognitive impairment cases and hence could not record the natural history of structural and electrophysiological changes, because of design limitations. Pattern electroretinogram is a more useful test for targetedly ascertaining ganglion cell dysfunction and this may be analysed in AD patients in a future study. We also lacked in the number of patients with severe AD who could cooperate for the study. The repeatability and consistency of the tests need to be ascertained by conducting large-scale population-based studies to minimise chances of false positives. Moreover, we did not use any targeted investigation to detect pathology in the photoreceptor layer of the macula which may have given rise to the electrical changes that we detected. Few studies believe that these changes are because of local A $\beta$  deposition, but whether this is a part of the overall AD pathogenesis is not clear. Larger studies utilising markers for such deposits and

correlating their presence with cognitive status of patients may give us some answers.

## Conclusion

Detection of inner retinal thinning, especially GCL thinning, along with pre-determined cut-offs by OCT may help improve the diagnostic accuracy of AD in the earliest stages, as observed by the correlation between these parameters and electrophysiological disturbances and disease severity, whereas neuroimaging modalities can only pick up changes in the central nervous system with established atrophy.

## AUTHORSHIP STATEMENT

Authors' contributions: SS, RS, MT, DV, PS, RT, SP were involved in study design. SS, RS, MT, and DV were involved in data collection. SS and RS performed the data analyses. RS, MT, and DV provided guidance about the data analysis, interpretation, and presentation of the data. PK helped in ophthalmic investigations. All authors critically reviewed and edited the article. The authors have no funding sources to declare.

## ORCID

Sagnik Sen  <http://orcid.org/0000-0001-5835-5371>

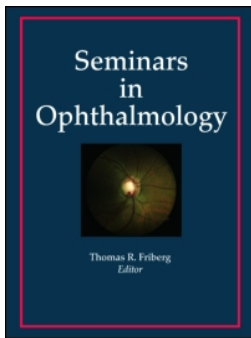
## DATA AVAILABILITY

With authors, will be made available on request.

## REFERENCES

1. Mathuranath PS, George A, Ranjith N, et al. Incidence of Alzheimer's disease in India: a 10 years follow-up study. *Neurol India*. 2012;60:625–630. doi:10.4103/0028-3886.105198.
2. Blacker D, Albert MS, Bassett SS, et al. Reliability and validity of NINCDS-ADRDA criteria for Alzheimer's disease. The National Health Institute of Mental Health Genetics initiative. *Arch Neurol*. 1994;51:1198–1204. doi:10.1001/archneur.1994.00540240042014.
3. Iseri PK, Altınış O, Tokay T, Yüksel N. Relationship between cognitive impairment and retinal morphological and visual functional abnormalities in Alzheimer disease. *J Neuroophthalmol*. 2006;26:18–24. doi:10.1097/01.wno.0000204645.56873.26.
4. Güneş A, Demirci S, Tök L, Tök Ö, Demirci S. Evaluation of retinal nerve fiber layer thickness in Alzheimer's disease using spectral-domain optical coherence tomography. *Turk J Med Sci*. 2014;44:1–4.
5. Guo L, Duggan J, Cordeiro MF. Alzheimer's disease and Retinal Neurodegeneration. *Curr Alzheimer Res*. 2010;7:3–14. doi:10.2174/156720510790274491.
6. Berisha F, Feke GT, Trempe CL, et al. Retinal abnormalities in early Alzheimer's disease. *Invest Ophthalmol Vis Sci*. 2007;48:2285–2289. doi:10.1167/iovs.06-1029.

7. Marziani E, Pomati S, Ramolfo P, et al. Evaluation of retinal nerve fiber layer and ganglion cell layer thickness in Alzheimer's disease using spectral domain optical coherence tomography. *Invest Ophthalmol Vis Sci.* 2013;54:5953–5958. doi:10.1167/iovs.13-12046.
8. Reisberg B, Ferris SH, de Leon MJ, Crook T. The global deterioration scale for assessment of primary degenerative dementia. *Am J Psychiatry.* 1982;139:1136–1139.
9. O'Bryant SE, Waring SC, Cullum CM, et al. Staging dementia using clinical dementia rating scale sum of boxes scores: a Texas Alzheimer's research consortium study. *Arch Neurol.* 2008;65:1091–1095. doi:10.1001/archneur.65.8.1091.
10. Hood DC, Bach M, Brigell M, et al. ISCEV standard for clinical multifocal electroretinography (mfERG) (2011 edition). *Doc Ophthalmol.* 2012;124:1–13. doi:10.1007/s10633-011-9296-8.
11. Odom JV, Bach M, Brigell M, et al. ISCEV standard for clinical visual evoked potentials: (2016 update). *Doc Ophthalmol.* 2016;133:1–9. doi:10.1007/s10633-016-9553-y.
12. Trick GL, Trick LR, Morris P, Wolf M. Visual field loss in senile dementia of the Alzheimer's type. *Neurology.* 1995;45:68–74. doi:10.1212/WNL.45.1.68.
13. Mendez MF, Mendez MA, Martin R, et al. Complex visual disturbances in Alzheimer's disease. *Neurology.* 1990;40:439–443. doi:10.1212/WNL.40.3\_Part\_1.439.
14. Garcia-Martin ES, Rojas B, Ramirez AI, et al. Macular thickness as a potential biomarker of mild Alzheimer's disease. *Ophthalmology.* 2014;121:1149–1153. doi:10.1016/j.ophtha.2013.12.023.
15. Ascaso FJ, Cruz N, Modrego PJ, et al. Retinal alterations in mild cognitive impairment and Alzheimer's disease: an optical coherence tomography study. *J Neurol.* 2014;261:1522–1530. doi:10.1007/s00415-014-7374-z.
16. Cheung CY, Ong YT, Hilal S, et al. Retinal ganglion cell analysis using high-definition optical coherence tomography in patients with mild cognitive impairment and Alzheimer's Disease. *J Alz Dis.* 2015;45:45–56. doi:10.3233/JAD-141659.
17. Golzan SM, Goozee K, Georgevsky D, et al. Retinal vascular and structural changes are associated with amyloid burden in the elderly: ophthalmic biomarkers of preclinical Alzheimer's disease. *Alzheimers Res Ther.* 2017;1(9):13. doi:10.1186/s13195-017-0239-9.
18. Blanks JC, Schmidt SY, Torigoe Y, Porrello KV, Hinton DR, Blanks RH. Retinal pathology in Alzheimer's disease. II. Regional neuron loss and glial changes in GCL. *Neurobiol Aging.* 1996;17:385–395. doi:10.1016/0197-4580(96)00009-7.
19. Blanks JC, Torigoe Y, Hinton DR, Blanks RH. Retinal pathology in Alzheimer's disease. I. Ganglion cell loss in foveal/parafoveal retina. *Neurobiol Aging.* 1996;17:377–384. doi:10.1016/0197-4580(96)00010-3.
20. Williams PA, Thirgood RA, Oliphant H, et al. Retinal ganglion cell dendritic degeneration in a mouse model of Alzheimer's disease. *Neurobiol Aging.* 2013;34:1799–1806. doi:10.1016/j.neurobiolaging.2013.01.006.
21. Moschos MM, Markopoulos I, Chatziralli I, et al. Structural and functional impairment of the retina and optic nerve in Alzheimer's disease. *Curr Alz Res.* 2012;9:782–788. doi:10.2174/156720512802455340.
22. Sartucci F, Borghetti D, Bocci T, et al. Dysfunction of the macular stream in Alzheimer's disease evaluated by pattern electroretinograms and visual evoked potentials. *Brain Res Bull.* 2010;82:169–176. doi:10.1016/j.brainresbull.2010.04.001.
23. Weinstein GW, Odom JV, Cavender S. Visually evoked potentials and electroretinography in neurological evaluation. *Neurol Clin.* 1991;9:225–242. doi:10.1016/S0733-8619(18)30312-8.
24. Krasodomska K, Lubinski W, Potemkowski A, et al. Pattern electroretinogram (PERG) and pattern visual evoked potential (PVEP) in the early stages of Alzheimer's disease. *Doc Ophthalmol.* 2010;121:111–121. doi:10.1007/s10633-010-9238-x.
25. Kromer R, Serbecic N, Hausner L, Froelich L, Beutelspacher SC. Comparison of visual evoked potentials and retinal nerve fiber layer thickness in Alzheimer's disease. *Front Neur.* 2013;4:1–6. doi:10.3389/fneur.2013.00203.
26. Holder GE. Electrophysiological assessment of optic nerve disease. *Eye.* 2004;18:1133–1143. doi:10.1038/sj.eye.6701573.
27. Blanks JC, Hinton DR, Sadun AA, et al. Retinal ganglion cell degeneration in Alzheimer's disease. *Brain Res.* 1989;501:364–372. doi:10.1016/0006-8993(89)90653-7.
28. Koronyo-Hamaoui M, Koronyo Y, Ljubimov AV, et al. Identification of amyloid plaques in retinas from Alzheimer's patients and noninvasive in vivo optical imaging of retinal plaques in a mouse model. *Neuroimage.* 2011;54:S204–S217. doi:10.1016/j.neuroimage.2010.06.020.
29. Hoh KJ, Lenassi E, Jeffery G. Viewing ageing eyes: diversities of amyloid beta accumulation in the ageing mouse retina and the upregulation of macrophages. *PLoS ONE.* 2010;5:e13127. doi:10.1371/journal.pone.0013127.
30. Perez SE, Lumayag S, Kovacs B, Mufson EJ, Xu S. Beta-amyloid deposition and functional impairment in the retina of the APP<sup>swE</sup>/PS1<sup>DeltaE9</sup> transgenic mouse model of Alzheimer's disease. *Invest Ophthalmol Vis Sci.* 2009;50:793–800. doi:10.1167/iovs.08-2384.
31. Alexandrov PN, Pogue A, Bhattacharjee S, Lukiw WJ. Retinal amyloid peptides and complement factor H in transgenic models of Alzheimer's disease. *Neuroreport.* 2011;22:623–627. doi:10.1097/WNR.0b013e3283497334.
32. Dutescu RM, Li QX, Crowston J, et al. Amyloid precursor protein processing and retinal pathology in mouse models of Alzheimer's disease. *Graefes Arch Clin Exp Ophthalmol.* 2009;247:1213–1221. doi:10.1007/s00417-009-1060-3.
33. Parthasarathy R, Chow KM, Derafshi Z, et al. Reduction of amyloid-beta levels in mouse eye tissues by intra-vitreally delivered neprilysin. *Exp Eye Res.* 2015;138:134–144. doi:10.1016/j.exer.2015.06.027.
34. Gupta VK, Chitranshi N, Gupta VB, et al. Amyloid beta accumulation and inner retinal degenerative changes in Alzheimer's disease transgenic mouse. *Neurosci Lett.* 2016;623:52–56. doi:10.1016/j.neulet.2016.04.059.
35. More SS, Vince R. Hyperspectral imaging signatures detect amyloidopathy in Alzheimer's mouse retina well before onset of cognitive decline. *ACS Chem Neurosci.* 2015;6:306–315. doi:10.1021/acscn.500242z.
36. Maass A, Lockhart SN, Harrison TM, et al. Entorhinal tau pathology, episodic memory decline, and neurodegeneration in aging. *J Neurosci.* 2018;38:530–543. doi:10.1523/JNEUROSCI.2028-17.2017.
37. Schön C, Hoffmann NA, Ochs SM, et al. Long-term in vivo imaging of fibrillar tau in the retina of P301S transgenic mice. *PLoS ONE.* 2012;7:e53547. doi:10.1371/journal.pone.0053547.
38. Pike KE, Savage G, Villemagne VL, et al. Beta amyloid imaging and memory in non-demented individuals: evidence for preclinical Alzheimer's disease. *Brain.* 2007;130:2837–2844. doi:10.1093/brain/awm238.
39. Fauw J, Ledsam JR, Romera-Paredes B, et al. Clinically applicable deep learning for diagnosis and referral in retinal disease. *Nat Med.* 2018;24:1342–1350. doi:10.1038/s41591-018-0107-6.
40. Wang T, Qiu RG, Yu M. Predictive modeling of the progression of Alzheimer's disease with recurrent neural networks. *Sci Rep.* 2018;8:9161. article number. doi:10.1038/s41598-018-27337-w.



## Multi-parametric magnetic resonance imaging characterization of orbital lesions: A triple-blind study

Camilla Russo, Diego Strianese, Marianna Perrotta, Adriana Iuliano, Roberta Bernardo, Valeria Romeo, Lorenzo Ugga, Lisa Brunetti, Fausto Tranfa & Andrea Elefante

To cite this article: Camilla Russo, Diego Strianese, Marianna Perrotta, Adriana Iuliano, Roberta Bernardo, Valeria Romeo, Lorenzo Ugga, Lisa Brunetti, Fausto Tranfa & Andrea Elefante (2020): Multi-parametric magnetic resonance imaging characterization of orbital lesions: A triple-blind study, *Seminars in Ophthalmology*, DOI: [10.1080/08820538.2020.1742358](https://doi.org/10.1080/08820538.2020.1742358)

To link to this article: <https://doi.org/10.1080/08820538.2020.1742358>



Published online: 16 Apr 2020.



Submit your article to this journal [↗](#)



View related articles [↗](#)



View Crossmark data [↗](#)



ORIGINAL ARTICLE

# Multi-parametric magnetic resonance imaging characterization of orbital lesions: A triple-blind study

Camilla Russo<sup>1</sup>, Diego Strianese<sup>2,3</sup>, Marianna Perrotta<sup>1</sup>, Adriana Iuliano<sup>3</sup>, Roberta Bernardo<sup>3</sup>, Valeria Romeo<sup>1</sup>, Lorenzo Ugga<sup>1</sup>, Lisa Brunetti<sup>4</sup>, Fausto Tranfa<sup>3</sup>, and Andrea Elefante<sup>1</sup>

<sup>1</sup>Department of Advanced Biomedical Sciences, Università Degli Studi Di Napoli "Federico II", Napoli, Italy, <sup>2</sup>Orbital Unit, CME Department, King Khalid Eye Specialist Hospital, Riyadh, Saudi Arabia, <sup>3</sup>Department of Neuroscience, Odontostomatological and Reproductive Sciences, Università Degli Studi Di Napoli "Federico II", Napoli, Italy, and <sup>4</sup>Neuroradiology Unit, Università Vita-Salute San Raffaele, Milano, Italy

## ABSTRACT

**Background:** Multi-parametric MRI used for preoperative assessment of orbital lesions does not routinely include DCE-MRI, since its accuracy in differential diagnosis of orbital mass is still under debate. Aim of this study is to characterize orbital lesions by multi-parametric MRI, analysing the incremental predictive value of DCE-MRI in differential diagnosis of orbital lesions.

**Methods:** In this prospective triple-blind study, 43 consecutive patients with unilateral orbital lesion underwent conventional multimodal MRI and DCE-MRI before biopsy in a tertiary referral centre. Pre-operative MRI examination including conventional unenhanced MRI protocol, DWI with ADC maps, static CE 3D-T1 w and dynamic CE T1 w sequences, was performed within 1 week from surgery (anterior/lateral orbitotomy depending on location of the lesion, to carry out incisional/excisional biopsy).

**Results:** Comparison between conventional T1 w/T2 w, DWI, CE 3D-T1 w and DCE-MRI groups showed a statistically significant difference in scores distribution ( $p < .001$ ). Statistically significant difference was found between conventional T1 w/T2 w and DWI ( $p < .005$ ), as well as between DWI and CE 3D-T1 w ( $p < .001$ ). Conversely, no significant difference was found between CE 3D-T1 w and DCE ( $p < .005$ ).

**Conclusions and Relevance:** This study confirmed the positive effect of DWI and CE 3D-T1 w on orbital lesions diagnosis when added to conventional T1 w/T2 w sequences, whereas no substantial impact on diagnostic performance was observed with the further addition of DCE-MRI. DCE does not strongly influence diagnostic performance and inter-rater agreement in characterizing orbital lesions; therefore, it should be recommended in selected patients whose assessment of flow dynamics is particularly useful for management.

**Abbreviations:** US = ultrasonography; MRI = magnetic resonance imaging; CT = computed tomography; STIR = Short-TI Inversion Recovery; DWI = diffusion weighted imaging; DCE-MRI = dynamic contrast-enhanced MRI; SE = Spin-Echo; TSE = Turbo Spin-Echo; THRIVE = T1-weighted high resolution Isotropic Volume Examination (dynamic contrast-enhanced ultrafast spoiled gradient echo); ROI = regions of interest; IRR = inter-rater reliability; TIC = time-intensity curve.

**Keywords:** diffusion weighted imaging, dynamic contrast enhancement, magnetic resonance imaging, orbital mass, perfusion

## INTRODUCTION

Orbital lesions encompass a broad spectrum of benign and malignant space-occupying masses associated with variable manifestations, the most common of which are

proptosis, diplopia and visual impairment.<sup>1,2</sup> Clinical assessment is crucial to guide the initial differential diagnosis and the subsequent instrumental investigations. The most frequent tools used for imaging of the orbital lesions are the CT scan and the MRI.<sup>3</sup>

Received 25 April 2019; accepted 8 March 2020; published online 17 April 2020.

Correspondence: Diego Strianese, Head of the Orbital Unit, Director of the Continuous Medical Education Department, King Khalid Eye Specialist Hospital, Riyadh, Saudi Arabia. E-mail: [diegostrianese@gmail.com](mailto:diegostrianese@gmail.com)



Ultrasonography (US) may provide information about tumour shape, internal reflectivity, and sound attenuation characteristics<sup>4-6</sup>, however, is operator-dependent procedure as well is the US with Doppler modality which may be useful in evaluating the vascular flow of the lesion.<sup>7,8</sup> Magnetic resonance imaging (MRI) is the mainstay imaging modality for orbital lesions, although computed tomography (CT) scan has still a relevant role in the evaluation of calcified/orbital bony lesions, or when MRI is formally contraindicated.<sup>1,9-11</sup>

The conventional MRI protocol for the evaluation of orbital masses usually includes multiplanar T1- and T2-weighted sequences, Short-TI Inversion Recovery (STIR) and T1-weighted sequences with fat saturation obtained after intravenous administration of gadolinium-based contrast media, with a recommended slice thickness of 2–3 mm.<sup>12-14</sup> Diffusion weighted imaging (DWI) has been also integrated in the standard MRI protocol, due to its pivotal role in differentiating between benign and malign tumours or inflammatory and infectious processes on the basis of ADC values.<sup>14-16</sup> Recently, dynamic contrast-enhanced (DCE) MRI, another non-invasive MRI technique has shown to improve the characterization of orbital lesions. This technique allows to obtain specific perfusion parameters, reflecting the microcirculatory structure of the tumour providing more information about tumour angiogenesis and capillary permeability; all these features are known to be related to aggressive behaviour, tumour grade, and overall prognosis.<sup>17</sup> Few studies on the use of DCE-MRI for orbital lesions, have shown specific perfusion patterns useful for differentiating benign to malignant lesions.<sup>17,18</sup> However, the actual diagnostic and prognostic impact of DCE-MRI in the assessment of orbital lesions in routinely practice is still under discussion. Aim of this study is to prospectively evaluate the role of DCE-MRI in diagnostic assessment of orbital masses, in comparison with routine MRI sequences conventionally performed for the study of the orbit.

## MATERIALS AND METHODS

### Participants, Imaging Acquisition and Data Interpretation

We prospectively evaluated 43 patients (20 females; 23 males; mean age  $47 \pm 19$ ) who suffered from acquired unilateral proptosis, who underwent multi-modal MRI examination between January 2016 and December 2018. All patients underwent preoperative MRI no later than 1 week before orbital biopsy on a 1.5 T MRI unit (Intera, Philips Medical Systems, Best, The Netherlands) with an 8-channel head coil. The imaging protocol consisted of: axial Spin-Echo

(SE) T1 w (TR-600, TE-15, FA-90, 256x256, slice thickness 3 mm); axial and coronal Turbo Spin-Echo (TSE) T2 w (TR-4400, TE-100, FA-90, 512x512, slice thickness 3 mm); coronal STIR (TR-2650, TE-90, FA-90, 288x288, slice thickness 3 mm); axial Multi-Shot DWI (TR-3800, TE-90, FA-90, 128x128,  $b = 0-800$  s/mm<sup>2</sup>, number of averages 2, slice thickness 5 mm) with relative ADC maps calculation; coronal dynamic contrast-enhanced ultrafast-spoiled gradient echo (THRIVE) (TR-1.772, TE-1.817, FA-10, 160x160, slice thickness 4 mm) with relative DCE maps calculation; axial post-contrast 3D T1 w SPIR (TR-40.374, TE-4.603, FA-30, 256x256, slice thickness 1.5 mm). ADC maps were obtained by using the Osirix plugin ADC calculation v1.9 ([github.com/mribri999/ADCmap](https://github.com/mribri999/ADCmap)); DCE maps were obtained by using the Olea Sphere® software v3.0 (Olea Medical, La Ciotat, France). Written informed consent was obtained from all patients included in the study. MRI evaluation was performed separately by three different neuroradiologists; all the operators independently drew regions of interest (ROIs) for ADC and DCE calculation. All observers were asked to make a diagnosis based on SE T1 w, TSE T2 w and STIR sequences, and assess whether DWI and relative ADC maps modify their original hypothesis as well as post-contrast T1 w SPIR, dynamic contrast-enhanced THRIVE and relative DCE maps. Final diagnosis was confirmed on tissue-biopsy pathological examination: 31 cases resulted benign; distributed as follow: vascular ( $n = 8$ ; [Figure 1](#)), inflammatory/infectious ( $n = 15$ ; [Figure 2](#)) neoplastic benign ( $n = 8$ ; [Figure 3](#)) while 12 resulted malignant ([Figure 4](#)). Results of histological specimen examination are listed in [Table 1](#).

### Statistical Analysis

At each observer for every step of the MRI evaluation has been attributed a value of 1 for the correct diagnosis and 0 for the incorrect diagnosis; for each patient, the final score was given by the sum of the three observers' scores. The proportion of correct observations for every case at each step of MRI evaluation is graphically represented as a percentage component bar chart in [Figure 5](#).

Upon completion of study data collection, a Friedman's test was then carried out on obtained scores to determine if there were differences in diagnostic performance among conventional T1 w/T2 w, DWI, CE 3D T1 w and DCE. A subsequent post-hoc analysis to assess which pairs of groups were significantly different then each other was performed by using Wilcoxon signed-ranks tests for pairwise comparisons. Finally, Fleiss' kappa statistics was used to compute the inter-rater reliability (IRR) among the three observers for each step of the MRI evaluation.



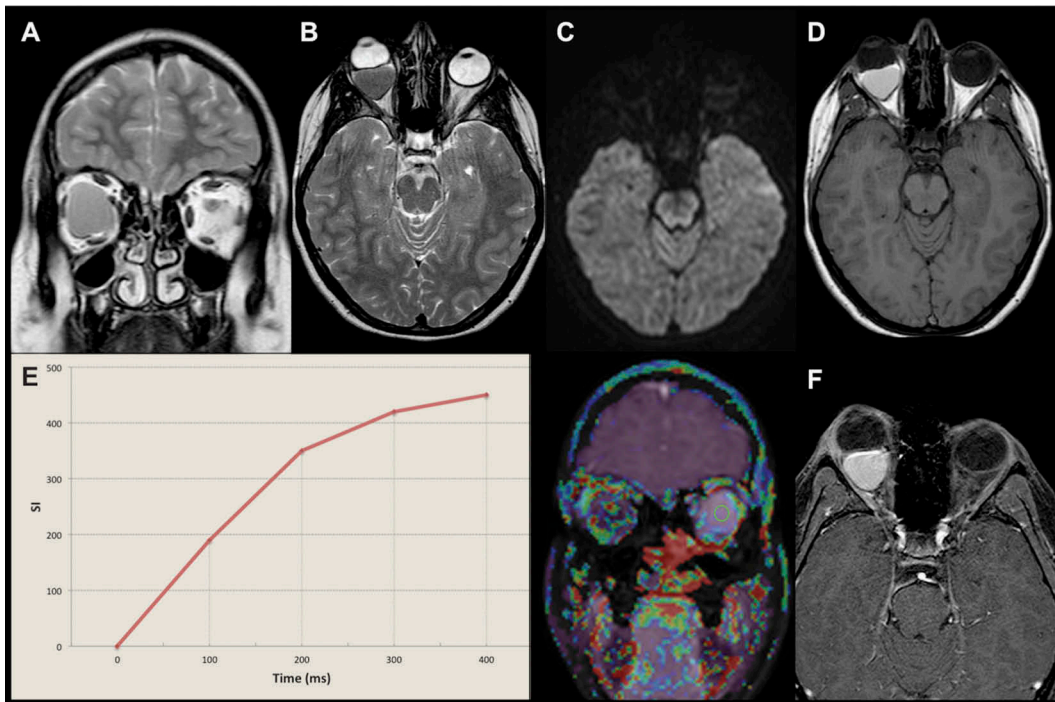


FIGURE 1. Right orbit hemolympangioma with associated exophthalmos in a 16-years-old girl. MRI at the most representative levels: coronal (a) and axial (b) TSE T2 w; axial Msh-DWI (c); axial unenhanced SE T1 w (d); coronal THRIVE and overlaid perfusion colorimetric map, with relative TIC from region of interest within the lesion (e); axial post-contrast 3D T1 w SPIR.

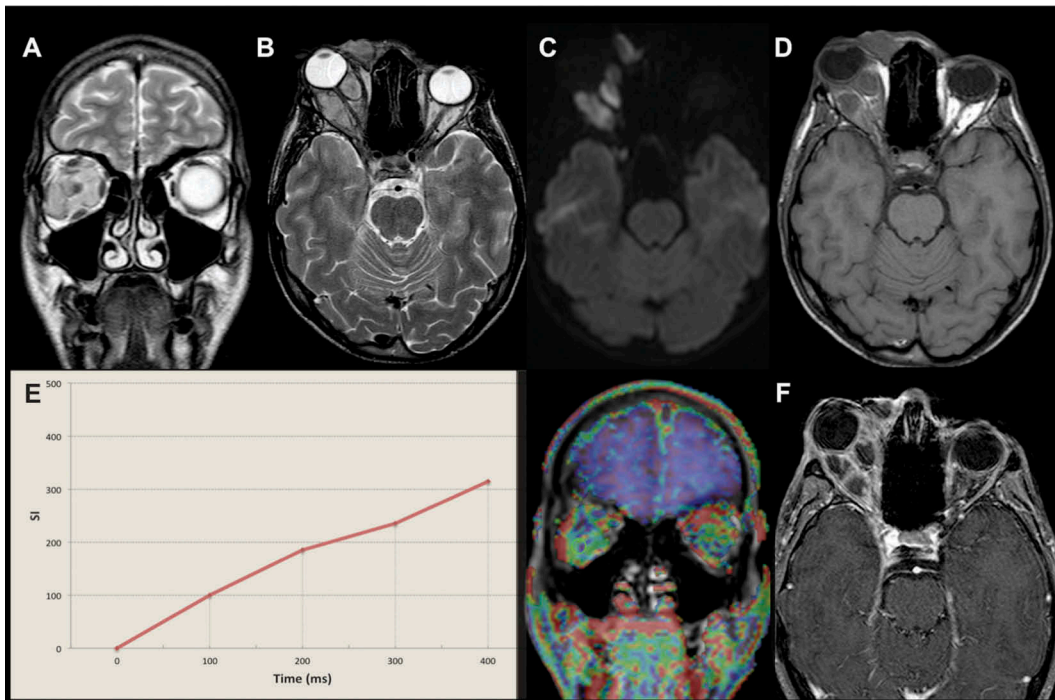


FIGURE 2. Right orbital cellulitis with multiple abscesses due to *S. aureus* infection in a 26-years-old man. MRI at the most representative levels: coronal (a) and axial (b) TSE T2 w; axial Msh-DWI (c); axial unenhanced SE T1 w (d); coronal THRIVE and overlaid perfusion colorimetric map, with relative TIC from region of interest within the lesion (e); axial post-contrast 3D T1 w SPIR.

## RESULTS

Comparison between conventional T1 w/T2 w, DWI, CE 3D T1 w and DCE groups obtained using

Friedman's test showed a statistically significant difference in the scores distribution ( $\chi^2$  r statistic: 22.6674, degrees of freedom: 3,  $p = .00005$ ,  $p < .001$ ). Wilcoxon signed-rank test post-hoc was used to

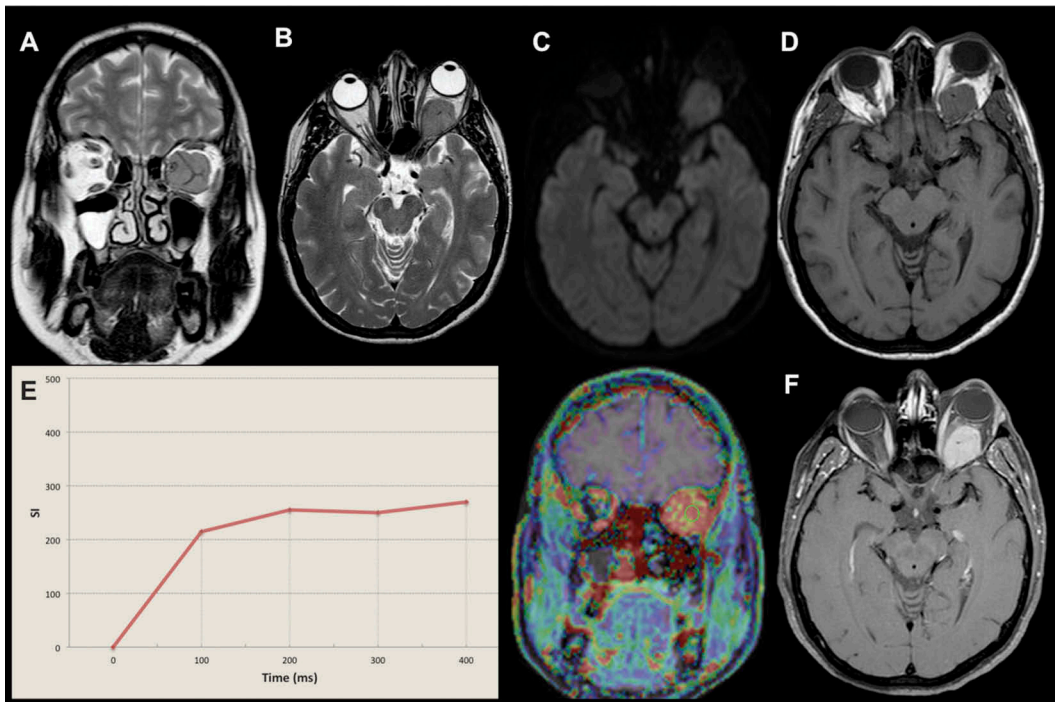


FIGURE 3. Left orbit rapidly growing meningioma with associated exophthalmos in a 60-years-old woman. MRI at the most representative levels: coronal (a) and axial (b) TSE T2 w; axial Msh-DWI (c); axial unenhanced SE T1 w (d); coronal THRIVE and overlaid perfusion colorimetric map, with relative TIC from region of interest within the lesion (e); axial post-contrast 3D T1 w SPIR.

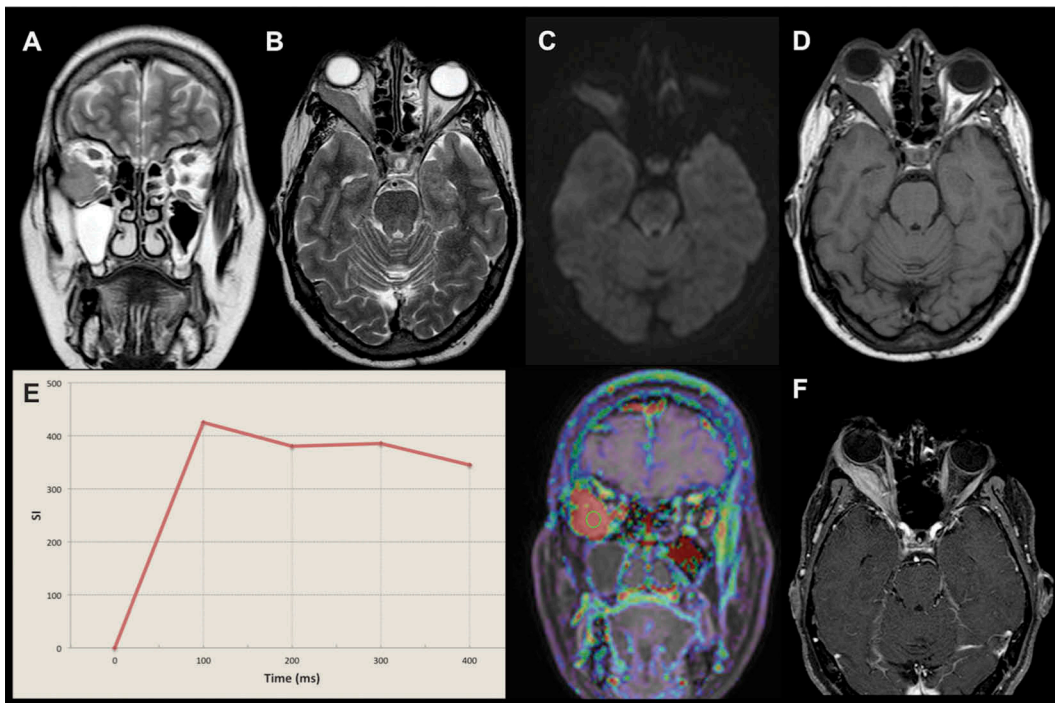


FIGURE 4. Right orbit B-cell non-Hodgkin lymphoma in a 64-years-old woman. MRI at the most representative levels: coronal (a) and axial (b) TSE T2 w; axial Msh-DWI (c); axial unenhanced SE T1 w (d); coronal THRIVE and overlaid perfusion colorimetric map, with relative TIC from region of interest within the lesion (e); axial post-contrast 3D T1 w SPIR.

evaluate the intergroup variation: a statistically significant difference was found between conventional T1 w/T2 w and DWI ( $p = .00169, p < .005$ ), as well as

between DWI and CE 3D T1 w ( $p = .00032, p < .001$ ). Conversely, no significant difference was found between CE 3D T1 w and DCE ( $p = .53517$ ,

TABLE 1. Results of histopathology specimens examinations.

Classification	Histopathological Diagnosis	N
Infective/ Inflammatory	Cholesterinic granuloma	1
	Mucocele	1
	Immunoglobulin IGG4-related ophthalmic disease	1
	Orbital cellulitis	3
Vascular	Idiopathic orbital inflammation	9
	Cavernous hemangioma	4
	Lympho-venous vascular malformation	3
Neoplastic, benignant	Fibrolipoma	1
	Optic nerve glioma	2
	Optic nerve meningioma	4
	Pleomorphic adenoma of ectopic lacrimal gland	1
Neoplastic, malignant	Esthesioneuroblastoma	1
	B-cell non-Hodgkin lymphoma	7
	Granulocitic myeloid sarcoma	1
	Orbital metastasis	2
	Syringoid carcinoma	1

TABLE 2. Post-hoc Wilcoxon signed-rank test results.

	T1 w/T2 w vs T1 w/T2 w + DWI	T1 w/T2 w + DWI vs T1 w/T2 w + DWI+CE 3D T1 w	T1 w/T2 w+ DWI +CE 3D T1 w vs T1 w/T2 w+ DWI +CE 3D T1 w+ DCE
<i>p</i> -value	0.00169	0.00032	0.53517

TABLE 3. Inter-rater reliability (IRR) with Fleiss' Kappa statistics.

	T1 w/ T2 w	T1 w/T2 w + DWI	T1 w/T2 w + DWI+ CE 3D T1 w	T1 w/T2 w + DWI+ CE 3D T1 w + DCE
IRR	0,63	0,68	0,82	0,82

*p* < .005). Above-described results are summarized in Table 2.

When testing for IRR with Fleiss' Kappa statistics, agreement improved from 0.63 to 0.68 by adding DWI to conventional T1 w/T2 w sequences, and from 0.68 to 0.82 by adding CE 3D T1 w to DWI + conventional T1 w/T2 w sequences, whereas no change occurred by adding DCE evaluation (0.82). IRR reliability in the four sub-groups is summarized in Table 3.

### DISCUSSION

The wide range of structures present within the orbit is often the site of origin of various tumours and tumour-like conditions, both in adults and children which are a common indication for the radiological evaluation of the orbit.<sup>19</sup> Knowledge of the clinical presentation and patient age helps to limit the differential diagnosis and to determine the appropriate

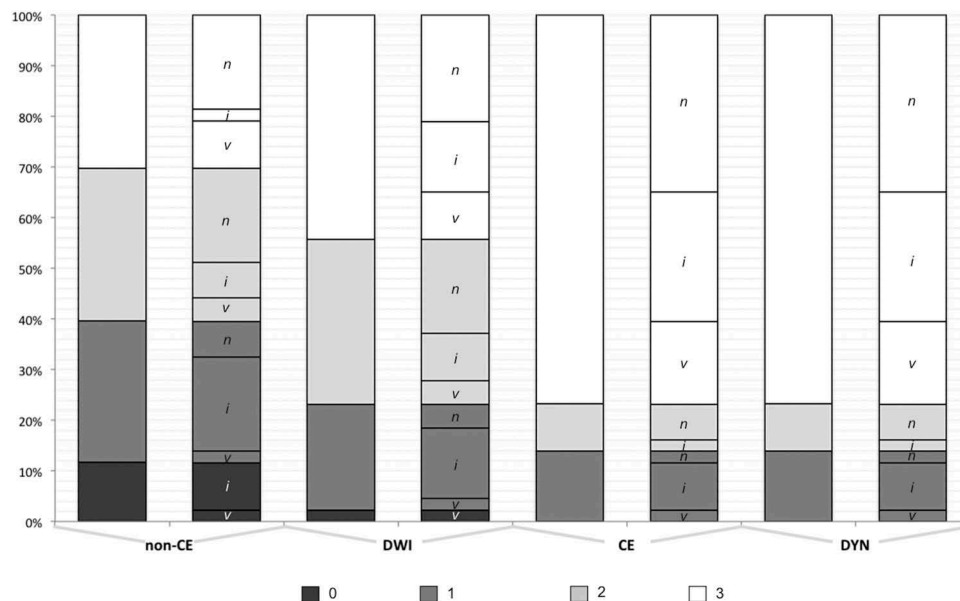


FIGURE 5. Percentage component bar chart representing the proportion of correct observations at each step of MRI evaluation. Black square = 0/3; dark grey square = 1/3; light grey square = 2/3; white square = 3/3. v = vascular; i = infective/inflammatory; n = neoplastic, both benign and malignant. Non-CE = standard MRI protocol without contrast-enhanced sequences; DWI = diffusion-weighted imaging; CE = static contrast-enhanced 3D T1 w SPIR; DYN = dynamic contrast-enhanced ultrafast-spoiled gradient echo.



imaging modality. Cross-sectional imaging is mandatory for the detection, characterization, and mapping of those lesions.

Routinely imaging assessment for orbital lesion largely relies on the combined use of CT scan and contrast-enhanced MRI. US and its colour-Doppler application although non-invasive, with high patient compliance, no significant contraindication and no exposition to ionizing radiations are scattered used depending on the local availability and expertise.<sup>20</sup> In recent years, MRI has become the benchmark for the assessment of orbital lesion, particularly to study the shape, the extension, the involvement of adjacent structures and, eventually the nature; the latter is based on the high tissue resolution and on the multi-parametric evaluation of tissue features.<sup>21,22</sup> On conventional MRI, there are several imaging clues that can help in distinguishing between benign lesions and possible malignancy, such as shape and margins, homogeneity on T1 w and T2 w imaging, pattern of enhancement after contrast media administration. A well-circumscribed mass with regular margins and no evidence of bone destruction might be suggestive of a benign lesion, whereas irregular shape, infiltrative appearance, perineural invasion and bone infiltration might indicate of an aggressive behaviour.<sup>10,21,22</sup> However, in many cases, a final diagnosis can be reached only after fine-needle aspiration or open biopsy because of the absence of specific MRI features or the presence of atypical findings.<sup>23–27</sup> In recent times, in order to improve the differential diagnosis flow-chart, new and more advanced techniques have been introduced.<sup>28,29</sup> It has been demonstrated that the use of advanced MRI imaging such as DWI with relative ADC maps and DCE perfusion imaging in head and neck surgery may add crucial information in therapeutic planning and patient management.<sup>14,30,31</sup>

DWI is known to be restricted in malignant tumours due to high cellularity compared to benign neoplastic and/or inflammatory lesions, whereas is less specific and pathognomonic in the differential diagnosis between abscesses and necrotic tumours.<sup>14,15,21,32</sup> Sepahdari *et al.* also proposed reference ADC values for distinguishing benign from malign orbital lesions, with a suggested cut-off of  $1.0 \times 10^{-3} \text{ mm}^2/\text{s}$  and an ADC ratio of less than  $1.2 \times 10^{-3} \text{ mm}^2/\text{s}$ .<sup>15</sup> According to literature, our study showed that DWI improved diagnostic performance when added to un-enhanced T1 w/T2 w sequences ( $p = .00169$ ), particularly contributing to the differential diagnosis between necrotic tumours and infectious-inflammatory lesions. We performed no quantitative ADC analysis to test the efficacy and the reproducibility of the proposed ADC range values in a heterogeneous clinical setting, the diagnostic performance was further increased when CE 3D T1 w was added to conventional T1 W/T2 W sequences and DWI ( $p = .00032$ ). This result is in line with previous literature evidences demonstrating the positive impact of

intravenous contrast media administration in characterizing orbital masses. In particular, static post-contrast 3D T1 w images combined with conventional sequences are demonstrated to implement the identification of subtle findings and the definition of anatomical relations with adjacent structures.<sup>10</sup>

Conversely, the clinical relevance of dynamic post-contrast T1 w images still remains controversial. Indeed, DCE offers information on the rate of uptake and clearance of contrast medium, allowing the extrapolation of information on tissue/tumour vascularity.<sup>14</sup> However, when testing the actual impact of DCE on diagnostic flow-chart of orbital masses, we documented no significant difference in diagnostic performance when DCE was added to non-contrast and static post-contrast images. In particular, the interpretation of the time-intensity curves (TIC) obtained from DCE acquisition as well as the evaluation of different perfusion patterns, although confirming the evoked hypothesis, never modified the primary diagnosis. Although in literature is reported that DCE has the potential value of helping in depicting TIC of benign versus malignant lesions<sup>33</sup>, in our experience these supplementary data did not significantly influence the diagnostic performance; a positive impact on diagnostic confidence was only observed in case of vascular lesions, when higher accuracy regarding flow dynamics and pattern of enhancement (i.e. progressive, centripetal, heterogeneous, etc.) is required.<sup>1,9,10,12</sup>

These data were further confirmed by IRR showing a higher agreement among observers when DWI is added to conventional T1 w/T2 w sequences (0,68), and a strong improvement when 3D T1 w CE is included in the protocol (0,82). No further improvement was obtained when DCE was added to conventional un-enhanced and static post-contrast sequences evaluation. Therefore, due to time-consuming post-processing elaboration with dedicated software to obtain TIC and other perfusion parameters, DCE should not be routinely included in acquisition protocols for orbital masses, but it should only be employed in selected cases where flow characteristics can be particularly useful.

This study confirmed the positive effect of the addition of DWI and CE 3D T1 w sequences on orbital lesions protocol diagnosis when added to conventional T1 w/T2 w sequences, whereas no substantial impact on diagnostic performance was observed with the further addition of DCE-MRI. In particular, when separately analysing different subgroups (such as neoplastic, vascular and inflammatory/infectious), DWI had a greater impact on the correct assessment of neoplastic lesions (both benignant and malignant) and infectious/inflammatory diseases, even on the basis of a simple qualitative analysis. On the other hand, 3D CE T1 w improved the diagnostic performance and confidence in the study and interpretation

of all the cited categories, with particular reference to neoplastic disorders.

Although the wide spectrum of disorders included in our analysis, the main limitation of this study is the relatively low number of patients for each cluster of pathology recruited. With this knowledge, it is therefore very difficult to draw general conclusions on a specific subgroup, as well as on different classes of pathology in each subgroup. In this light, further studies on larger series are still required, with particular reference to vascular lesions that were relatively poorly represented in the sample. Moreover, these results should be further expanded in patients undergoing specific therapies, in order to evaluate the possible role of the above-mentioned sequences in early prediction of treatment response and long-term follow-up.<sup>18,33</sup>

In conclusion, DWI and T1 3D CE are useful non-invasive imaging tools for the evaluation of orbital and anterior visual pathways lesions, helping the operator in the differential diagnosis of orbital masses; therefore, their inclusion in the MRI routine study of orbital lesions should be considered. Conversely, DCE does not strongly influence diagnostic performance and inter-rater agreement in the study of orbital lesions, increasing the diagnostic confidence only in case of vascular ones; therefore its use should be recommended only in selected patients where the assessment of flow dynamics can be particularly useful for the therapeutic planning. However, further prospective studies on larger cohorts are still required to define the actual impact of dynamic post-contrast sequences compared to non-contrast and static post-contrast images in specific clinical settings, such as early prediction of treatment response.

### DISCLOSURE STATEMENT

The authors declare that there is no conflict of interests regarding the publication of this paper.

### ETHICAL APPROVAL

All procedures performed in studies involving human participants were in accordance with the ethical standards of the institutional and/or national research committee and with the 1964 Helsinki declaration and its later amendments or comparable ethical standards. The IRB for this study was approved by the IRB interdepartmental committee.

### INFORMED CONSENT

Informed consent was obtained for all participants included in the study.

### DATA AVAILABLE ON REQUEST FROM THE AUTHORS


The data that support the findings of this study are available from the corresponding author, upon reasonable request.

### AUTHORS CONTRIBUTION

All authors make substantial contributions to conception and design, and/or acquisition of data, and/or analysis and interpretation of data according to ICMJE recommendations.

All those who have made substantive contributions to the article have been named as authors.

### ORCID

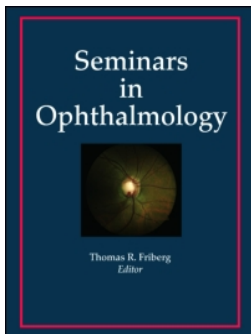
Camilla Russo  <http://orcid.org/0000-0002-2256-7281>

### REFERENCES

- Gündüz K, Yanık Ö. Myths in the diagnosis and management of orbital tumors. *Middle East Afr J Ophthalmol.* 2015;22(4):415–420. doi:10.4103/0974-9233.167823.
- Szabo I, Szabo B. Expanding masses of the posterior orbit. *Oftalmologia.* 2003;3:39–44.
- Bingham CM, Sivak-Callcott JA, Gurka MJ, et al. Axial globe position measurement: a prospective multicenter study by the international thyroid eye disease society. *Ophthalm Plast Reconstr Surg.* 2016;32(2):106–112. doi:10.1097/IOP.0000000000000437.
- Dubois J, Patriquin HB, Garel L, et al. Soft-tissue hemangiomas in infants and children: diagnosis using doppler sonography. *AJR.* 1998;171(July):247–252. doi:10.2214/ajr.171.1.9648798.
- Paltiel HJ, Burrows PE, Kozakewich HPW, Zurakowski D, Mulliken JB. Soft-tissue vascular anomalies: utility of US for diagnosis. *Radiology.* 2000;748(3):747–754. doi:10.1148/radiology.214.3.r00mr21747.
- Bourne RRA, Flaxman SR, Braithwaite T, et al. Magnitude, temporal trends, and projections of the global prevalence of blindness and distance and near vision impairment: a systematic review and meta-analysis. *Lancet Glob Health.* 2017;5(9):e888–e897. doi:10.1016/S2214-109X(17)30293-0.
- Berrocal T, De Orbe A, Prieto C, et al. Us and color doppler imaging of ocular and orbital disease in the pediatric age group. *Radiographics.* 1996;16(2):251–272. doi:10.1148/radiographics.16.2.8966285.
- Neudorfer M, Leibovitch I, Stolovitch C, et al. Intraorbital and periorbital tumors in children—value of ultrasound and color doppler imaging in the differential diagnosis. *Am J Ophthalmol.* 2004;137(6):1065–1072. doi:10.1016/j.ajo.2004.01.050.
- Taylor TD, Gupta D, Dalley RW, Keene CD, Anzai Y. Orbital neoplasms in adults: clinical, radiologic, and pathologic review. *Radiographics.* 2013;33(6):1739–1759. doi:10.1148/rg.336135502.
- Purohit BS, Vargas MI, Ailianou A, et al. Orbital tumours and tumour-like lesions: exploring the armamentarium of multiparametric imaging. *Insights Imaging.* 2016;7(1):43–68. doi:10.1007/s13244-015-0443-8.



11. Strianese D, Piscopo R, Elefante A, et al. Unilateral proptosis in thyroid eye disease with subsequent contralateral involvement: retrospective follow-up study. *BMC Ophthalmol.* 2013;13(1):21. doi:10.1186/1471-2415-13-21.
12. Purohit BS, Vargas MI, Ailianou A, et al. Orbital tumours and tumour-like lesions: exploring the armamentarium of multiparametric imaging. *Insights Imaging.* 2015. doi:10.1007/s13244-015-0443-8.
13. Tortora F, Prudente M, Cirillo M, et al. Diagnostic accuracy of short-time inversion recovery sequence in Graves' ophthalmopathy before and after prednisone treatment. *Neuroradiology.* 2014;56(5):353–361. doi:10.1007/s00234-014-1332-4.
14. Ro S, Asbach P, Siebert E, Eckart B, Hamm B, Erb-Eigner K. Characterization of orbital masses by multiparametric MRI. *Eur J Radiol.* 2015. doi:10.1016/j.ejrad.2015.11.041.
15. Sepahdari AR, Aakalu VK, Kapur R, et al. MRI of orbital cellulitis and orbital abscess: the role of diffusion-weighted imaging. *AJR.* 2009;193(September):244–250. doi:10.2214/AJR.08.1838.
16. Kapur R, Sepahdari AR, Mafee MF, et al. MR imaging of orbital inflammatory syndrome, orbital cellulitis, and orbital lymphoid lesions: the role of diffusion-weighted imaging. *AJNR.* 2009;30(Jan):64–70. doi:10.3174/ajnr.A1315.
17. Jittapiromsaka N, Houc P, Liuc H-L, Sund J, Schiffmane JS, Chia TL. Dynamic contrast-enhanced MRI of orbital and anterior visual pathway. *Magn Reson Imaging.* 2018;51(April):44–50. doi:10.1016/j.mri.2018.04.016.
18. Yuan Y, Kuai XP, Chen XS, Tao XF. Assessment of dynamic contrast-enhanced magnetic resonance imaging in the differentiation of malignant from benign orbital masses. *Eur J Radiol.* 2013;82(9):1506–1511. doi:10.1016/j.ejrad.2013.03.001.
19. Bonavolontà G, Strianese D, Grassi P, et al. An analysis of 2480 space-occupying lesions of the orbit from 1976 to 2011. *Ophthalm Plast Reconstr Surg.* 2013;29(2):79–86. doi:10.1097/IOP.0b013e31827a7622.
20. Nagaraju RM, Gurushankar G, Bhimarao KB. Efficacy of high frequency ultrasound in localization and characterization of orbital lesions. *J Clin Diagn Res.* 2015;9(9):1–6. doi:10.7860/JCDR/2015/13021.6428.
21. Sun B, Song L, Wang X, et al. Lymphoma and inflammation in the orbit: diagnostic performance with diffusion-weighted imaging and dynamic contrast-enhanced MRI. *J MAGN Reson IMAGING.* 2016;1–8. doi:10.1002/jmri.25480.
22. Sun B, Song L. Orbital malignant lesions in adults: multiparametric MR imaging. *Jpn J Radiol.* 2017;35(8):454–462. doi:10.1007/s11604-017-0653-8.
23. Akansel G, Hendrix L, Erickson BA, Demirci A, Papke A, Arslan A. MRI patterns in orbital malignant lymphoma and atypical lymphocytic infiltrates. *Eur J Radiol.* 2005;53(2):175–181. doi:10.1016/j.ejrad.2004.04.005.
24. Ma KK, Callahan AB, Wang SJ, Goldman JE, Kazim M. Atypical rapidly enlarging orbital schwannoma. *Am Soc Ophthalmic Plast Reconstr Surg.* 2017;33(3S Suppl 1):S111–S114. doi:10.1097/IOP.0000000000000740.
25. D, Elefante A, Matarazzo F, Panico A, Ferrara M, Tranfa F. Orbital lymphoma mimicking lacrimal gland pleomorphic adenoma. *Case Rep Ophthalmol.* 2013;4(3):109–113. Published 2013 Sep 17. doi: 10.1159/000354963
26. Velayudhan V, Chaudhry ZA, Smoker WRK, Shinder R, Reede D. Imaging of intracranial and orbital complications of sinusitis and atypical sinus infection: what the radiologist needs to know. *Curr Probl Diagn Radiol.* 2017;46(6):441–451. doi:10.1067/j.cpradiol.2017.01.006.
27. Mombaerts I, Rose GE, Garrity JA. Orbital inflammation: biopsy first. *Surv Ophthalmol.* 2016;61(5):664–669. doi:10.1016/j.survophthal.2016.03.002.
28. Xian J, Zhang Z, Wang Z, et al. Value of MR imaging in the differentiation of benign and malignant orbital tumors in adults. *Eur Radiol.* 2010;20(7):1692–1702. doi:10.1007/s00330-009-1711-0.
29. Ben Simon GJ, Annunziata CC, Fink J, Villablanca P, McCann JD, Goldberg RA. Rethinking Orbital Imaging. *Orbital Imaging.* 2005;112(12):2196–2207. doi:10.1016/j.ophtha.2005.09.013.
30. Elefante A, Cavaliere M, Russo C, et al. Diffusion weighted MR imaging of primary and recurrent middle ear cholesteatoma: an assessment by readers with different expertise. *Biomed Res Int.* 2015;2015:1–8. doi:10.1155/2015/597896.
31. Elkhamary SM, Galindo-ferreiro A, Alghafri L, Khandekar R, Artioli Schellini S. Characterization of diffuse orbital mass using apparent diffusion coefficient in 3-tesla MRI. *Eur J Radiol Open.* 2018;5(November 2017):52–57. doi:10.1016/j.ejro.2018.03.001.
32. Comerchi M, Elefante A, Strianese D, et al. Semiautomatic regional segmentation to measure orbital fat volumes in thyroid-associated ophthalmopathy. A validation study. *Neuroradiol J.* 2013;26(4):373–379. doi:10.1177/197140091302600402.
33. Yuan Y, Kuai X, Chen X, Tao X. Assessment of dynamic contrast-enhanced magnetic resonance imaging in the differentiation of malignant from benign orbital masses. *Eur J Radiol.* 2013;82(9):1506–1511. doi:10.1016/j.ejrad.2013.03.001.



## Ocular Hypertension Following Intravitreal Injection of 0.7mg Dexamethasone Implant versus 2mg Triamcinolone

Brandon Kuley, Philip P. Storey, Maitri Pancholy, Anthony Obeid, James Murphy, Jake Goodman, Turner D. Wibbelsman, Carl Regillo & Allen Chiang

To cite this article: Brandon Kuley, Philip P. Storey, Maitri Pancholy, Anthony Obeid, James Murphy, Jake Goodman, Turner D. Wibbelsman, Carl Regillo & Allen Chiang (2020): Ocular Hypertension Following Intravitreal Injection of 0.7mg Dexamethasone Implant versus 2mg Triamcinolone, *Seminars in Ophthalmology*, DOI: [10.1080/08820538.2020.1758161](https://doi.org/10.1080/08820538.2020.1758161)

To link to this article: <https://doi.org/10.1080/08820538.2020.1758161>



Published online: 28 Apr 2020.



Submit your article to this journal [↗](#)



View related articles [↗](#)



View Crossmark data [↗](#)



# Ocular Hypertension Following Intravitreal Injection of 0.7mg Dexamethasone Implant versus 2mg Triamcinolone

Brandon Kuley, Philip P. Storey, Maitri Pancholy , Anthony Obeid, James Murphy, Jake Goodman, Turner D. Wibbelsman, Carl Regillo, and Allen Chiang

*Mid Atlantic Retina, Wills Eye Hospital, Thomas Jefferson University, Philadelphia, PA, USA*

## ABSTRACT

**Background:** To compare the incidence and outcomes of ocular hypertension (OHT) after intravitreal injection of 0.7 mg dexamethasone (DEX) and 2 mg triamcinolone acetonide (IVT).

**Methods:** In a single-center, retrospective comparative case series, all patients with at least 3 months follow-up receiving 2 mg IVT 3/1/2012 – 3/1/2017 or 0.7 mg dexamethasone 10/1/2014 – 3/1/2017 were included. Ocular hypertension was defined as an intraocular pressure (IOP)  $\geq$  25 mmHg. Patients with a minimum of 3 months follow-up were included. Patients receiving any other form of topical, oral, or intravitreal steroid were excluded.

**Results:** 106 eyes in 100 patients receiving IVT and 114 eyes in 102 patients receiving DEX were included. The mean number of injections was 2.9 for patients receiving IVT and 2.4 for patients receiving DEX ( $p = .11$ ). Fourteen eyes (13.2%) in 14 patients receiving IVT developed OHT compared to 17 eyes (15.1%) in 15 patients receiving DEX ( $p = .85$ ). All cases of OHT were managed with IOP lowering drops or observation alone.

**Conclusions:** Rates of ocular hypertension following 2 mg IVT and DEX are similar. All patients developing OHT were successfully managed without surgical intervention.

**Keywords:** Dexamethasone, triamcinolone, ocular hypertension, corticosteroids, intravitreal injection

## BACKGROUND AND OBJECTIVE

Intravitreal corticosteroid injections are commonly used to treat macular edema secondary to various retinal diseases.<sup>1-4</sup> Elevated intraocular pressure (IOP), also known as ocular hypertension (OHT), is a potential complication of corticosteroid use that has been reported with various routes of administration including but not limited to intravitreal, topical, and periocular delivery.<sup>5,6</sup> The severity of OHT may be influenced by the specific type of corticosteroid, dose, and route of administration. Intravitreal triamcinolone acetonide (IVT) and the dexamethasone implant (DEX) (Ozurdex, Allergan, Inc., Irvine, CA) are two commonly used intravitreal corticosteroids with the latter being FDA approved for the treatment of macular edema following central or branch retinal vein occlusion, diabetic macular edema, and uveitis. Recent studies have suggested lower doses of IVT

may reduce OHT while achieving similar therapeutic efficacy to higher doses.<sup>7,8</sup> The reported rates of OHT following 2 mg of IVT, as reported in a recent study by our group,<sup>9</sup> and 0.7 mg of DEX range from approximately 13-38% and 13-33%, respectively.<sup>10-13</sup> However, no studies have directly compared the rates of ocular hypertension between IVT and DEX. The purpose of our current study is to compare rates of OHT following 0.7 mg of DEX and 2 mg of IVT.

## PATIENTS/MATERIALS AND METHODS

### Inclusion and Exclusion Criteria

Institutional Review Board approval was obtained for this retrospective review. All patients receiving 2 mg IVT at Mid Atlantic Retina/Wills Eye Hospital

Received 26 June 2019; accepted 15 April 2020; published online xx xxx xxxx.

Correspondence: Allen Chiang, Mid Atlantic Retina, the Retina Service of Wills Eye Hospital, Thomas Jefferson University, 840 Walnut Street, Suite 1020, Philadelphia, PA, 19107. E-mail: [Bxk029@jefferson.edu](mailto:Bxk029@jefferson.edu)

Retina Service for any retinal pathology between March 1, 2012 and March 1, 2017 and DEX implant between June 1, 2014 and March 1, 2017 were identified through billing data with Healthcare Common Procedure Coding System (HCPCS) codes J3300 (IVT) and J7312 (DEX). Chart review was used to collect demographic variables and outcome measures. Patients with less than 3 months of follow-up after first DEX implant or 2 mg IVT were excluded. In an attempt to isolate the effects of DEX and IVT, patients receiving any topical, periocular, or intravitreal steroid other than 0.7 mg DEX or 2 mg intravitreal triamcinolone within 3 months of the first DEX implant or IVT injection or after DEX or IVT treatment was initiated were excluded. Baseline IOP was calculated as the mean of the three most recent IOP measurements of the involved eye prior to first DEX implant or IVT injection. For patients who received an injection at their first visit, the IOP of the involved eye measured at that visit was considered to be the baseline pressure.

### Intravitreal Injection Technique

Intravitreal implant of 0.7 mg dexamethasone (Ozurdex, Allergan Inc., Irvine, CA, USA) and intravitreal injection of 2 mg triamcinolone (Triesence, Alcon Laboratories) were performed in an office-based setting. A 27- or 30-gauge needle was used to perform each IVT injection 3.5 mm from the limbus if pseudophakic and 4.0 mm if phakic. The standard injector for the DEX implant that has a 22-gauge needle was used to perform each DEX implant 3.5 or 4.0 mm from the limbus if pseudophakic or phakic, respectively.

### Outcomes

The primary outcome of the study was the incidence of ocular hypertension (OHT), which was defined as an intraocular pressure (IOP) measurement 25 mmHg or higher at any follow-up visit after first DEX or first IVT. Secondary outcomes measures included peak IOP, elevation in IOP >10 above baseline, and treatment for OHT, either medical or surgical. IOP was measured with a Tono-Pen XL (Reichert Inc., Depew, NY). The routine in practice is to confirm any IOP measured  $\geq 25$  mmHg by Tono-Pen XL with Goldmann applanation.

### Statistical Analysis

Demographic, IOP, and treatment data were compared using t-tests. The occurrence of OHT, medical history, and adverse outcome data were compared

using the chi-square test. All statistical tests were performed using SPSS, Version 24 (SPSS, Inc., Chicago, IL).

## RESULTS

### Demographics

For the 2 mg IVT group, a total of 106 eyes in 100 patients were included. For the DEX group, a total of 114 eyes in 102 patients were included. Mean patient age was 65.6 years (range 20.0 to 90.0 years) for the dexamethasone group compared to 69.0 years (range 33.3 to 97.9 years) for the IVT group ( $p = .055$ ). A history of glaucoma was present in 14 patients (12.2%) for the DEX group compared to 22 patients (20.8%) for the IVT group ( $p = .14$ ). Of the 14 patients with a history of glaucoma receiving DEX, 12 patients had primary open angle glaucoma (POAG) and 2 had steroid induced glaucoma. In comparison, of the 22 patients with a history of glaucoma receiving IVT, 21 patients had POAG and 1 patient had steroid induced glaucoma ( $p = .55$ ). Mean duration of patient follow-up was similar between groups: 17.4 months (range 4.0–45.0 months) for DEX group and 15.1 months (range 3.0–52.5 months) for the IVT group ( $p = .10$ ). Rates of follow-up at 3 months, 6 months, and 12 months were similar between groups (3 months- IVT: 99.1% vs DEX: 98.2% ( $p > .99$ ), 6 months- IVT: 90.6% vs. DEX: 91.2% ( $p > .99$ ), 12 months- IVT: 57.5% vs. DEX: 65.8% ( $p = .22$ )). Overall, eyes received a mean of 2.4 DEX injections (range 1–10 injections) compared to 2.9 IVT injections (range 1–17 injections) ( $p = .11$ ). Ocular conditions in eyes treated with DEX implant were diabetic macular edema (52.6%), retinal vein occlusion (20.1%), uveitis (16.7%), other etiologies (4.3%), and Irvine-Gass syndrome (3.5%). Ocular conditions in eyes treated with IVT were diabetic macular edema (40.6%), Irvine-Gass syndrome (25.5%), retinal vein occlusion (18.9%), other etiologies (11.3%), and uveitis (10.4%).

### Incidence of Ocular Hypertension

A total of 17 eyes (14.9%) in 15 patients (Table 1) developed OHT after DEX implant compared to a total of 14 eyes (13.2%) in 14 patients after IVT (Table 2) ( $p = .85$ ). OHT occurred after a mean of 1.6 DEX implant injections with a median of 1 (range 1–3) (Table 1) compared to a mean of 2.4 IVT injections with a median of 1.5 (range 1–9) (Table 2) ( $p = .16$ ). Of the 17 eyes with OHT after receiving DEX implant, ten eyes (58.8%) developed OHT after 1 injection, four eyes (23.5%) developed OHT after 2 injections, and three eyes (17.6%) developed OHT after 3 injections. Of the 14 eyes with OHT after receiving IVT, seven

TABLE 1. Eyes with ocular hypertension following intravitreal injection of 0.7 mg dexamethasone.

Patient	Baseline IOP (mmHg)	History of glaucoma	Number of injections prior to OHT	Time of OHT after DEX (Months)	Peak IOP (mmHg)	Treatment
1	19	No	2	0.5	27	Brimonidine
2	16	Yes	1	1.0	29	Travoprost, Timolol
3-1	14	No	2	5.6	33	Brimonidine, Timolol
3-2	18	No	2	8.6	26	None
4	16	No	3	2.8	28	Brimonidine
5	22	No	2	2.3	30	Dorzolamide, Brimonidine
6	20	No	1	5.3	42	Lataonoprost, Dorzolamide, Brimonidine
7	21	No	1	1.2	28	Timolol
8	17	No	1	0.9	31	Dorzolamide, Timolol
9	16	No	1	2.6	28	Brimonidine
10	17	No	1	2.3	38	Lataonoprost, Brimonidine
11	25	Yes	3	0.2	48	Dorzolamide, Timolol, Bimatoprost
12	15	Yes	3	4.2	28	Dorzolamide, Bimatoprost
13	19	No	1	0.9	38	Brimonidine, Dorzolamide
14	17	No	1	0.9	28	Latanoprost
15-1	13	No	1	1.7	35	Brimonidine, Timolol
15-2	14	No	1	1.7	31	Brimonidine, Timolol

IOP = intraocular pressure; OHT = ocular hypertension; DEX = intravitreal dexamethasone.

eyes (50%) developed OHT after 1 injection, 2 eyes (14.2%) developed OHT after 2 injections, 3 eyes (21.4%) developed after 3 injections, 1 eye (7.1%) developed OHT after 5 injections and 1 eye (7.1%) developed OHT after 9 injections. The mean peak IOP in patients developing OHT was 32.2 mmHg (range 26–48 mmHg) for patients receiving DEX implant compared to 29.0 mmHg (range 25–38 mmHg) for patients receiving IVT ( $p = .086$ ). A total of 8 eyes (7.0% overall) recorded an IOP of 30 mmHg or higher in patients receiving DEX implant compared to 4 eyes (3.8% overall) in patients receiving IVT ( $p = .38$ ). A total of 4 eyes (3.5% overall)

recorded an IOP of 35 mmHg or higher at any follow-up visit in patients receiving DEX compared to 1 eye (0.94% overall) in patients receiving IVT ( $p = .37$ ). Ocular hypertension occurred within 1 month of DEX implant in 6 eyes (35.2%) compared to 4 eyes (28.5%) in patients receiving IVT ( $p = .70$ ), between 1–2 months of DEX implant in 3 eyes (17.6%) compared with 6 eyes (42.9%) in patients receiving IVT ( $p = .23$ ), between 2–3 months of DEX implant in 4 eyes (23.5%) compared to 1 eye (7.1%) in the IVT group ( $p = .35$ ), and more than 3 months after DEX implant in 4 eyes (23.5%) compared to 3 eyes (21.4%) in patients receiving IVT ( $p > .99$ ) (Tables 1 and 2).

TABLE 2. Eyes with ocular hypertension following intravitreal injection of 2 mg triamcinolone.

Patient	Baseline IOP (mmHg)	History of glaucoma	Number of injections prior to OHT	Time of OHT after IVT (Months)	Peak IOP (mmHg)	Treatment
1	12	No	2	1.8	28	Brimonidine
2	21	No	1	0.8	38	Brimonidine, Timolol, Dorzolamide
3	12	No	1	3.3	25	Observation
4	16	No	3	1.4	32	Brimonidine, Timolol
5	20	No	1	2.6	29	Brimonidine
6	14	No	1	1.7	31	Observation
7	22	No	3	1.9	29	Observation
8	12	No	5	1.9	26	Timolol, Dorzolamide, Bimatoprost
9	15	No	9	4.2	31	Timolol, Dorzolamide
10	10	No	3	3.3	28	Brimonidine
11	20	Yes	1	1.0	28	Timolol, Dorzolamide
12	17	Yes	1	0.3	29	Timolol, Brimonidine (Brinzolamide at baseline)
13	9	Yes	1	1.0	26	Observation (Timolol, Dorzolamide at baseline)
14	15	Yes	2	1.8	26	Observation (Timolol, Dorzolamide, Tafluprost at baseline)

IOP = intraocular pressure; OHT = ocular hypertension; IVT = intravitreal triamcinolone.



## Patients with a History of Glaucoma

Of the fourteen eyes of 14 patients receiving DEX implant with a history of glaucoma, 3 eyes of 3 patients (21.4%) developed OHT compared to 22 patients with a history of glaucoma receiving IVT in which 4 eyes of 4 patients (18.2%) developed OHT ( $p > .99$ ). In patients with a history of glaucoma receiving DEX implant, OHT occurred after a median of 3.0 injections (range 1–3) with a mean peak IOP of 35.0 mmHg (range 28–48 mmHg) (Table 1) compared to a median of 1.0 injection (range 1–2) with an mean peak IOP of 27.3 mmHg (range 26–29 mmHg) (Table 2) in patients with a history of glaucoma receiving IVT ( $p = .22$ ). Overall, 7 of 36 eyes between both groups with a history of glaucoma developed OHT compared to 24 of 184 eyes without a history of glaucoma ( $p = .46$ ).

## Treatment

In terms of treatment for OHT, all patients were successfully treated to an IOP  $\leq 25$  mmHg with topical medical therapy or observation alone (Tables 1 and 2). In patients with OHT, IOP lowering drops were used in 13 eyes receiving DEX implant (76.5%) compared to 9 eyes in the IVT group (64.3%) ( $p = .69$ ). One eye with OHT (5.8%) was managed with observation alone in patients receiving DEX implant compared to 5 eyes in patients receiving IVT (35.7%) ( $p = .07$ ). Overall, the mean duration of OHT before IOP returned  $\leq 25$  mmHg was 1.9 months. After OHT was first noted, twenty-four of 32 eyes (75.0%) achieved IOP control on the next follow-up visit. Mean duration of OHT until return to  $\leq 25$  mmHg was 1.3 months for patients receiving IVT compared to 2.4 months for patients receiving DEX implant ( $p = .052$ ). No patients required surgical or laser intervention in either group.

A total of 17 eyes (14.9%) were started on IOP lowering medication at any point during the study in patients receiving DEX implant compared to 21 eyes (19.8%) in patients receiving IVT ( $p = .38$ ). Four eyes in 4 patients without OHT were started on IOP lowering drops in patients receiving DEX implant (3.9%) compared to 8 eyes in 7 patients receiving IVT (7.5%) ( $p = .24$ ). The mean IOP at the time of starting IOP lowering drops was 20.5 mmHg in patients receiving DEX implant without OHT (range 12–24 mmHg) compared to 18.6 mmHg (range 12–24 mmHg) in patients receiving IVT without OHT ( $p = .51$ ).

## DISCUSSION

In this study, eyes that received intravitreal injections of either 0.7 mg DEX or 2 mg IVT had similar rates of OHT with no statistically significant differences in the

time to OHT or peak IOP. All cases of OHT were successfully managed with either IOP lowering drops or observation alone.

We identified OHT in 14.9% of eyes following 0.7 mg DEX, which is similar to other studies that have reported a range of 13–33%<sup>6,10,11,13,14</sup> In one large retrospective study of 421 eyes across all etiologies, the rate of OHT (defined as IOP  $\geq 25$  mmHg) was 20%.<sup>6</sup> One prospective study of patients receiving 0.7 mg DEX for macular edema secondary to retinal vein occlusion (RVO) found the rate of OHT to be 16%.<sup>12</sup> Another retrospective study of DEX for RVO found a rate of 33.7%.<sup>15</sup> While one prospective study of patients receiving DEX for diabetic macular edema (DME) found the rate to be 32.0%,<sup>13</sup> a separate retrospective study found the rate to be 10.2%.<sup>16</sup>

Comparing our rate of OHT following 0.7 mg DEX implant to other studies is difficult due to differences in sample size, patient population, range of follow-up, and indication. Our rate of OHT (defined as IOP  $\geq 25$  mmHg) was 14.9%, which falls within the range of 13–33% reported in the literature.<sup>6,12–14</sup> This range may be attributable to the different pathology examined across these studies (DME, RVO separately in other studies vs. DME, RVO, uveitis together in our study), variability in mean follow-up time, or study method (prospective or retrospective).

In this study OHT following 2 mg IVT was 13.2%, which is generally lower than previously reported rates, although few studies have investigated the 2 mg dose of IVT. In one retrospective study comparing the rate of OHT between 4 mg IVT and 2 mg IVT in RVO patients, the rate of OHT (defined as IOP  $> 21$  mmHg) was 38.9% in patients receiving 2 mg IVT.<sup>17</sup> In another small, prospective study comparing 2 mg IVT vs 4 mg IVT in DME patients, the rate of OHT (defined as IOP  $\geq 25$  mmHg) was 50% for 2 mg IVT and 31% for 4 mg IVT.<sup>18</sup>

Although many studies have reported varying rates of OHT for different agents separately, few have directly compared them. There are limited studies of OHT following 4 mg IVT and 0.7 mg DEX implant, but no studies comparing 2 mg IVT to 0.7 mg DEX implant. A prospective study comparing 4 mg IVT and 0.7 mg DEX implant, in patients with uveitic macular edema demonstrated a rate of OHT (as defined as IOP  $\geq 25$  mmHg) of 30% in patients receiving IVT and 41% in patients receiving DEX implant with no significant difference between the medications.<sup>19</sup> While the rates of OHT in our study for both agents compare similarly to rates reported in existing literature,<sup>6,11,13,17,20,21</sup> definitive cross-study comparisons cannot be made.

Patients with a history of primary open angle glaucoma (POAG) have demonstrated higher IOP following DEX implant injection compared to controls in previous studies. One retrospective study found that of patients with a history of POAG, the mean peak IOP was significantly higher compared to controls

(25.1 mmHg and 20.8 mmHg, respectively).<sup>22</sup> In our study, 21.4% of eyes in patients receiving DEX implant with a history of glaucoma developed OHT (IOP  $\geq$ 25 mmHg) compared to 14% in patients without history of glaucoma ( $p = .44$ ). While our findings did not reach statistical significance, our relatively small sample size of 36 eyes with glaucoma limits this sub-group analysis.

The strengths of our study include a moderately sized and consistent sample of eyes across both agents while importantly excluding patients with concurrent, cross-over, or recent history of topical, periocular, or intravitreal steroids to better isolate any IOP elevation to the effects of 2 mg IVT or 0.7 mg DEX implant. Limitations to our study include the acquisition of IOP measurements using a Tono-pen tonometer instead of Goldmann applanation tonometry which may be more precise but logistically more difficult in a busy retina clinic setting. A challenging aspect of all studies of OHT is defining a threshold IOP value. Several studies selected an IOP of  $>21$  mmHg<sup>17,23-25</sup> while others chose a threshold of  $\geq 25$  mmHg.<sup>12,26,27</sup> Our group chose  $\geq 25$  mmHg in effort to stay within reasonable range of the existing literature. With regard to the difference in the timeframe of data collection, our more frequent use of DEX implant since its FDA approval necessitated an extension in the timeframe for the IVT group in order to obtain a similarly sized group for comparison. We did not find any indication of this difference influencing the primary outcome measure of this study. Another limitation is the variety of indications included in our study (DME, RVO, uveitis, PCME, etc.). For example, some studies have found uveitis to be a risk factor for developing OHT after injection.<sup>28,29</sup> Given that there is some variability between the distribution of indications for both groups, this could represent bias in the study. While our study did not find any significant differences between treatments, our study was limited by sample size and therefore may have been underpowered to detect a difference. In addition, while the rate of follow-up at 3, 6, and 12 months was similar across groups, the precise timing of IOP measurements was variable among patients which could be a confounder. The study was also retrospective and choice of treatment was not randomized, therefore the choice between DEX and IVT could represent a bias. Finally, it should be noted that our study was intentionally limited in scope and did not assess or compare the efficacy of these two agents. Visual acuity and central macular thickness are not reported in this study and we do not draw conclusions regarding these particular treatment outcomes.

In summary, our study compared the development of OHT between 2 mg IVT and 0.7 mg DEX implant and we found no difference in the incidence of OHT, peak IOP, or subsequent OHT management. All eyes that developed OHT were successfully managed with IOP lowering medications or observation and no patients

required surgical intervention. Our findings suggest the risk of OHT is not significantly different between these two common intravitreal corticosteroids.

## DECLARATION OF INTEREST

The authors have no competing interests or financial disclosures regarding this study.

## MEETING PRESENTATIONS

Association for Research in Vision and Ophthalmology Annual Meeting, Vancouver, 2019

Unidentified data is available upon request from Brandon Kuley. Please email [bxk029@jefferson.edu](mailto:bxk029@jefferson.edu) for inquiries.

## SUMMARY STATEMENT

In a study comparing 114 eyes receiving 0.7mg intravitreal dexamethasone and 106 eyes receiving 2mg intravitreal triamcinolone acetonide, no significant difference in the rate of ocular hypertension ( $\geq 25$ mmHg) was found (14.9% vs. 13.2%,  $p=.846$ ).

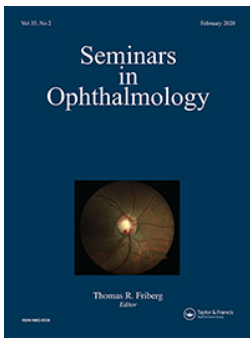
## ORCID

Maitri Pancholy  <http://orcid.org/0000-0002-9417-7629>

## REFERENCES

1. Challa JK, Gillies MC, Penfold PL, Gyory JF, Hunyor ABL, Billson FA. Exudative macular degeneration and intravitreal triamcinolone: 18 month follow up. *Aust N Z J Ophthalmol.* 1998;26(4):277-281. doi:10.1111/j.1442-9071.1998.tb01330.x.
2. Antcliff RJ, Spalton DJ, Stanford MR, Graham EM, TJ F, Marshall J. Intravitreal triamcinolone for uveitic cystoid macular edema: an optical coherence tomography study. *Ophthalmology.* 2001;108(4):765-772. doi:10.1016/S0161-6420(00)00658-8.
3. Greenberg PB, Martidis A, Rogers AH, Duker JS, Reichel E. Intravitreal triamcinolone acetonide for macular oedema due to central retinal vein occlusion. *Br J Ophthalmol.* 2001;86(2):247-248. doi:10.1136/bjo.86.2.247.
4. Jonas JB, Hayler JK, Söfker A, Panda-Jonas S. Intravitreal injection of crystalline cortisone as adjunctive treatment of proliferative diabetic retinopathy. *Am J Ophthalmol.* 2001;131(4):468-471. doi:10.1016/S0002-9394(00)00882-5.
5. Byun YS, Park Y. Complications and safety profile of posterior subtenon injection of triamcinolone acetonide. *J Ocul Pharmacol Ther.* 2009;25(2):159-162. doi:10.1089/jop.2008.0087.
6. Malcles A, Dot C, Voirin N, et al. Safety of intravitreal dexamethasone implant (ozurdex): the SAFODEX study. incidence and risk factors of ocular hypertension. *Retina.* 2017;37(7):1352-1359. doi:10.1097/IAE.0000000000001369.

7. Michael S. Ip, Allison R. Edwards, Roy W. Beck, Neil M. Bressler. A randomized trial comparing intravitreal triamcinolone acetonide and focal/grid photocoagulation for diabetic macular edema. *Ophthalmology*. 2008;115(9):1447–1459.e10. doi:10.1016/j.ophtha.2008.06.015.
8. Hauser D, Bukelman A, Pokroy R, et al. Intravitreal triamcinolone for diabetic macular edema: comparison of 1, 2, and 4 mg. *Retina*. 2008;28(6):825–830.doi:10.1097/IAE.0b013e318165767e.
9. Storey PP, Obeid A, Pancholy M, et al. Ocular hypertension after intravitreal injection of 2-mg triamcinolone. *Retina*. 2018. doi:10.1097/IAE.0000000000002361.
10. Smithen LM, Ober MD, Maranan L, Spaide RF. Intravitreal triamcinolone acetonide and intraocular pressure. *Am J Ophthalmol*. 2004;138(5):740–743. doi:10.1016/j.ajo.2004.06.067.
11. Bakri S, Beer P. Intravitreal triamcinolone injection for diabetic macular edema: A clinical and fluorescein angiographic case series. *Can J Ophthalmol*. 2004;39:755–760. doi:10.1016/S0008-4182(04)80069-3.
12. Haller JA, Bandello F, Belfort R, et al. Randomized, sham-controlled trial of dexamethasone intravitreal implant in patients with macular edema due to retinal vein occlusion. *Ophthalmology*. 2010;117(6):1134–1146.e3. doi:10.1016/j.ophtha.2010.03.032.
13. Boyer DS, Yoon YH, Belfort R, et al. Three-year, randomized, sham-controlled trial of dexamethasone intravitreal implant in patients with diabetic macular edema. *Ophthalmology*. 2014;121(10):1904–1914.doi:10.1016/j.ophtha.2014.04.024.
14. Haller JA, Bandello F, Belfort R, et al. Dexamethasone intravitreal implant in patients with macular edema related to branch or central retinal vein occlusion: twelve-month study results. *Ophthalmology*. 2011;118(12):2453–2460.doi:10.1016/j.ophtha.2011.05.014.
15. Capone A Jr, Singer MA, Dodwell DG, et al. Efficacy and safety of two or more dexamethasone intravitreal implant injections for treatment of macular edema related to retinal vein occlusion (shasta study). *Retina*. 2014;34(2):342–351. doi:10.1097/IAE.0b013e318297f842.
16. Malcles A, Dot C, Voirin N, et al. Real-life study in diabetic macular edema treated with dexamethasone implant: the reldex study. *Retina*. 2017;37(4):753–760.doi:10.1097/IAE.0000000000001234.
17. Chuang LH, Yeung L, Wang NK, Chen HS, Ku WC, Lai CC. Secondary ocular hypertension after intravitreal injection with 2 mg or 4 mg of triamcinolone in retinal vein occlusion. *J Ocul Pharmacol Ther*. 2010;26(4):325–328. doi:10.1089/jop.2010.0039.
18. Audren F, Lecleire-Collet A, Erginay A, et al. Intravitreal triamcinolone acetonide for diffuse diabetic macular edema: phase 2 trial comparing 4 mg vs 2 mg. *Am J Ophthalmol*. 2006;142(5):794–799.doi:10.1016/j.ajo.2006.06.011.
19. Thorne JE, Sugar EA, Holbrook JT, et al. Periocular triamcinolone vs. intravitreal triamcinolone vs. intravitreal dexamethasone implant for the treatment of uveitic macular edema: the PeriOcular vs. INTravitreal corticosteroids for uveitic macular edema (POINT) trial. *Ophthalmology*. 2018. doi:10.1016/j.ophtha.2018.08.021.
20. Rhee DJ, Peck RE, Belmont J, et al. Intraocular pressure alterations following intravitreal triamcinolone acetonide. *Br J Ophthalmol*. 2006;90(8):999–1003. <http://www.ncbi.nlm.nih.gov/pmc/articles/PMC1857192/>.
21. Bakri SJ, Beer PM. The effect of intravitreal triamcinolone acetonide on intraocular pressure. *Ophthalmic Surg Lasers Imaging*. 2003;34:386–390.
22. Bahadorani S, Krambeer C, Wannamaker K. et al. The effects of repeated ozurdex injections on ocular hypertension. *Clin Ophthalmol*. 2018;12:639–642. doi:10.2147/OPHTH.S148990.
23. Ozkok A, Saleh OA, Sigford DK, Heroman JW, Schaal S, STUDY: THEOMAR. Comparison of ozurdex and triamcinolone acetonide for refractory cystoid macular edema in retinal vein occlusion. *Retina*. 2015;35(7):1393–1400. doi:10.1097/IAE.0000000000000475.
24. Jonas JB, Degenring RF, Kreissig I, Akkoyun I, Kamppeiter BA. Intraocular pressure elevation after intravitreal triamcinolone acetonide injection. *Ophthalmology*. 2005;112(4):593–598. doi:10.1016/j.ophtha.2004.10.042.
25. Jonas JB, Kreissig I, Degenring R. Intraocular pressure after intravitreal injection of triamcinolone acetonide. *Br J Ophthalmol*. 2003;87(1):24–27. doi:10.1136/bjo.87.1.24.
26. Storey PP, Ho V, Yeh S, et al. Incidence of sustained ocular hypertension using prepackaged versus freshly prepared intravitreal bevacizumab for neovascular age-related macular degeneration. *Retina*. 2015;35(10):1992–2000. [https://journals.lww.com/retinajournal/Fulltext/2015/10000/INCIDENCE\\_OF\\_SUSTAINED\\_OCULAR\\_HYPERTENSION\\_USING.10.aspx](https://journals.lww.com/retinajournal/Fulltext/2015/10000/INCIDENCE_OF_SUSTAINED_OCULAR_HYPERTENSION_USING.10.aspx).
27. Choi DY, Ortube MC, McCannel CA, et al. Sustained elevated intraocular pressures after intravitreal injection of bevacizumab, ranibizumab, and pegaptanib. *Retina*. 2011;31(6):1028–1035.doi:10.1097/IAE.0b013e318217ffde.
28. Galor A, Margolis R, Brasil OM, et al. Adverse events after intravitreal triamcinolone in patients with and without uveitis. *Ophthalmology*. 2007;114(10):1912–1918. doi:10.1016/j.ophtha.2007.05.037.
29. Jonas JB, Schlichtenbrede F. Visual acuity and intraocular pressure after high-dose intravitreal triamcinolone acetonide in selected ocular diseases. *Eye (Lond)*. 2008;22(7):869–873. doi:10.1038/sj.eye.6702734.



## Retraction: Effective Lens Position According to Incision Width in Cataract Surgery Using Phacoemulsification and Posterior Chamber Lens Implantation

To cite this article: (2020) Retraction: Effective Lens Position According to Incision Width in Cataract Surgery Using Phacoemulsification and Posterior Chamber Lens Implantation, *Seminars in Ophthalmology*, 35:2, 147-147, DOI: [10.1080/08820538.2020.1750267](https://doi.org/10.1080/08820538.2020.1750267)

To link to this article: <https://doi.org/10.1080/08820538.2020.1750267>



Published online: 21 Apr 2020.



Submit your article to this journal [↗](#)



Article views: 71



View related articles [↗](#)



View Crossmark data [↗](#)





## **Retraction: Effective Lens Position According to Incision Width in Cataract Surgery Using Phacoemultification and Posterior Chamber Lens Implantation**

We, the Editors, Publishers, and Authors of *Seminars in Ophthalmology*, have retracted the following article:

Jiwon Baek, Kee-Sun Tae, Anna Lee, Man Soo Kim, and Eun Chul Kim (2018). Effective Lens Position According to Incision Width in Cataract Surgery Using Phacoemultification and Posterior Chamber Lens Implantation, *Seminars in Ophthalmology* 33:7-8, 846-851, DOI: 10.1080/08820538.2018.1534977

The article is being retracted at the request of the authors and their institution, the Catholic University of Korea, Bucheon St. Mary's Hospital, after authors identified errors in subject randomization and concluded the resulting data and results are unreliable.

We have been informed in our decision-making by our policy on publishing ethics and integrity and the COPE guidelines on retractions.

The retracted article will remain online to maintain the scholarly record, but it will be digitally watermarked on each page as "Retracted."